Reviews of Geophysics

REVIEW ARTICLE
10.1029/2024RG000858

**Key Points:**

- Effects of e[$O_3$], water and salinity stresses, and adoption of drip irrigation all lower total growing–season $ET_a$ for almost all crops
- Effects of e[$CO_2$], warming, heat stress, mulching, planting density, and nitrogen addition on total growing–season $ET_a$ appear inconsistent
- Existing $ET_a$ models can describe the response of $ET_a$ to many factors and stresses except for e[$O_3$], heat stress, and nitrogen application

**Correspondence to:**
R. Qiu,
qiurangjian@whu.edu.cn

**Citation:**
Qiu, R., Katul, G. G., Zhang, L., Qin, S., & Jiang, X. (2025). The effects of changing environments, abiotic stresses, and management practices on cropland evapotranspiration: A review. *Reviews of Geophysics*, *63*, e2024RG000858. https://doi.org/10.1029/2024RG000858

Received 26 JUL 2024
Accepted 3 DEC 2024

**Author Contributions:**
**Conceptualization:** Rangjian Qiu, Gabriel G. Katul
**Data curation:** Rangjian Qiu
**Formal analysis:** Rangjian Qiu
**Funding acquisition:** Rangjian Qiu
**Investigation:** Rangjian Qiu
**Methodology:** Rangjian Qiu
**Validation:** Rangjian Qiu, Gabriel G. Katul, Lu Zhang, Shunjing Qin, Xuelian Jiang
**Visualization:** Rangjian Qiu
**Writing – original draft:** Rangjian Qiu, Shunjing Qin, Xuelian Jiang
**Writing – review & editing:** Rangjian Qiu, Gabriel G. Katul, Lu Zhang, Shunjing Qin, Xuelian Jiang



# The Effects of Changing Environments, Abiotic Stresses, and Management Practices on Cropland Evapotranspiration: A Review

**Rangjian Qiu[1], Gabriel G. Katul[2], Lu Zhang[1], Shunjing Qin[1], and Xuelian Jiang[3]**

[1]State Key Laboratory of Water Resources Engineering and Management, School of Water Resources and Hydropower Engineering, Wuhan University, Wuhan, China, [2]Department of Civil and Environmental Engineering, Duke University, Durham, NC, USA, [3]Weifang Municipal Key Laboratory of Agricultural Planting Quantization and Application, Weifang University, Weifang, China

**Abstract** The significance of crop evapotranspiration ($ET_a$) to climate science, agronomic research, and water resources is not in dispute. What continues to draw attention is how variability in $ET_a$ is driven by changing environments, abiotic stresses, and management practices. Here, the impacts of elevated $CO_2$ concentration (e[$CO_2$]), elevated ozone concentration (e[$O_3$]), warming, abiotic stresses (water, salinity, heat stresses), and management practices (planting density, irrigation methods, mulching, nitrogen application) on cropland $ET_a$ were reviewed, along with their possible causes and estimation. Water and salinity stresses, e[$O_3$], and drip irrigation adoption generally led to lower total growing–season $ET_a$. However, total growing–season $ET_a$ responses to e[$CO_2$], warming, heat stress, mulching, planting density, and nitrogen supplement appear inconsistent across empirical studies. The effects of e[$CO_2$], e[$O_3$], water and salinity stresses on total growing–season $ET_a$ are attributed to their influence on stomatal conductance, root water uptake, root and leaf area development, microclimate, and potentially phenology. Total growing–season $ET_a$ in response to warming is affected by variations in ambient growing–season mean air temperature and phenology. The differences in crop $ET_a$ under varying planting densities are due to their differences in leaf area. The responses of $ET_a$ to heat stress, mulching, and nitrogen application represent trade–off between their opposite effects on transpiration and evaporation, along with possibly phenology. Modified $ET_a$ models currently in use can estimate the response of $ET_a$ to the many aforementioned factors except for e[$O_3$], heat stress, and nitrogen application. These factors offer a blueprint for future research inquiries.

**Plain Language Summary** Evapotranspiration ($ET_a$) describes the net amount of water vapor molecules that are transported from ecosystems to the overlying drier atmosphere per unit ground area per unit time. It is a topic that cuts across agronomy, climate science, hydrometeorology, plant physiology, radiation and energy balances, soil physics, thermodynamics, turbulence, water resources, and many others. Cropland $ET_a$ pose additional challenges because crop growth is rapid in agroecosystems and physiological function spanning germination, flowering, and biological aging (or senescence) evolves dramatically over a single growing season instead of a decade as in forests. Moreover, crops are and continue to be subjected to many stresses and management practices, and their response to them is reflected through $ET_a$. The review here covers the effects of key changing environments (e[$CO_2$], e[$O_3$], warming), abiotic stresses (water, salinity, heat stresses), management practices (planting density, irrigation methods, mulching, nitrogen supplement) on cropland $ET_a$. The focus is on potential causes, quantification methods, and what was found from field studies across crop types, soil, climate, and management practices. Operational formulations for $ET_a$ as well as measurement techniques in use are also discussed.

## 1. Introduction

The term evapotranspiration ($ET_a$) represents the combined sum of evaporation from the soil (or water) surface to the atmosphere and the uptake of liquid water by roots that is then transported to the leaves where evaporation occurs to enable carbon dioxide uptake from the atmosphere. Because $ET_a$ involves a phase transition from liquid water to water vapor within soil pores near the soil-atmosphere interface and in the sub-stomatal cavities of leaves, the review commences with the topic of evaporation for the purposes of defining terminology and identifying key challenges to $ET_a$. Thermodynamic textbooks deal with this topic by considering what is termed as a closed system, a system that does not allow mass exchange with the surrounding but allows energy inputs.

Within this closed system, liquid water and the overlying air are considered within a container. Continual loss of water molecules due to external heating of the container saturates the overlying air and an equilibrium state is reached whereby the number of molecules escaping from the liquid phase is balanced by the number of molecules colliding with the liquid surface from the air aloft (condensation). When such an equilibrium is reached, the net rate of water vapor molecules exchanged between water and the overlying air is zero. At this state, the vapor pressure in the air defines the so-called saturation vapor pressure as described by the Clausius–Clapeyron equation (Bolton, 1980), and the air relative humidity (RH) is at 100%. In such cases, the saturation vapor pressure only varies with the equilibrium temperature—that is the overall temperature of the air-water system. A situation such as this may exist in the sub-stomatal cavity when stomatal pores are actually closed. If the same experiment is repeated in what is termed as an open system (i.e., a system with mass and energy exchanges across its boundaries are allowed) and where the atmosphere deviates from saturation (i.e., RH < 100%), water vapor molecules can be transported away from the evaporating site by turbulent eddies (Brutsaert, 1965), and the chance that these escaped water vapor molecules collide again and condense onto the evaporating surface is small compared to a closed system. For this reason, the vapor pressure deficit (VPD) between the surrounding atmosphere and the evaporating surface ensures that the atmosphere has the capacity to accommodate more water vapor molecules escaping from the evaporating surface. Wind can enhance the transfer of these water vapor molecules away from the evaporating surface thereby increasing the atmospheric transfer efficiency or reducing the aerodynamic resistance (Brutsaert, 1982; Campbell & Norman, 1998; Katul & Liu, 2017). This was the basis for some of the early theories on evaporation in the early 1800 (Dalton, 1802) as reviewed elsewhere (McMahon et al., 2016). Interestingly, measurements of evaporation from water surfaces were conducted much earlier as by Edmund Halley in 1686 (Halley, 1687) using evaporation pans—a concept that still in use today.

Moving from a free water surface to a bare soil surface in an open system adds another layer of complexity. When the soil surface is saturated, soil evaporation depends primarily on meteorological conditions (stage I evaporation). In this stage, the ability of the atmosphere to provide the requisite energy and transport water vapor away from the surface dictates the evaporation rate. However, as the soil dries, soil evaporation rate declines with increased time (Brutsaert, 2014; Jury & Horton, 2004; Parlange et al., 1992) and becomes controlled by the ability of underlying soil pores to transmit liquid water to the evaporating surface (stage II evaporation). The physics describing this liquid movement is encoded in the so–called Richards–Richardson equation (Raats & Knight, 2018; L. A. Richards, 1931; Richardson, 1993), whose solution yields evaporation rates decreasing with square root of inverse time. For very dry conditions, the ability of water vapor, produced by evaporation in the deeper soil pores, to diffuse in the air space to the soil surface becomes the limiting rate for evaporation (stage III evaporation). At this stage, the evaporation rate is diminished substantially compared to its stage I counterpart. These three stages have been extensively studied in the soil science literature since the 1950s (H. R. Gardner & Gardner, 1969; W. R. Gardner, 1959) and have informed some of the debate about advantages and disadvantages of soil tillage (Liebhard et al., 2022).

Plant transpiration ($T_r$) is another process whereby liquid water also vaporizes inside the plant tissue and enters the atmosphere predominately but not exclusively through stomata (Figure 1). Thus, evaporation and transpiration are thermodynamically equivalent as they both involve the same first–order phase transition as noted earlier. The reason why these two mechanisms are distinguished in $ET_a$ models is attributed to the differences in liquid pathways they follow before the phase transition. The stomatal aperture is controlled by guard cells and those determine the vapor exchange from the intercellular space of the leaf to the atmosphere (Darwin, 1898). For every water molecule lost to the atmosphere, stomata must adjust their aperture and thus their leaf water potential to lift the entire liquid water column all the way up from the roots (source) to the leaf (sink) by one water molecule to avoid dehydration (Johnson et al., 2022). In doing so, water becomes under tension as it is transported from the soil pores to the roots (mainly dictated by the soil physics of the rhizosphere), then moved in the crop tissues (as described by cohesion–tension theory), and finally lost to the atmosphere thereby setting $T_r$. This description has a long tradition in soil–plant relations (Bonner, 1959; Dixon & Joly, 1894; Van den Honert, 1948). Only a tiny proportion (<1%) of this water is kept within the plant to sustain the water demands for leaf photosynthesis ($A_n$)—meaning the water needed to convert carbon dioxide to sugars and oxygen is only a tiny fraction compared to water losses to the desiccating atmosphere when stomata open up to uptake carbon dioxide molecules. This fact means that when crops open their stomata, $A_n$ and crop leaf transpiration ($T_{r\text{—leaf}}$) occur simultaneously and are conventionally approximated by a Fickian diffusive mass transport given by (Cowan & Troughton, 1971)

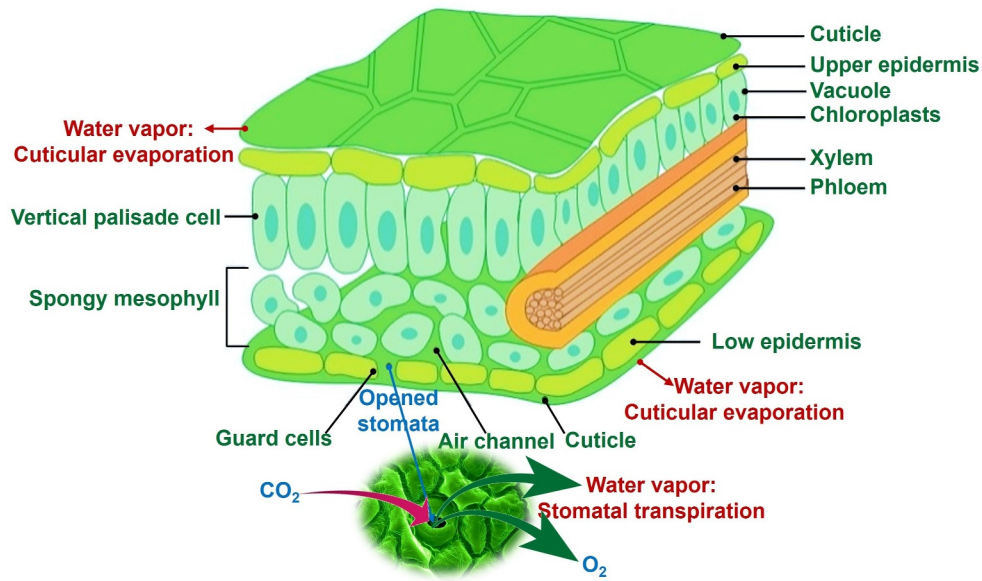


**Figure 1.** Flowchart of the transfer of water from the leaf to atmosphere.

$$A_n = g_c(c_a - c_i), \tag{1}$$

$$T_{r-\text{leaf}} = g_s(e_i - e_a) \approx 1.6 g_c \text{VPD}, \tag{2}$$

where $g_s$ and $g_c$ is the leaf stomatal conductance to $H_2O$ and $CO_2$, respectively (mol m$^{-2}$ leaf area s$^{-1}$) ($g_s = 1.6\ g_c$), $c_a$ and $c_i$ are the ambient and intercellular $CO_2$ concentrations (μmol mol$^{-1}$), $e_a$ and $e_i$ are the ambient and intercellular water vapor concentrations (kPa), and VPD is the vapor pressure deficit (kPa). Hence, $T_{r-\text{leaf}}$ links crop physiological activities, growth, and reproduction, and $g_s$ acts as a bridge between the carbon and water cycles. In fact, this bridge can be made explicit when considering the above–ground biomass ($B$, g m$^{-2}$) of plants given by (F. J. Richards, 1959; Von Bertalanffy, 1957)

$$\frac{dB}{dt} = A_{c,*} P_g L - k_m B, \tag{3}$$

where $A_{c,*}$ is the amount of photosynthate allocated to $B$ (that evolves with the crop growth stage), $P_g$ is the gross photosynthesis per unit leaf area reduced by photorespiration and synthesis respiration (g C m$^{-2}$ leaf area$^{-1}$ d$^{-1}$), $L$ is the active leaf area (related to $B$ depending on crop growth stage), and $k_m$ is the rate of maintenance respiration plus tissue death (g C g$^{-1}$ dry mass d$^{-1}$). This carbon budget reflects the dominant balance between carbon uptake and respiration losses. Because $P_g$ is proportional to $A_n$, and $A_n$ is proportional to $g_s$ as before, stomata exert first–order controls on plant growth (Niklas, 1994). The link between $T_r$ and growth can be summarized by (Mrad et al., 2020)

$$\frac{dB}{dt} = A_{c,*} T_r c_a \frac{1 - c_i/c_a}{1.6\text{VPD}} - k_m B. \tag{4}$$

Compared to carbon gain, $T_r$ (plant scale) and $T_{r-\text{leaf}}$ (leaf scale) are commonly considered a "cost" needed to maintain leaves well hydrated to enable plant physiological activities (Hsiao, 1973). However, in the subsurface, the reverse is true. Plants are required to "invest" assimilated carbon to construct roots that are used to acquire water and nutrients from the soil (Guswa, 2008, 2010). Returning to the stomates, how to maximize carbon gain for a given amount of water in the soil root system may be used as a plausibility conjecture to decide on how stomatal aperture is to be adjusted in time (Cowan & Farquhar, 1977; Hari et al., 1986; Makela et al., 2002; Mrad et al., 2019). While this approach has been extensively studied and recently reviewed (Katul et al., 2012;

Nakad et al., 2023), it has not permeated into the crop literature except for few studies (Qiu & Katul, 2020; Volpe et al., 2011). In some cases, $T_r$ may be beneficial to plants because of evaporative cooling (Campbell & Norman, 1998; C. Huang et al., 2015; Konrad et al., 2021). Such cooling may avoid leaves suffering from heat injury or decline in photosynthesis due to heat stress (Zahra et al., 2023).

Equation 4 suggests that increasing VPD may lead to a decline in $B$. However, to assess the role of VPD on $B$ requires deeper understanding of how $c_i/c_a$ and transpiration are both impacted by VPD discussed next. At the leaf scale, the response of $T_{r\text{—leaf}}$ to VPD (Equation 2) is expected to be non–monotonic. While $g_s$ monotonically declines with increasing VPD, the driving force for transpiration (i.e., Dalton's law) increases with increasing VPD. To illustrate, considering the $g_s$ represented by (Oren, Sperry, et al., 1999)

$$g_s = g_{\text{ref}}[1 - m\log(\text{VPD})], \tag{5}$$

where $g_{\text{ref}}$ is a reference conductance evaluated at VPD = 1 kPa for optimal temperature, saturating light conditions, and moist soils, with $m$ being roughly a constant coefficient that varies between 0.5 and 0.6 (Katul et al., 2009), then a maximum $T_{r\text{—leaf}}$ is expected to occur at a critical VPD ($\text{VPD}_{\text{crit}}$) given by

$$\text{VPD}_{\text{crit}} = \exp\left(\frac{1-m}{m}\right) \approx 1.94\text{kPa}. \tag{6}$$

For VPD $<$ $\text{VPD}_{\text{crit}}$, increases in VPD will lead to increases in $T_{r\text{—leaf}}$. Conversely, if VPD $>$ $\text{VPD}_{\text{crit}}$, increases in VPD will lead to a decline in $T_{r\text{—leaf}}$. For these reasons, semi–arid areas may experience a decline in $T_{r\text{—leaf}}$ with increased VPD while humid areas will experience an increase in $T_{r\text{—leaf}}$ with increasing VPD.

At the whole plant scale, $T_r$ depends on meteorological conditions (i.e., received energy, VPD, and wind speed), as well as soil moisture, the ability of the soil to conduct water to roots, water logging, soil salinity, crop and soil characteristics, changing environments, management practices, among others (R. G. Allen et al., 1998).

Thus, at the "field–scale," cropland $\text{ET}_\text{a}$ consists of $T_r$ and soil (or water in case of paddy rice field) evaporation ($E_s$). Since $T_r$ and $E_s$ occur simultaneously, it is difficult to distinguish between these two processes from a micro–meteorological perspective (i.e., what the atmosphere senses as a source of water vapor) as reported by numerous studies (Z. Hu et al., 2009; Kool et al., 2014; Schlesinger & Jasechko, 2014; Scott et al., 2021). For crops, the proportion of $T_r$ to $\text{ET}_\text{a}$ varies during the plant growing season and is mainly controlled by the leaf area index (LAI) or crop canopy coverage. Water is primarily consumed by $E_s$ for small LAI, and by $T_r$ under high LAI when water is sufficient. There are linear and non-linear (logarithmic, exponential, polynomial, etc) correlations between cropland $T_r/\text{ET}_\text{a}$ and LAI (P. Zhao et al., 2018). Since $E_s$ is not beneficial for crop production (except through some evaporative cooling or reduction in overall VPD), one of the methods to improve crop water productivity in water scarce regions is increasing the fraction of $T_r$ in $\text{ET}_\text{a}$ while minimizing $E_s$. Such an approach may include mulching (placement of material on the soil surface) and micro irrigation (i.e., low–pressure application of water) methods. For instance, the $T_r/\text{ET}_\text{a}$ for maize increased by 6%–12% under transparent plastic film mulching compared to no mulching (Y. Zhang et al., 2018), and by 5% on average under drip irrigation than border (Y. Wang et al., 2020).

Moving from mass to energy transport (Figure 2), and upon neglecting heat advection, photosynthetic energy consumption, and energy storage by the plant canopy, the $\lambda\text{ET}_\text{a}$ (energy form of $\text{ET}_\text{a}$) over cropland can be determined as a residual in the energy balance (Kimball et al., 1994)

$$\lambda\text{ET}_\text{a} = R_n - G_0 - H, \tag{7}$$

where $R_n$ is the incident net radiation (W m$^{-2}$), $G_0$ is the surface soil heat flux (W m$^{-2}$), $H$ is the sensible heat flux (W m$^{-2}$), and $\lambda$ is the latent heat of vaporization (MJ kg$^{-1}$). The $\lambda\text{ET}_\text{a}$ is a primary component of surface energy balance and reflects the energy associated with evaporating water. Terrestrial $\lambda\text{ET}_\text{a}$ consumes about 60% $R_n$ on average (K. Wang & Dickinson, 2012), while growing–season mean $\lambda\text{ET}_\text{a}/R_n$ over cropland was higher—0.77–0.86 for rice (B. Liu et al., 2019), 0.77–0.79 for maize (Jiao et al., 2018), 0.64–0.69 for winter wheat (X. Y. Feng et al., 2023), 0.63–0.70 for soybean (Suyker & Verma, 2009), and 0.75–0.76 for cotton (Tian et al., 2017). Advection of sensible heat between a field and its surroundings may occasionally occur in

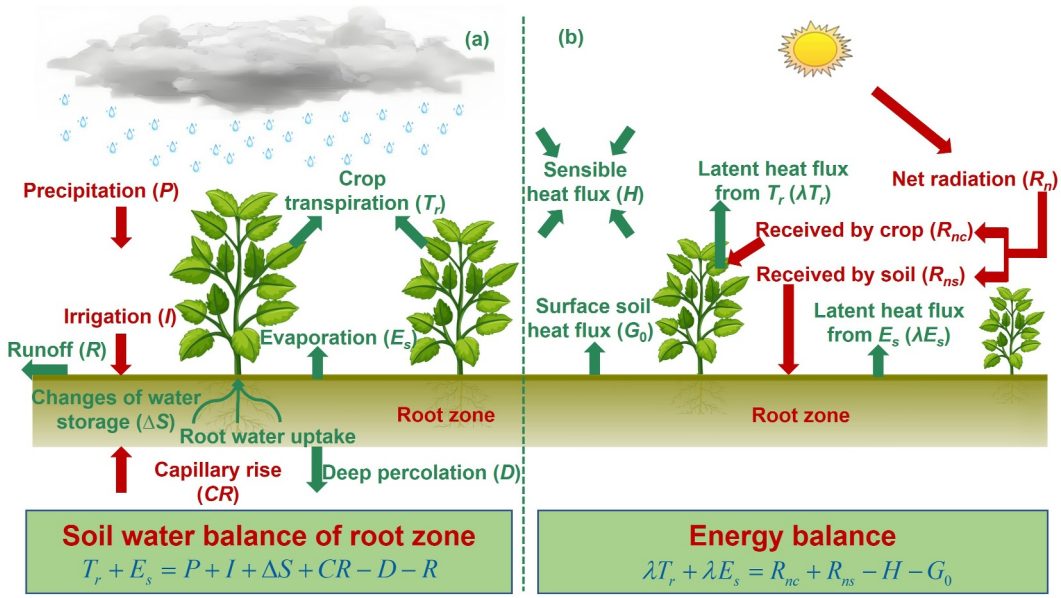


**Figure 2.** Soil water balance in the root zone (a) and the energy balance (b) to determine crop evapotranspiration.

cropland so that $\lambda ET_a$ becomes larger than available energy ($R_n$—$G_0$) on certain growing days depending on the size of the field and adjacent land cover (Alfieri et al., 2012; Lei & Yang, 2010; L. Li & Yu, 2007; Qiu et al., 2019; T. Wang et al., 2024). To highlight the frequency of occurrence of such advective events, we report few cases from field studies. The number of advective days were eight for the early rice season, 30 for the late rice season (B. Liu et al., 2022), and 10 for the summer maize season (Ding et al., 2015). The advection of sensible heat can be identified by negative daytime $H$ or the Bowen ratio $\left(\beta_o = \frac{H}{\lambda ET_a}\right)$ (Kool et al., 2018) and has been reported in a number of studies that sought to generalize combination equations (Katul & Parlange, 1992). This advection provides additional energy to the field, enhancing cropland $ET_a$, which can be quantified by the differences between measured $ET_a$ and equilibrium evaporation (Ding et al., 2015; L. Li & Yu, 2007; McNaughton, 1976; S. Wang et al., 2019). The reported contribution of advection to daily $ET_a$ was 4.4%–28.0% for maize (Ding et al., 2015), 0.6%–37.7% for rice (B. Liu et al., 2022), over 50% for winter wheat (L. Li & Yu, 2007), and 1.4%–57.4% for an irrigated vineyard (S. Wang et al., 2019). Even for an irrigated bare soil, the advection can be severe and contribute some 20% extra daytime evaporation as discussed elsewhere (Parlange and Katul, 1992).

From a mass transport perspective (Figure 2), the $ET_a$ can be determined based on root–zone soil water balance as

$$ET_a = P + I + \Delta S + CR - D - R, \tag{8}$$

where $P$ is the precipitation amount adjusted by interception losses (mm), $I$ is the irrigation amount (mm), ΔS is the change of water storage within the root zone (mm), CR is the capillary rise (mm), $D$ is the deep percolation (mm), and $R$ is the surface runoff (mm). This water balance also reflects the relation between water supply and water demand. The $ET_a$ is a primary component of the water balance and reflects the dominant water loss, especially in arid and semi–arid regions. The $ET_a$ accounts for 59%–67% of the terrestrial precipitation (K. Wang & Dickinson, 2012) and about 90%–100% of annual rainfall in arid and semi–arid regions (Katul et al., 2012; Y. Liu et al., 2022). Nearly 70% of total water use worldwide is consumed in agriculture (Kang et al., 2017), where ~99% of agricultural water is lost by cropland $ET_a$ (Rana & Katerji, 2000). Hence, cropland $ET_a$ reflects the final consumption of water in agriculture.

In addition, variation of regional cropland $ET_a$ reflects the changes of the regional agro–ecological environment. The varying vegetation cover and irrigation methods in cropland will lead to differences in mass and energy exchanges between the surface and the atmosphere, which in turn further affect the local climate and atmospheric circulation. For instance, increasing water–saving irrigation has been reported to restrain cooling effects in

**Table 1**
*Summary of Recently Published Reviews Concerning Evapotranspiration ($ET_a$)*

| Perspective | Reference |
|---|---|
| The role of $ET_a$ in the global, terrestrial, and local water cycles | Katul et al. (2012) |
| The modeling, climatology, and climatic variability of global terrestrial $ET_a$ | K. Wang and Dickinson (2012) |
| Best practices for measuring $ET_a$ | R. G. Allen et al. (2011a, 2011b) |
| $ET_a$ partitioning methods | Kool et al. (2014); W. Xiao et al. (2018) |
| Land–scale $ET_a$ from a boundary–layer meteorology perspective | Cuxart and Boone (2020) |
| Theoretical origin, basic assumptions, and limitations in major conventional $ET_a$ approaches | Y. Liu et al. (2022) |
| Spatiotemporal patterns of global $ET_a$ variations and their relations with vegetation greening | Y. Yang, Roderick, et al. (2023) |
| Cropland $ET_a$ in response to changing environments, abiotic stresses, and management practices | This study |

Xinjiang, China (C. Zhang et al., 2023). Intensive irrigation in India cools air by some 0.5°C but increases the specific humidity thereby resulting in an enhanced moist heat stress (Mishra et al., 2020). Furthermore, $ET_a$ trends in time appear non–monotonic with projected changes in climate. Unsurprisingly, global terrestrial $ET_a$ is projected to increase due to warming and increasing precipitation. However, $ET_a$ is projected to also decrease as a result of limiting soil moisture and elevating atmospheric $CO_2$ concentration (e[$CO_2$]) due to partial stomatal closure (Jung et al., 2010; Pan et al., 2015; Y. Yang, Roderick, et al., 2023). Some studies indicated that marked variations of global crop water demand were primarily driven by climate and e[$CO_2$], and these trends increased faster in 1981–2013 (Urban et al., 2017).

Given the significance of $ET_a$, there are numerous reviews covering this subject, and detailing all of them is well beyond the scope of this effort. Table 1 summarizes the varying perspectives concerning $ET_a$ of recently published reviews. There appears to be a recalcitrant gap in covering issues related to cropland $ET_a$—given the dynamic nature of agroecosystems (rapid changes in leaf area, nutritional status, plant height, root area, root depth, physiological properties, etc). Cropland $ET_a$ exhibits high variability due to its fast response to numerous factors (Figure 3), including meteorological conditions (their effect on $ET_a$ can be expressed using reference evapotranspiration, $ET_o$), changing environments, various abiotic stresses, management practices, crop–specific and soil factors, among others. To date, there is a need to re–examine the primary factors (such as key changing environments, abiotic stresses, and management practices) influencing cropland $ET_a$ given the proliferation of

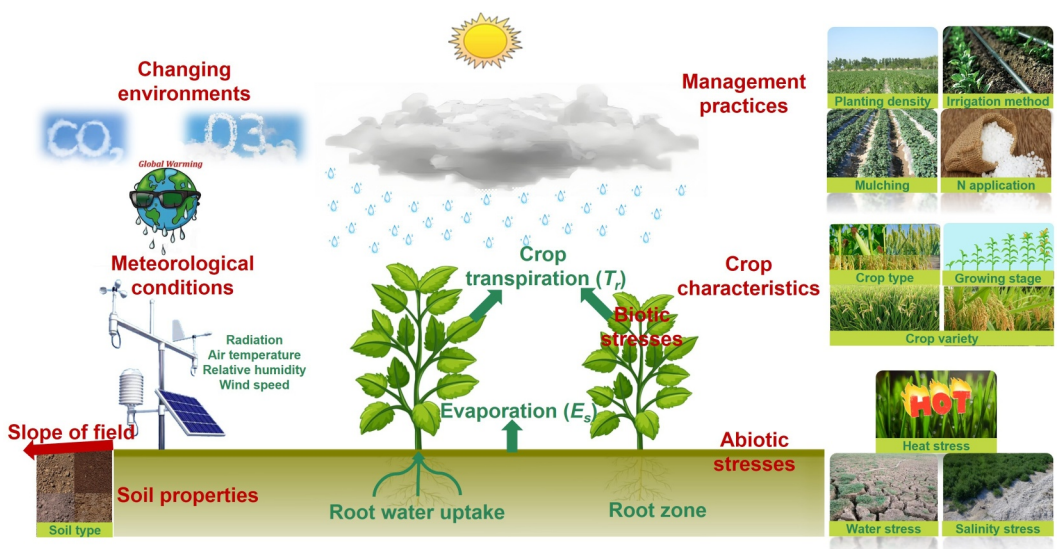


**Figure 3.** Factors affecting cropland evapotranspiration ($ET_a$). The effect of meteorological conditions on $ET_a$ can be expressed by using a reference evapotranspiration (R. G. Allen et al., 1998).

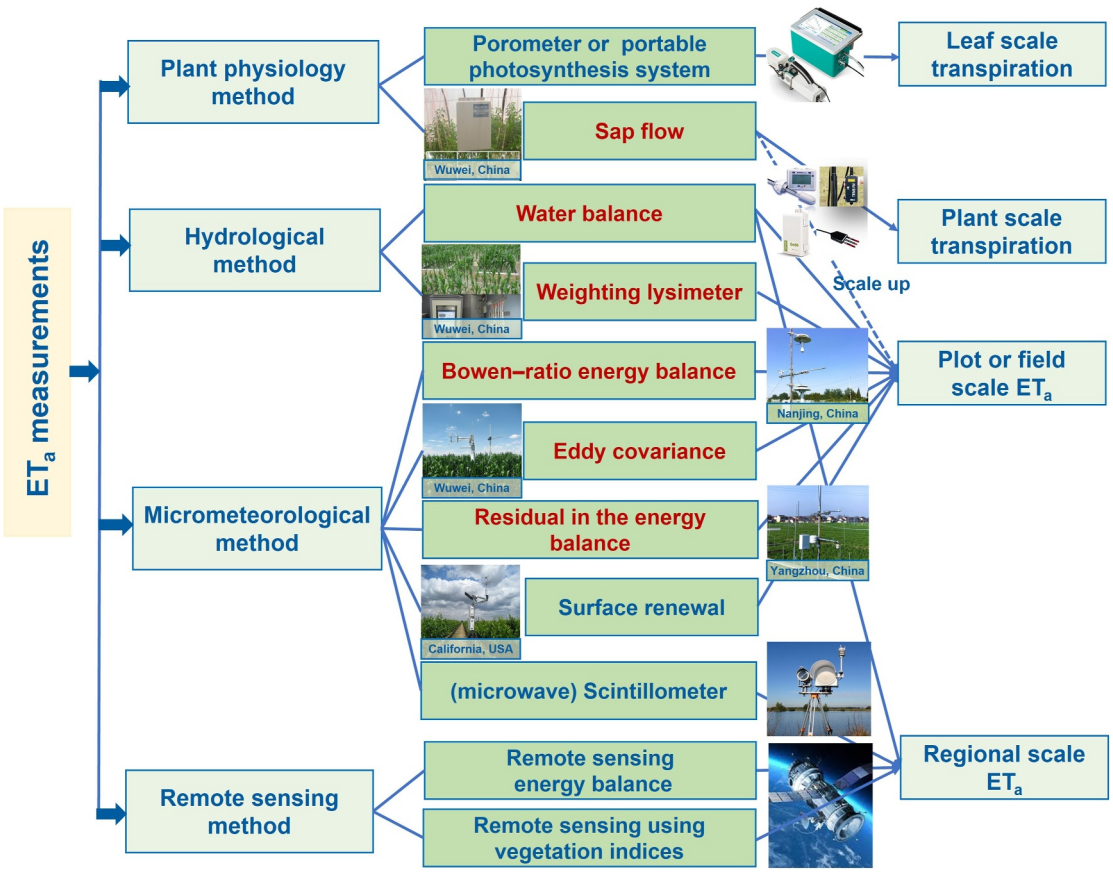


**Figure 4.** Measurement methods for cropland evapotranspiration ($ET_a$). Methods (dark-red font) used to investigate plot or field scale $ET_a$ in response to varying factors are reviewed.

long–term manipulation experiments, advancements in estimation models, and exponential growth in new and improved measuring methods at multiple spatial and temporal scales.

In this review, the focus is on factors encompassing key changing environments, abiotic stresses, and management practices that impact cropland $ET_a$, along with their quantification methods. In Section 2, a brief introduction to the methods employed for measuring $ET_a$ is provided. These methods are instrumental in analyzing $ET_a$ in response to the plethora of factors considered in later sections. Sections 3 delves into reported effects of key changing environments (e[$CO_2$], elevated ozone concentration (e[$O_3$]), global warming), abiotic stresses (water, salinity, heat stresses), management practices (planting density, irrigation methods, mulching, nitrogen (N) supplement) on cropland $ET_a$, along with their potential causes and estimation methods. Additionally, other reported considerations are also presented that forms the basis for models. The review concludes by highlighting key themes and suggests further experiment and modeling needs for analyzing the effects of e[$O_3$], heat stress, warming, and compound factors on cropland $ET_a$. Despite this restricted scope, it is envisaged that such a review of $ET_a$ provides foundational knowledge for the development of irrigation systems, establishment of crop planting zones, implementation of regional water–saving agriculture practices, efficient assessment of water resources, and effective development, management, and allocation of water resources, among others (R. G. Allen et al., 2011b).

## 2. $ET_a$ Measurement Methods for Investigating Different Affecting Factors

The $ET_a$ can be measured by using several methods (Figure 4) such as the hydrological balance, the energy balance at multiple scales (local and satellite space based), several micro–meteorological approaches, and heat transport in plants summarized in Table 2. The merit and demerit of each method and recommendation for proper and best operation have been discussed elsewhere (R. G. Allen et al., 2011a). Only a brief introduction to the

10.1029/2024RG000858

**Table 2**
*Summary of Evapotranspiration ($ET_a$) Measurement Methods*

| Method | Spatial scale | Temporal scale | Typical error (%)[a] | Advantage | Disadvantage |
|---|---|---|---|---|---|
| Sap flow | $10^1$–$10^4$ $cm^2$ | Seconds to yearly | 15–50 | Measuring short–term transpiration ($T_r$); separating $T_r$ from $ET_a$ coupled with other $ET_a$ measurements | Only measuring individual $T_r$; uncertain in scaling up from plants to ecosystem |
| Weighing Lysimeter | 0.2–40 $m^2$ | Minutes to yearly | 5–15 | Accurate; long–term automatic continuous measurement | Edge effects; small spatial scale; difficult to measure plants having large spacing |
| Residual in the energy balance | 4–$10^2$ $m^2$ | Seconds to yearly | – | Clear principles; relatively accurate $ET_a$ in plots, such as in the FACE systems | Small spatial scale; requiring accurate determining surface temperature |
| Surface renewal | Hundreds $m^2$ to several $km^2$ | Seconds to yearly | – | Relatively inexpensive and easily operated; useful for rough or non–homogenous surfaces | Caution to use in high humidity and wind conditions; requiring high-frequency air temperature measurements |
| Bowen–ratio and Energy Balance | Hundreds $m^2$ to several $km^2$[b] | Seconds to yearly | 10–20 | Accurate; non-destructive; long-term automatic continuous measurement | Large error when Bowen–ratio is near −1; requiring uniform fetch of sufficient distance |
| Eddy covariance | Hundreds $m^2$ to several $km^2$[b] | Seconds to yearly | 15–30 | Accurate; high frequency; non-destructive; long-term automatic continuous measurement | Needing "corrections"; energy balance closure issue; requiring uniform fetch of sufficient distance |
| Remote sensing energy balance | $10^1$–$10^4$ $km^2$ | Several days to yearly | 10–20 | Large areas; high spatial resolution | Time gaps to obtain images; satellite pixels over narrow vegetation may overlay |
| Remote sensing using vegetation indices | $10^1$–$10^4$ $km^2$ | Several days to yearly | 15–40 | Large areas; high spatial resolution | Relations may vary with type of vegetation; Time gaps to obtain images |
| (Microwave) Scintillometer | $10^1$–$10^4$ $km^2$ | Seconds to yearly | 10–35[c] | Capture H (and $ET_a$) directly over large areas; stable footprints | Expensive; advection effect |
| Soil water balance | Several $m^2$ to $10^4$ $km^2$ | 3–15 days to yearly | 10–30 | Cheap and simple; wide spatial range | Cannot obtain reliable short-term $ET_a$; requiring accurate determining each water balance component |

*Note.* Remote sensing energy balance, remote sensing using vegetation indices, and (microwave) scintillometer methods measuring $ET_a$ over 10 $km^2$ are rarely reported to investigate cropland $ET_a$ in response to varying factors. Surface renewal is a micrometeorological method that requires high frequency (10 Hz) sampling of air temperature or water vapor and its description as well as advantages and disadvantages can be found elsewhere (Y. Hu et al., 2018; Paw U et al., 1995). The method seeks to estimate turbulent fluxes from ramp-like patterns in air temperature and water vapor. Because ramps also explain much of the temperature variance over a 30-min duration, flux-variance methods can also be used to supplement or even calibrate surface renewal methods (Fischer et al., 2023). [a]The data were from R. G. Allen et al. (2011a). [b]The fetch requirement generally 50–100 times the height of the instrument above the zero plane displacement. [c]The value is for scintillometer.

measurement methods used to investigate plot and field scale crop $ET_a$ in response to varying factors is offered. Remote sensing energy balance, remote sensing with vegetation indices, and (microwave) scintillometer methods measuring regional $ET_a$ (>10 $km^2$) are not covered.

### 2.1. Soil Water Balance Method

For plot–scale experiments, the soil water balance method uses the changes in soil moisture (Equation 8) within the rooting zone to determine crop $ET_a$. This method is deemed reasonable on time scales of 3–15 days (R. G. Allen et al., 1998; Qiu et al., 2015a). The key is to determine soil water content, which can be measured by oven–drying method (cheapest). However, for periodical or continuous soil moisture measurements, neutron-probes, time domain reflectometry, time domain transmission, and capacitance–based probes and sensors (Figure 4) have been used (R. G. Allen et al., 2011a). In arid and semi–arid regions, the hydrological components CR, $D$, and $R$ for determining plot–scale crop $ET_a$ on 3–15 days can be ignored. Uncertainty in CR, $D$, and $R$ remains high for the soil water balance method in sub–humid and humid regions where there is frequently heavy rain or shallow groundwater.

The soil water balance is common to determine cropland $ET_a$ under conditions involving water stress (J. L. Chen et al., 2014; Göksoy et al., 2004; Kang, Zhang, Liang, et al., 2002; Karam et al., 2003), salinity stress (Tripler et al., 2011), varying irrigation methods (B. Li et al., 2020, 2021; Patra et al., 2023; T. Zhang et al., 2021), various planting densities (Eberbach & Pala, 2005; Jiang et al., 2014; Sandhu & Irmak, 2019; Y. Zhang et al., 2019), mulching schemes (N. Chen et al., 2021; Fan et al., 2017; J. Wang et al., 2018; Xie et al., 2005), and N application (S. Lenka et al., 2009; Zhong & Shangguan, 2014).

### 2.2. Weighting Lysimeter

If well managed, weighting lysimeters (Figure 4) provide accurate short–term $ET_a$ by weighing the entire unit to determine changes in the mass of the lysimeters even on a 30-min basis (Katul & Parlange, 1992). Hence, this method can be used as a baseline for developing, calibrating, and validating other $ET_a$ methods (R. G. Allen et al., 2011a; Ding et al., 2010). The individual weighting lysimeter (a point measurement) can measure crop $ET_a$ with surface areas from 0.2 to 40 $m^2$. The same vegetation cover grown in the lysimeters must also be planted surrounding the weighting lysimeters to ensure the lysimeter is not experiencing distorted micro–climatic conditions. The precision of measurements by weighting lysimeters ranges from 0.02 to 0.6 mm (R. G. Allen et al., 2011a; Ding et al., 2010; C. Liu et al., 2002). Since large–scale weighting lysimeters are expensive, there are only few studies comparing $ET_a$ under water stress condition (Gong et al., 2020; M. Liu, Shi, et al., 2022), different cropping systems (Y. Yang, Yang, et al., 2023), and different irrigation methods (Flumignan et al., 2011).

Another design employs the so-called "floating drag plate lysimeter" whereby turbulent stresses and $ET_a$ are simultaneously measured (Pruitt et al., 1973). This method, when combined with mean water vapor concentration profiles, proved effective in determining the so-called stability correction functions for water vapor within the context of Monin-Obukhov similarity theory (Monin & Obukhov, 1954) even before the weighty Kansas and Minnesota experiments (Kaimal & Wyngaard, 1990) that form the basis of numerous micrometeorology textbooks. A comparison between $ET_a$ measured by the floating and weighing lysimeters suggest that both approaches can be used on short time scales (<30 min) as presented elsewhere (Katul & Parlange, 1992).

### 2.3. Sap Flow Method

Measuring sap flow from temperature changes is appealing as the advection of heat is primarily conducted by liquid water movement in plants. This method was originally proposed for trees in the early to mid–1970s (Čermák et al., 1973, 1976)—and in some literature—it is referred to as the Granier sap–flow method (Granier, 1987; Phillips et al., 1996). Several reviews about its utility and limitations have already been presented (Grime et al., 1995; Kjelgaard et al., 1997; Köstner et al., 1998; Smith & Allen, 1996). The method can directly measure short–term $T_r$ by inserting a low–grade heat source into the plant stem and measuring the water flow in the xylem through either the velocity of a heat pulse or the dissipation of heat energy in the stem (R. G. Allen et al., 2011a). The heat pulse, heat dissipation, and heat balance methods are the three main methods used today. The heat pulse and heat dissipation methods are suitable for measuring $T_r$ in orchards and forests (Oren, Phillips, et al., 1999), and the heat balance method can be used to determine $T_r$ in trees with trunk diameter <165 mm and

various crops, such as maize, pepper, tomato, cotton, soybean, rice, and sugarcane (Qiu et al., 2015a; Y. Q. Zhang et al., 2011). The heat balance system, Flow 32–1K system (Figure 4) with micro flow, stem flow, and trunk gages (Dynamax inc., Houston, USA), is commonly adopted to measure $T_r$ in stems with diameters varying from 2 to 165 mm. When applying the Flow 32–1K system, weather shields are required to avoid variable radiation load that distort the thermal flow regime. Hence, this system can only measure the short–term $T_r$ of some crops for growing stages when they meet the installation requirement of the sensors.

Since the sap flow method only measures $T_r$ from individual branches or plants, scaling up to stand level $T_r$ is required, which introduces errors. Leaf area, cross–sectional area, or planting density are the common factors used to scale up $T_r$ (Jiang et al., 2016; C. W. Liu et al., 2012; Y. Wang et al., 2021; Y. Q. Zhang et al., 2011) and have received significant attention in forests (Ewers & Oren, 2000; Oren et al., 1998). In addition, the sap flow method is commonly incorporated with micro lysimeters (determining daily $E_s$) to determine daily $ET_a$ (Jiang et al., 2016; Y. Q. Zhang et al., 2011). The sap flow method coupled with other $ET_a$ measurements methods such as Bowen–ratio energy balance and eddy covariance methods can be also used to partition $ET_a$ into $T_r$ and $E_s$ (Jiang et al., 2016; Rafi et al., 2019; Williams et al., 2004) provided the variability in the footprint is accommodated (Oishi et al., 2008, 2010).

The sap flow method has been used to compare $T_r$ under various conditions, such as water stress (Cammalleri et al., 2013; Y. Feng, Cui, et al., 2017; Nguyen et al., 2022; Rousseaux et al., 2009), nitrogen stress (Qiu et al., 2015b), contrasting groundwater table depth (X. Wang et al., 2020), female and male parents of maize for seed production (Jiang et al., 2016), varying irrigation methods (S. Qin et al., 2019), and mulching practices (Y. Zhang et al., 2018).

### 2.4. Residual in the Energy Balance Method

Residual in the energy balance method (Equation 7) has been commonly reported to determine crop $ET_a$ in plot experiments due to the small flux fetch available. These small fetch studies cover experiments conducted under e[$CO_2$] and e[$O_3$] in the Free–Air Concentration Enrichment (FACE) system (Bernacchi et al., 2011; Hussain et al., 2013; Kimball et al., 1994, 1999; Triggs et al., 2004; Vanloocke et al., 2012; Yoshimoto et al., 2005). In this method, the $R_n$ and $G_0$ can be directly measured, and the $H$ can be calculated based on bulk heat transport equations as

$$H = \rho_a C_p \frac{T_c - T_a}{r_a}, \tag{9}$$

where $\rho_a$ is the mean air density (kg m$^{-3}$), $C_p$ is the heat capacity of dry air at constant pressure (J kg$^{-1}$ °C$^{-1}$), $T_c$ and $T_a$ are the surface and air temperatures (°C), and $r_a$ is the aerodynamic resistance (s m$^{-1}$) linked to the eddy diffusivity for heat $K_{t,h}$ using $r_a = \int_{z_s}^{z_r} \frac{dz}{K_{t,h}(z)}$, where $z_s$ is related to the heat roughness length above the zero plane displacement $d_o$ of the crop (m) and $z_r$ is the measurement height associated with $T_a$ (m). In a neutrally stratified atmospheric surface layer, $K_{t,h} = \kappa (z - d_o) u_*$, where $\kappa = 0.4$ is the von Karman constant, $z$ is the vertical distance from the ground (m), and $u_*$ (m s$^{-1}$) is the friction velocity that can be linked to the mean velocity at $z_r$ using the log–law or the law–of–the wall (Brutsaert, 1982). The $T_c$, a key variable for this method, is commonly measured by infrared radiometers, which require calibration before each growing season (Triggs et al., 2004).

### 2.5. Bowen–Ratio Energy Balance (BREB) and Eddy Covariance (EC) Methods

While the Bowen ratio energy balance (BREB) method (Figure 4) was initially derived and used for lake evaporation studies (Bowen, 1926; Lewis, 1995), it has proliferated in the crop–water requirement communities along with the eddy–covariance (EC) method (Figure 4) introduced some 20 years after the BREB (Barrett & Suomi, 1949; Montgomery, 1948; Swinbank, 1951). In the BREB method,

$$\lambda ET_a = \frac{R_n - G}{1 + \beta_o}, \tag{10}$$

where $\beta_o = \frac{H}{\lambda ET_a} \neq -1$ is the Bowen ratio determined from mean air temperature and mean water vapor concentration measurements at two heights above the canopy assuming the eddy diffusivity for heat is identical to the

eddy diffusivity for water vapor. The mean here reflects averaging intervals over 0.5 hr or some appropriate time scale separating turbulence from meso–scale motion. Typical values for the Bowen ratio across a gradient in aridity are $\beta_o > 3$ over semiarid regions, $\beta_o \sim 0.5$ over grasslands and forests, $\beta_o \sim 0.2$ over irrigated orchards or grass, $\beta_o \sim 0.1$ over large open water bodies. A $\beta_o < 0$ is commonly associated with advection of hot and dry air into the study area so that $\lambda \mathrm{ET_a}$ can exceed the available energy provided by $R_n - G_0$ (Katul & Parlange, 1992).

The EC system estimates

$$\lambda \mathrm{ET_a} = \lambda \overline{w'q'}, \tag{11}$$

where $w'$ and $q'$ are the vertical velocity and water vapor concentration fluctuation, and overline is time averaging (typically over 0.5 hr as in the BREB). The EC system requires sensors that can detect at very high frequency (usually 10 Hz) the turbulent contributions of vertical velocity and water vapor concentration to the covariance $\overline{w'q'}$.

The key assumption to interpreting the BREB and EC measured $\lambda \mathrm{ET_a}$ is that the flow over the study area must be stationary (i.e., a flow whose statistics are steady), planar homogeneous (i.e., a flow whose statistics do not vary appreciably in the plane paralleling the ground), high Reynolds number (i.e., a flow where turbulent transport is far more efficient than molecular transport), and lacking any subsidence (i.e., the mean vertical velocity is negligible). These conditions require that the air flow attains a certain equilibrium with the underlying surface and the adjustment distance as the flow encounters the target area is small compared to the overall study area. For these reasons, BREB and EC systems measure uniform crop $\mathrm{ET_a}$ in fields with uniform planar areas from hundreds of $m^2$ to several $km^2$, depending on the height of the upper sensors for temperature and humidity in the BREB system or the $CO_2/H_2O$ measurement sensors in the EC system (Allen et al., 2011a). Another challenge is the positioning of sensors too close to the canopy top for the BREB. Because the upper sensors are restricted by footprint considerations and gradient measurements require large signal–to–instrument noise ratio, these requirements may necessitate the placement of lower–level sensors near the canopy top. This placement is problematic because the assumption that heat and water vapor eddy diffusivities are the same breaks down (i.e., $K_{t,h} \neq K_{t,q}$ the water vapor eddy diffusivity) in the canopy roughness sublayer (Garratt & Hicks, 1973; Harman & Finnigan, 2008; Zahn et al., 2016).

The BREB (D. Yang et al., 2020, 2023) and EC systems (S. Qin et al., 2016; S. Qin, Fan, et al., 2023; Y. Wang et al., 2020) have been used extensively to explore how irrigation methods impact $\mathrm{ET_a}$ over maize and wheat fields. Other studies (Reavis et al., 2021) used two EC systems to compare rice $\mathrm{ET_a}$ under alternate wetting and drying and delayed flood irrigation regimes. Measurement of $\mathrm{ET_a}$ over both flooded and aerobic rice fields (1 km apart) was also carried out by using only one portable EC system rotated from one site to another every week (Alberto et al., 2011). These studies provide a comparison of field–scale $\mathrm{ET_a}$ under different irrigation management conditions. However, the high cost of BREB and EC systems and the large fetch requirement restricts their replication.

To overcome the limited fetch requirement, one method that is gaining some traction is the so-called surface renewal method (Paw U et al., 1995). In this method, high frequency (usually 10 Hz) time series of air temperature is used accompanied by a ramp detection scheme (Fischer et al., 2023). Because ramp-like patterns are responsible for much of the heat flux-bearing events, especially in the roughness sublayer just above the canopy, estimating the mean ramp slope enables the determination of the heat source over some averaging interval (30 min or so). Upon integrating the heat source with respect to height (or eddy penetration depth) yields the sensible heat flux. This estimate may then be used in conjunction with the surface energy balance to compute $\mathrm{ET_a}$. Some success using this method was reported in many agricultural crops as well as screenhouses, where fetch was quite restricted (Rosa et al., 2013). Comparisons between this method and a simpler flux-variance method based on similarity theory (Albertson et al., 1995; Tillman, 1972) seem to indicate that both methods can reproduce sensible heat flux reasonably. This agreement is partly due to the fact that the flux-bearing ramps also contribute most to the overall variance of air temperature (Katul et al., 1996). Both methods also do not require any measurements of velocity statistics, only high frequency temperature.

## 3. Primary Factors Affecting Cropland $ET_a$

Cropland $ET_a$ is affected by the meteorological conditions (radiation, $T_a$, RH, and wind speed), changing environments (e.g., e[$CO_2$], e[$O_3$], global warming), various abiotic stresses (e.g., water, salinity, heat stresses, waterlogging), management practices (e.g., planting density, mulching, irrigation method, fertilizers application, control of diseases and pests, soil management), underlaying surface (e.g., geography, soil types), and crop–specific factors (e.g., crop type, variety, and development stages) as discussed elsewhere (R. G. Allen et al., 1998). The effect of meteorological conditions on $ET_a$ can be surrogated to a reference evapotranspiration (R. G. Allen et al., 1998), where soil type and hydroclimatic conditions for the reference crop resemble those of the target crop. By using the same reference crop across different regions allows for a systematic comparison of how soil type and hydroclimatic conditions as well as changing environmental conditions impact reference evapotranspiration much the same way pan evaporation was used to guestimate potential evaporation across different climatic conditions. Here, the focus is mainly on reviewing the impacts of key changing environments (e[$CO_2$], e[$O_3$], and global warming), abiotic stresses (water, salinity, and heat), and management practices (planting density, mulching, irrigation method, and N application) on cropland $ET_a$ (Figure 3), as discussed below. In addition, other reported considerations are also presented or reviewed.

### 3.1. Effects of Changing Environments

#### 3.1.1. e[$CO_2$]

Atmospheric $CO_2$ concentration has been increasing from about 280 ppm in 1750 to 410 ppm in 2019 (IPCC, 2021), and is projected to be about 800 ppm in the 2071–2100 (Y. T. Yang et al., 2019). Although some studies reported unchanged (Kimball et al., 1994; Wei et al., 2022) and positive (Wei et al., 2021) effect of e[$CO_2$] for crop $ET_a$, the majority of studies report a negative effect (reduction of 2%–22%) depending on crop species and levels of e[$CO_2$] (Bernacchi et al., 2006; Hussain et al., 2013; Kang, Zhang, Hu, & Zhang, 2002; Kimball et al., 1999; F. S. Li et al., 2004; Triggs et al., 2004; Yoshimoto et al., 2005) as summarized in Table 3.

This variability of responses of $ET_a$ to e[$CO_2$] is due to the adverse effect of e[$CO_2$] on $g_s$ at the leaf level, but a positive effect on leaf area, root biomass, and other hydroclimatic conditions (Figure 5a). (a) The e[$CO_2$] on $g_s$ is much more studied and a number of reviews have already been offered documenting its magnitude. A meta–analysis showed that e[$CO_2$] reduced $g_s$ by 26%–30% for $C_3$ and $C_4$ crops (Ainsworth & Rogers, 2007). The main mechanism for this reduction is conventionally (Larcher, 2003) attributed to an increase in carbonic acid ($CO_2 + H_2O = H_2CO_3$) within the sap of guard cells because of e[$CO_2$]. Increases in carbonic acid are accompanied by a reduction in pH, which then favors production of starch instead of sucrose as products of $A_n$. Starch is a less efficient outcome for biomass production because enzymes must expend more energy at its conversion to biomass compared to sugars. Hence, from a leaf level perspective, a reduction in $g_s$ due to e[$CO_2$] leads to a reduction in $T_{r-\text{leaf}}$, which in turn, decreases $ET_a$. (b) However, e[$CO_2$] also accelerates the growth and maximum leaf area of crops because of increased $A_n$, which in turn, increases overall $T_r$ despite a reduction of $T_{r-\text{leaf}}$. Moreover, increasing leaf area directly reduces the incident radiation load and aerodynamic conductance at the soil surface thereby reducing $E_s$ (F. S. Li et al., 2004; X. J. Li et al., 2018). (c) The enhanced root growth because of $dB/dt$ also promotes root water uptake for e[$CO_2$]. A number of studies report root biomass increases of 43%, 22%, and 33%, respectively, for spring wheat, maize, and cotton when e[$CO_2$] reached 300 μmol $mol^{-1}$ above ambient (Kang, Zhang, Hu, & Zhang, 2002). (d) Moreover, partial stomatal closure induced by e[$CO_2$] also reduced evaporative cooling, which results in a warmer canopy temperature and lower RH, in turn leading to higher leaf-to-air VPD. This leads to an increased driving force for $ET_a$, hence compensating for the reduction of $g_s$ induced by e[$CO_2$] (Hussain et al., 2013; Triggs et al., 2004; Yoshimoto et al., 2005). For instance, higher canopy temperature under e[$CO_2$] was observed for rice (daily 0.2–1.0°C) (Yoshimoto et al., 2005), maize (midday 0.2–0.7°C; daytime 0.5–0.6°C) (Hussain et al., 2013), sorghum (midday 1.47–1.85°C) (Triggs et al., 2004), and potato canopy (daytime 0.6–0.9°C) (Magliulo et al., 2003) in FACE experiments where crop phenology was not markedly affected by e[$CO_2$] (C. Cai et al., 2016).

The effect of various stresses on $g_s$ can be estimated based on a Jarvis type multiplicative function (Jarvis, 1976; B. Z. Zhang et al., 2008)

$$g_s = g_{s\max} \prod_i f(X_i), \tag{12}$$

**Table 3**
*The Effect of Elevated Atmospheric $CO_2$ Concentration (e[$CO_2$]) on Total Growing–Season Crop Evapotranspiration*

| Facility | Study area | Crop type | Percentage change relative to ambient (%) | e[$CO_2$] (μmol mol$^{-1}$) | Source |
|---|---|---|---|---|---|
| FACE | Braunschweig, Germany | Barley ($C_3$) | −9 | 170 | Burkart et al. (2011) |
| | | Sugar beet ($C_3$) | −18 | 170 | |
| | | Wheat ($C_3$) | −12 | 170 | |
| | Champaign-Urbana, USA | Soybean ($C_3$) | −9 to −16 | 175 | Bernacchi et al. (2006) |
| | Rapolano Terme, Italy | Potato ($C_3$) | −12 | 185 | Magliulo et al. (2003) |
| | Champaign-Urbana, USA | Maize ($C_4$) | −7 to −11 | 200 | Hussain et al. (2013) |
| | Maricop, USA | Wheat ($C_3$) | −7 | 200 | Kimball et al. (1999) |
| | Maricop, USA | Sorghum ($C_4$) | −12 to −14 | 200 | Triggs et al. (2004) |
| | Iwate, Japan | Rice ($C_3$) | −8 | 200 | Yoshimoto et al. (2005) |
| | Maricop, USA | Cotton ($C_3$) | NS | 280 | Kimball et al. (1994) |
| OTC | Bhopal, India | Wheat ($C_3$) | −2 | 150 | N. K. Lenka et al. (2021) |
| Chambers | Yangling, China | Spring wheat ($C_3$) | −17 | 300 | Kang, Zhang, Hu, and Zhang (2002) |
| | | Maize ($C_4$) | −22 | 300 | |
| | | Cotton ($C_3$) | −6 | 300 | |
| | – | Spring wheat ($C_3$) | −4 | 350 | F. S. Li et al. (2004) |
| | – | Soybean ($C_3$) | −9 | 350 | L. H. Allen et al. (2003) |
| Climate–controlled greenhouse | Yangling, China | Barley ($C_3$) | +8 | 400 | Wei et al. (2021, 2022) |
| | | Maize ($C_4$) | NS | 400 | |
| | | Tomato ($C_3$) | NS | 400 | |
| Climatic phytotron | Wuwei, China | Maize ($C_4$) | −13 | 150, 300, and 500 | X. J. Li et al. (2018) |

*Note.* The FACE and OTC stand for Free–Air $CO_2$ Enrichment and Open Top Chambers, respectively. NS, no significant difference.

where $g_{s\ \max}$ is the maximum $g_s$ under optimal conditions (m s$^{-1}$); $X_i$ is a specific restricting variable introducing deviations from optimal conditions such as irradiance, $T_a$, VPD, water and salinity stresses, e[$CO_2$], and e[$O_3$]; $f(X_i)$ is a restricted function of $X_i$ bounded between [0, 1]. The reported forms of $f(CO_2)$ including linear or hyperbolic types are summarized in Table 4, which should be tested before being employed for a specific crop. The Jarvis function considering e[$CO_2$] can then be incorporated into a Penman–Monteith model to estimate the effect of e[$CO_2$] on $ET_a$ (X. J. Li et al., 2019; Pan et al., 2015; Y. T. Yang et al., 2019).

### 3.1.2. e[$O_3$]

Ozone is an air pollutant restricting crop growth and food production (Ainsworth, 2008; Z. Z. Feng & Kobayashi, 2009). Its impact on food security has been studied extensively using climate models (Chameides et al., 1994). The global annual mean surface $O_3$ concentrations ([$O_3$]) in the Northern Hemisphere have increased from 10 to 15 ppb in 1850 to ∼50 ppb at present (Cooper et al., 2014; Z. Z. Feng et al., 2022), and is projected to increase globally by up to 5 ppb in 2100 using the RCP 8.5 scenario (Turnock et al., 2020).

Ozone diffuses into leaves through stomata, and because of its oxidizing power, it damages the ability of the plant to regulate its guard cells. For this reason, patches of stomates exposed to e[$O_3$] lose their ability to close stomates and ultimately experience desiccation at those and hydraulically connected locations to them. Hence, the leaf $g_s$ will decline because the number of "active" stomatal sites declines on a given leaf with time.

There are limited studies on crop (mainly for soybean) $ET_a$ in response to e[$O_3$] and those studies uniformly document the adverse effect of e[$O_3$] on crop $ET_a$. Total growing–season $ET_a$ of soybean has been reported to be reduced by 28% under e[$O_3$] of 60–75 ppb in Open Top Chambers (OTC) experiments (Booker et al., 2004; Bou Jaudé et al., 2008). It was reported to decrease by 11%–13% with e[$O_3$] of 22%–37% above background (46–68 ppb) in the four of five growing seasons for soybean in a FACE experiment (Bernacchi et al., 2011). Total

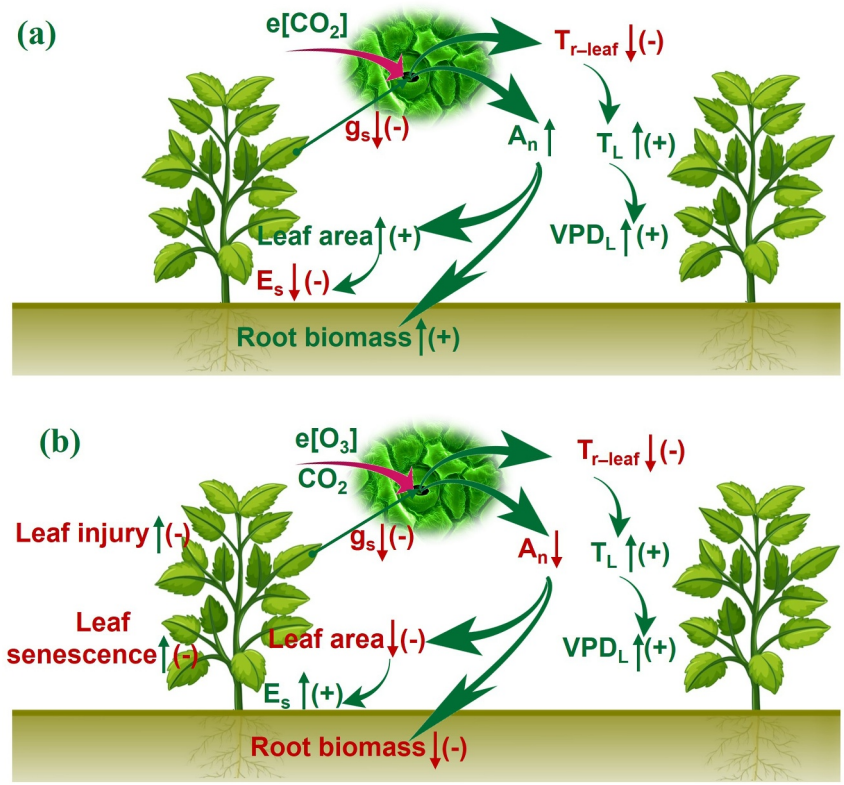


**Figure 5.** The main pathways detailing how elevated $CO_2$ concentration (e[$CO_2$]) (a) and elevated ozone concentration (e[$O_3$]) (b) impact crop evapotranspiration ($ET_a$). The $g_s$ is the leaf stomatal conductance to $H_2O$, $A_n$ is the net photosynthesis, $T_{r-\text{leaf}}$ is the leaf transpiration, $E_s$ is the soil evaporation, $T_L$ is the leaf temperature, $VPD_L$ is the leaf–to–air vapor pressure deficit. (+) and (−) indicate positive and negative effects on crop $ET_a$. Upper and lower arrows show increase and decline.

growing–season $ET_a$ of soybean also linearly decreased as e[$O_3$] increased with the highest [$O_3$] treatment (116 ppb) reducing $ET_a$ by 26% with respect to [$O_3$] of 40 ppb treatment (Vanloocke et al., 2012).

This reduction of $ET_a$ caused by e[$O_3$] may be due to its negative effect on $g_s$, root and leaf development and phenology, despite increasing driving force (Figure 5b). (a) e[$O_3$] lowers $g_s$ thereby reducing $T_{r-\text{leaf}}$. In a meta–analysis, it was shown that $g_s$ was reduced by 23% for rice with mean [$O_3$] of 62 ppb (Ainsworth, 2008), by 22% for wheat when mean [$O_3$] was 79 ppb (Z. Z. Feng et al., 2008), and by 17% for soybean when [$O_3$] was 30–120

**Table 4**
*Summary for Reported Leaf Stomatal Conductance ($g_s$) Functions in Response to Elevated $CO_2$ Concentration ($f(CO_2)$) in the Jarvis Model*

| Functions | Type | Sources |
|---|---|---|
| $f(CO_2) = -0.001CO_2 + 1.35$ | Linear model | Pan et al. (2015) |
| $f(CO_2) = 1 - 0.4(CO_2/330 - 1)$ | Linear model | Easterling et al. (1992); Y. Wu et al. (2012) |
| $f(CO_2) = 1 - (1 - a_3)(CO_2/350 - 1)$ | Linear model | Medlyn et al. (2001) |
| $f(CO_2) = \frac{1}{1+CO_2/C_{so}}$ | Hyperbolic model | J. L. Wang et al. (2005) |
| $f(CO_2) = \frac{1}{1+a_0(CO_2/330-1)}$ | Hyperbolic model | X. J. Li et al. (2019) |
| $f(CO_2) = a_1\frac{1}{1+a_2(CO_2-300)}$ | Hyperbolic model | Y. T. Yang et al. (2019) |

*Note.* The $C_{so}$ is an empirical parameter (=305 μmol mol$^{-1}$ based on pooled data from the literature (X. J. Li et al., 2019)); $a_0$–$a_3$ are empirical parameters.

ppb (Morgan et al., 2003). (b) e[$O_3$] also limit root biomass, which was reduced by 35% for rice, 27% for wheat, and 21% for soybean (Z. Z. Feng et al., 2008; Morgan et al., 2003; Shang et al., 2022), limiting the ability of roots to uptake water. (c) The $O_3$ exposure can induce visible leaf injury (Vandermeiren et al., 2005), which can be up to >80% reduction in green leaf area for wheat and soybean (Booker, 2004; Z. Z. Feng et al., 2008; Morgan et al., 2003). (d) The reduced leaf area, especially green leaf, under e[$O_3$] may be another explanation, which will enhance reductions in $T_r$, although some crops such as wheat were not significantly affected. Leaf area was reported to be 8% lower under e[$O_3$] in rice (Ainsworth, 2008). Likewise, e[$O_3$] reduced the total leaf area of soybean by ~10%, the number of leaves per plant by 5%, and especially the green leaf area by 32% (Morgan et al., 2003). (e) e[$O_3$] accelerates leaf senescence (Morgan et al., 2006) and shortened the growth period. Some studies reported a growth period that is 4% shorten for wheat (Z. Z. Feng et al., 2008) in e[$O_3$], leading to a low total growing–season $ET_a$. (f) Exposure to e[$O_3$] also resulted in warmer canopies and lower humidity and therefore higher VPD, which may partially offset the reduced $ET_a$ induced by e[$O_3$]. FACE experiments showed that midday values of canopy temperature were more than 2°C warmer for the highest [$O_3$] treatment (116 ppb) than the lowest (40 ppb) (Vanloocke et al., 2012).

The $g_s$ in response to e[$O_3$] has been quantified using a modified Jarvis model as in Equation 12. This approach remains the workhorse formulation for determining the stomatal $O_3$ flux at present (Azuchi et al., 2014; Mills et al., 2011; Shang et al., 2021) and is written as

$$g_s = g_{s\,\max} \times \min(f(\text{phen}),\, f(\text{O}_3)) \times f(R_s) \times \max\{g_{s\,\min},\ (f(T_a) \times f(\text{VPD}) \times f(\theta))\}, \tag{13}$$

where $g_{s\min}$ is the minimum $g_s$; $f$(phen), $f(R_s)$, $f(T_a)$, $f$(VPD), $f(\theta)$, and $f(O_3)$ represent the restricted functions of $g_s$ in $g_{s\,\max}$ that are related to the effects of phenology, irradiance, $T_a$, VPD, soil water potential, plant water potential, or available soil water content, and [$O_3$], respectively. As before, all these functions are bounded between [0, 1]. These response functions can be generally parameterized based on a boundary line analysis (Y. S. Xu et al., 2021). Further details on $f$(phen), $f(R_s)$, $f(T_a)$, and $f$(VPD) calculations are provided elsewhere (E. Z. Hu et al., 2015). This response of $g_s$ to e[$O_3$] may be used for estimating $ET_a$ under e[$O_3$] in a Penman–Monteith model but is rarely investigated until recently.

### 3.1.3. Global Warming

Compared to 1850–1900, global surface temperature has increased by 0.95–1.20°C in 2011–2020, and is projected to be even higher by 1.0–5.7°C in 2081–2100 (IPCC, 2021). Furthermore, greater increment in daily minimum temperature than maximum was noted over the last 50 years (Peng et al., 2013). These varying types of warming should have variable effect on crop $ET_a$. The daily $ET_a$ in response to warming is affected by canopy coverage. With increase in $T_a$, daily $ET_a$ almost always increases linearly under low canopy coverage ($E_s$ dominant), while it increases rapidly at high canopy coverage ($T_r$ dominant) until $T_a$ reaches a critical value (related to optimal plant growth $T_a$), followed by gradually decreases (Qiu et al., 2021). The dynamics of canopy coverage or LAI are closely related to accumulated thermal time and is altered by warming. The development of canopy coverage is projected to be slower, faster, or experiencing small variations under varying types of warming compared to ambient conditions depending on ambient total growing–season average $T_a$ and its deviation (Qiu et al., 2021). A FACE experiment also observed that LAI of rice under +2.0°C all–day warming was reduced by 10%–24% for four growing stages in a warm season. However, this warming did not have marked effect in a cool season (C. Cai et al., 2016).

Total growing–season $ET_a$ in response to global warming is largely affected by variations in phenology and ambient growing–season average $T_a$. Growing season of rice have been observed to be shortened by 1–5 days for all–day warming of 1.4–2.1°C (C. Cai et al., 2016; Dong et al., 2011; W. L. Wang et al., 2018), 0–3 days for day–time warming by 1.1°C and night–time warming by 0.5–1.8°C (J. Chen et al., 2017; Dong et al., 2011). In addition, it is projected to be shortened by 0–23 days for varying types of warming (i.e., all–day, day–time, night–time, and asymmetric warming) by 1.0–3.0°C for cool season, while prolonged by 0–4 days for warm seasons (Qiu et al., 2021). Furthermore, the growth duration is closely related with growing season averaged $T_a$. An increment of 1°C for growing–season average $T_a$ leads to a shortened growth duration of 4–5 days (P. L. Lu et al., 2008). A negative relation was also found between the growth duration and growing–season average $T_a$ (T. Y. Zhang

et al., 2013), and greater warming level resulted in higher temperature sensitivity to changed growth season (Qiu et al., 2021).

Combined with warming induced variations in growth duration and direct effects on $ET_a$, inconsistent responses of total growing–season $ET_a$ are reported across studies. The changes in total growing–season $ET_a$ of rice were projected to be within the range of −18.2%–5.6% for all–day warming by 1∼3°C using crop models (Asseng et al., 2004; Tao et al., 2008), and −60.1 to 16.5, −29.7 to 11.6, −40.2 to 5.3, and −50.6 to 10.8 mm, respectively, for all–day, day–time, night–time, and asymmetric warming by 1∼3°C using a modified Priestley–Taylor model (Qiu et al., 2021). In addition, with the increase in ambient growing–season average $T_a$, the total growing–season $ET_a$ of rice increased linearly (for night–time warming) or parabolically (for all–day, day–time, and asymmetric warming) under a preset level of warming, whereas it decreased linearly or parabolically when not considering changes in phenology (Qiu et al., 2021). The total growing–season $ET_a$ of wheat was also projected to increase by 18 mm under all–day warming of 3°C, whereas it is reduced if considering a 13 days shorter growing duration (Asseng et al., 2004). These results suggest that phenology plays a leading role in assessing the effects of warming on total growing–season $ET_a$.

The effect of warming on $ET_a$ at large scales was generally assessed using crop models (Asseng et al., 2004; Kim et al., 2013; Tao et al., 2008). However, these models are running on daily time–scales and can only interrogate the effect of all–day warming on $ET_a$. A dynamic Priestley–Taylor model that can estimate the effect of all–day, daytime, nighttime, and asymmetric warming on crop $ET_a$ have been proposed recently (Qiu et al., 2021). This revised Priestley–Taylor model introduces a plant temperature constraint on $T_r$, adopts a function based on canopy coverage instead of LAI to partition the absorbed energy between the canopy and water (or soil) surface, and employs Wang–Engel curvilinear temperature response function to calculate accumulated thermal time, which affects phenology and subsequent development of canopy coverage. During global warming (such as +1.5°C and +2°C warmer) experiments, the likelihood of crops (especially rice) experiencing heat stress may increase. Whether this revised Priestley–Taylor model adopting such simplified temperature response function to assess crop $ET_a$ under combined warming and heat stress still requires further investigation.

### 3.2. Effects of Abiotic Stresses

#### 3.2.1. Water Stress

Water (or drought) stress is one of the main limitations affecting $ET_a$ and crop production. Future warming will cause more frequent and intense water (or drought) stress events. Across arid and semi–arid regions, the frequency of an agricultural and ecological drought event that occurred once in 10 years on average will likely occur 2.4 times in 10 years for a future with a +2.0°C warming level (compared to 1850–1900). The increase in intensity of +0.6sd (sd: standard deviation) dryer is also projected to occur (IPCC, 2021). Even in humid regions, seasonal droughts are occasionally occurring as documented by the intense summer droughts in the middle and lower reaches of Changjiang River of China in 1978, 2001, 2011, and 2022 (Y. Liu et al., 2023; Z. Song et al., 2020).

Water stress generally results in lower total growing–season $ET_a$. For instance, deficit irrigation (56% of full irrigation each time) had 17%–23% lower total growing–season $ET_a$ for greenhouse–grown tomato than full irrigation as measured from weighing lysimeters (Gong et al., 2020). Total growing–season $ET_a$ of maize was also reduced by 33% under water stress (60% of full irrigation each time) compared to full irrigation (Karam et al., 2003).

Generally, severe water stress and its occurrence at key growing period leads to substantial reduction of total growing–season $ET_a$. For instance, lower total growing–season $ET_a$ for greenhouse–grown pepper induced by water stress have been reported at early fruit bearing and harvesting stage (27% and 12%, respectively, for receiving 1/3 and 2/3 irrigation amount of full irrigation) than at flowering and fruit setting stage (9% and 5%, respectively). Similar reductions were reported at the late fruit bearing and harvesting stages (19% and 7%, respectively) in the 2009–2010 season (H. Yang et al., 2016). Some studies (Karam et al., 2007) showed that water stress reduced more total growing–season $ET_a$ of sunflower at early and middle flowering stages (22% and 16% respectively) than at early seed formation stage (9%). Total growing–season $ET_a$ of greenhouse–grown tomato had greater reduction under water stress at fruit ripening stage (25% and 14%, respectively, for receiving 1/3 and 2/3 irrigation amount of full irrigation) than at flowering and fruit development stage (16% and 4%, respectively) (J. L. Chen et al., 2014).

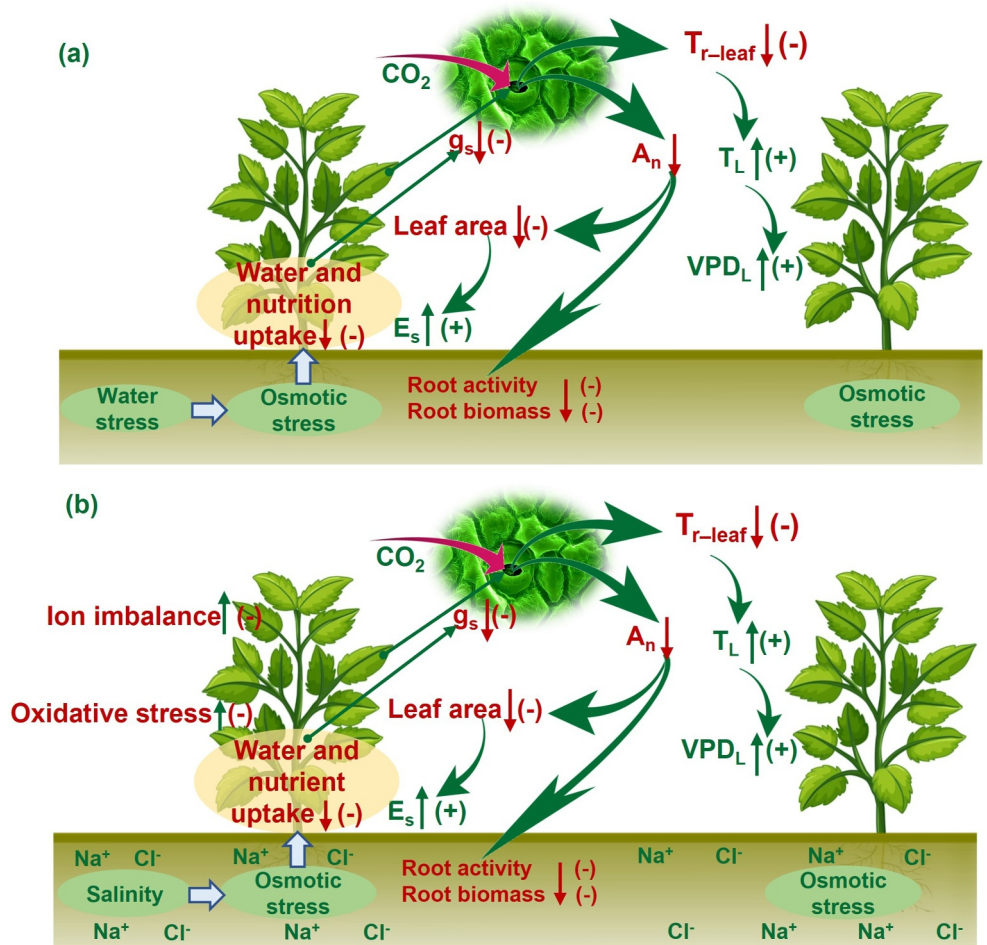


**Figure 6.** The main pathways of water (a) and salinity (b) stresses on crop evapotranspiration ($ET_a$). The $g_s$ is the leaf stomatal conductance to $H_2O$, $A_n$ is the net photosynthesis, $T_{r\text{–leaf}}$ is the leaf transpiration, $E_s$ is the soil evaporation, $T_L$ is the leaf temperature, $VPD_L$ is the leaf–to–air vapor pressure deficit. (+) and (−) indicate positive and negative effects on crop evapotranspiration. Upper and lower arrows show increasement and decline.

The response of $ET_a$ to water stress has been studied through its adverse effects on root water uptake, $g_s$, xylem hydraulic conductivity, leaf area, root growth, despite increasing VPD (Figure 6a). (a) When suffering from water stress, the plant is experiencing a soil water potential that is low. Hence, to pull water from drying soils all the way up to the leaf, the plant has to perform more work by lowering further its leaf water potential. There are three main "bottlenecks" when leaf water potential is low (Manzoni et al., 2013): The first is in the rhizosphere—where the main restriction to water flow is due to reduced soil–root conductivity (Manoli et al., 2014; Siqueira et al., 2008). The second restriction is associated with loss of xylem hydraulic conductance. Water under tension is in a metastable state and is prone to embolism (bubble formation) and subsequent cavitation spread (air spreading within the xylem network). Once enough conduits are filled with air, the overall xylem hydraulic conductance is reduced and the ability of the plant to deliver water to the leaf is impaired (J. Liu et al., 2020; Mrad et al., 2018). Last, low leaf water potential can also lead to direct reductions in $g_s$ (Damour et al., 2010; Manzoni et al., 2011; X. Song et al., 2020), and further amplify non–stomatal limitations such as loss of mesophyll conductance (Dewar et al., 2018; Qiu & Katul, 2020), or phloem failure (Jensen et al., 2016; Konrad et al., 2019; Nakad et al., 2022). These non-stomatal limitations have been recently modeled to explain differing functional traits using a multi-scale optimality framework where both short-term limitations and long-term effects of those limitations are coupled (Matthews et al., 2024). The leaf water potential has been reported to decrease from −1.1 MPa in sufficient irrigation areas to −1.6 MPa in severe water deficit (1/3 of sufficient irrigation) (Tezara et al., 2002).

Stem–specific hydraulic conductivity under varying water stress levels was reported to be reduced ranging from 14% (75%–55% field water capacity) to 30% (65%–45% field water capacity) (J. Liu et al., 2020). The $g_s$ of sunflower decreased from 0.8 mmol $m^{-2}$ $s^{-1}$ in full irrigation to 0.1 mmol $m^{-2}$ $s^{-1}$ in mild water deficit and to 0.05 mmol $m^{-2}$ $s^{-1}$ to severe water deficit (Tezara et al., 2002). The mild and severe water deficit also had 57% and 86% lower middle–day $g_s$ of maize than full irrigation (Kang, Zhang, Hu, & Zhang, 2002). (b) Long–term water stress also restricts leaf expansion and tillering, forms small and succulent leaves, thereby reduces leaf area, which then reduces the canopy transpiration (Farooq et al., 2009), but may increase $E_s$ rates just after irrigation. The maximum LAI have been reported to be 7%–29% lower in aerobic rice fields than flooded fields (Alberto et al., 2011), 17%–29% lower for greenhouse–grown tomato under mid water deficit than full irrigation (Gong et al., 2020), 25% lower for maize under water deficit (60% of full irrigation) than control (Karam et al., 2003). (c) Root activity and growth are also affected by long–term water stress further limiting root water uptake. A meta–analysis showed that although water stress increased root hair density and root hair length by 49.4% and 35.8%, it reduced root dry weight and root length by 21.9% and 19.8% (Kou et al., 2022). (d) Similar to the effect of e[$O_3$], water stress leads to warmer canopies and higher VPD, partially offsetting the decreased $ET_a$ induced by water stress. The average $T_a$ increased by 0.2°C while average RH was 3.1% lower, resulting in 0.12 kPa greater VPD over the entire growing season of aerobic rice fields compared to flooded ones (Alberto et al., 2009).

The effect of water stress on $g_s$ can also be described by a modified Jarvis model by introducing a function for water stress $f(\theta)$ in Equation 12, as

For paddy rice (J. Z. Xu et al., 2017)

$$f(\theta) = (\theta - \theta_W)/(\theta_S - \theta_W), \tag{14a}$$

For other crops (B. Z. Zhang et al., 2008)

$$f(\theta) = (\theta - \theta_W)/(\theta_F - \theta_W), \tag{14b}$$

where $\theta$ is the actual root-zone soil moisture content ($cm^3$ $cm^{-3}$); $\theta_S$ and $\theta_F$ are the saturated soil water content and field water capacity ($cm^3$ $cm^{-3}$); and $\theta_w$ is the soil water content at wilting point ($cm^3$ $cm^{-3}$). This modified Jarvis function with water stress can be then incorporated into the Penman–Monteith or Shuttleworth–Wallace models to estimate the effect of water stress on crop $ET_a$ such as for rice (J. Z. Xu et al., 2017), maize (S. Li et al., 2013; X. J. Li et al., 2019), tomato (Ortega-Farias et al., 2006), soybean (Ortega-Farias et al., 2004), and wheat (D. Yang et al., 2020).

The effect of water stress on crop $ET_a$ can also be quantified by the FAO 56 single (Equation 15a) or dual crop coefficient (Equation 15b) methods. These methods incorporate a water stress coefficient ($K_s$) as (R. G. Allen et al., 1998)

$$\mathrm{ET_a} = K_s K_c \mathrm{ET_o}, \tag{15a}$$

$$\mathrm{ET_a} = T_r + E_s = (K_s K_{cb} + K_e)\,\mathrm{ET_o}, \tag{15b}$$

where $K_c$ is the crop coefficient, $K_{cb}$ is the basal crop coefficient, $K_e$ is the evaporation coefficient, and $ET_o$ is the reference evapotranspiration as before. For crops others than rice, $K_s$ can be determined as (R. G. Allen et al., 1998)

$$K_s = \begin{cases} \dfrac{\mathrm{TAW} - D_{r,i}}{\mathrm{TAW} - \mathrm{RAW}} = \dfrac{\mathrm{TAW} - D_{r,i}}{(1-p)\,\mathrm{TAW}} & D_{r,i} > \mathrm{RAW} \\ 1 & D_{r,i} \le \mathrm{RAW} \end{cases}, \tag{16a}$$

where TAW and RAW are the root zone total available and readily available soil water content (mm); $p$ is the fraction of TAW that plants can extract water from the soil before being subjected to water stress. Values of $p$ for varying crops are shown elsewhere (R. G. Allen et al., 1998); $D_{r,i}$ is the water depletion at the end of day $i$ (mm).

The $K_s$ for rice is different as a result of flooding and can be determined based on the relative soil moisture content, $\theta_r$ (=$\theta/\theta_S$) (Lv et al., 2018; J. Z. Xu et al., 2017) and is given as

$$K_s = \begin{cases} 1 & \theta_r \geq \theta_{r1} \\ \ln(1 + 100\theta_r)/\ln(\alpha_1) & \theta_{r2} < \theta_r < \theta_{r1}, \\ \alpha_2 \exp((\theta_r - \theta_{r2})/\theta_{r2}) & \theta_r \leq \theta_{r2} \end{cases} \tag{16b}$$

where $\theta_{r1}$ and $\theta_{r2}$ are the two critical values of $\theta_r$. The $\alpha_1$ and $\alpha_2$ are coefficients that depend on values of $\theta_{r1}$ and $\theta_{r2}$.

### 3.2.2. Salinity Stress

Salinity affects over 800 million ha of land worldwide (Munns, 2005). It is one of main factors inhibiting $ET_a$ and crop production. Irrigation with saline water measured by its electrical conductivity ($EC_{iw}$) immediately inhibits $ET_a$ as a result of osmotic stress, but daily $ET_a$ experiences a linear reduction with increased $EC_{iw}$ after several applications of saline water (Qiu et al., 2017). Salinity reduces plant water flow (Y. Y. Lu & Fricke, 2023) and limits the $ET_a$ during day and night. The nighttime $ET_a$ of hot pepper as well as hourly $ET_a$ during all daytime conditions have been reported to be linearly decreased as $EC_{iw}$ increased at 24, 28 and 66 days after application of saline water (Qiu et al., 2017). Total growing–season $ET_a$ also showed a linear reduction with increasing $EC_{iw}$ when $EC_{iw}$ exceeded a threshold for many crop types, including corn, melon (Shani & Dudley, 2001; Skaggs et al., 2006), bell pepper, sunflower, onion, and tomato (Ben-Gal et al., 2003, 2008; Shani et al., 2007).

The $ET_a$ in response to salinity stress is analogous to water stress (Figure 6b). (a) Salinity decreases soil water availability by decreasing the osmotic potential (Corwin et al., 2007; Katerji et al., 2003), which then leads to lower free energy of water and thus requires extra biological energy for the roots to pull water (S. Chen et al., 2016; Homaee & Schmidhalter, 2008; Homaee et al., 2002; Ramos et al., 2012). (b) The $g_s$ is inhibited by salinity (Assouline et al., 2006; J. Qin et al., 2010; Volpe et al., 2011), and is linearly reduced with increasing $EC_{iw}$ thereby limiting $T_{r-\text{leaf}}$ (Qiu et al., 2017). (c) Salinity has an adverse effect on the leaf growth rate both on short– and long–term, enhancing the reductions in $T_r$ (Assouline et al., 2006; Maggio et al., 2004; Munns, 2002). (d) Root properties, such as root turgor pressure, root density and activity, are restricted by salinity, limiting root water uptake rate and inhibiting $T_r$ (Maggio et al., 2004; Skaggs et al., 2006). (e) Salinity stress causes oxidative stress and excessive $Na^+$ and a reduction in $K^+$ in plant tissues restricting $A_n$ and growth rate of root and leaf, in turn further limiting $T_r$ (Hatamnia et al., 2013; Munns, 2002; Qiu et al., 2018). (f) Similar to water stress, warmer canopy and higher VPD under saline stress may offset the adverse effect of salinity on $ET_a$ by increasing the driving force.

Irrigation with saline water ultimately leads to soil salt accumulation. Therefore, application of extra clean water to leach salts from the root zone is required (Letey & Feng, 2007). High leaching fraction allows excess salt to leach out of the root zone thereby increasing $ET_a$. The total growing–season $ET_a$ of hot pepper has been reported to increase by 5%–9% as a result of lower root zone soil salinity, lower absorbed $Na^+$, and greater LAI in high leaching fractions. However, the leaching fraction does not immediately affect $ET_a$. Daily $ET_a$ experienced a statistically significant reduction after 55 days from when salinity was imposed (Qiu et al., 2017).

A reduction in $ET_a$ due to salinity leads to reductions in yield or biomass, which can be described by a linear response function (Equation 17) (Maas & Hoffman, 1977) or by a sigmoidal logistic response function (Equation 18) (Van Genuchten & Hoffman, 1984), as

$$\frac{ET_a}{ET_m} = \begin{cases} 1 & 0 \leq EC_e \leq EC_{et} \\ 1 - b(EC_e - EC_{et}) & EC_{et} < EC_e < EC_{eo}, \\ 0 & EC_e > EC_{eo} \end{cases} \tag{17}$$

$$\frac{ET_a}{ET_m} = \frac{1}{1 + (EC_e/EC_{e50})^{\alpha}}, \tag{18}$$

**Table 5**
*Summary of Stress Coefficients Due To Osmotic Stress Induced by Salinity and Water Deficit ($K_{EC}$)*

| Equations | Sources |
|---|---|
| $K_{EC} = \frac{TAW - D_{r,i}}{TAW - RAW}\left(1 - \frac{b(EC_e - EC_{et})}{100K_y}\right)$ | R. G. Allen et al. (1998) |
| $K_{EC} = \frac{TAW - D_{r,i}}{TAW - RAW}\left(1 + \frac{(a-1) - b(EC_e - EC_{et})}{K_y}\right)$ | Sepaskhah et al. (2006) |
| $K_{EC} = \frac{TAW_{salt} - D_{r,i}}{TAW_{salt} - RAW_{salt}}\left(1 - \frac{b(EC_e - EC_{et})}{100K_y}\right)$ | Pereira et al. (2007); Rosa et al. (2016); Minhas et al. (2020); M. Liu, Shi, et al. (2022); M. Liu, Paredes, et al. (2022) |
| $K_{EC} = 1 - \frac{b}{100K_y}\left(\frac{C_{rz}\theta_{rz}}{\theta_{rz,s}} - EC_{et}\right)$ | Xiong et al. (2019) |

*Note.* The $EC_e$ is the electrical conductivity of soil saturated paste extract (dS $m^{-1}$), $EC_{et}$ is the threshold $EC_e$ beyond which yield is reduced (dS $m^{-1}$). TAW and RAW are the total and readily available root zone soil water content (mm), $TAW_{salt}$ and $RAW_{salt}$ are the total and readily available root zone soil water content under saline conditions (mm), $D_{r,i}$ is the water depletion in the root zone at the end of day $i$ (mm), $K_y$ is a factor showing the reduction of relative yield due to decline of relative evapotranspiration (−). $b$ is the slope parameter (% m $dS^{-1}$ or m $dS^{-1}$). The values of $K_y$, $EC_{et}$ and $b$ are crop specific, and the latest updated values of these parameters are shown elsewhere (Minhas et al., 2020), $a$ is a coefficient >1 for crops (e.g., sugar beet). The $C_{rz}$ is the average root zone salinity (dS $m^{-1}$), $\theta_{rz}$ and $\theta_{rz,s}$ is the average and saturated root zone soil water content ($cm^3$ $cm^{-3}$).

where $ET_m$ is the maximum $ET_a$, $EC_e$ is the electrical conductivity of soil saturated paste extract (dS $m^{-1}$), $EC_{et}$ is the threshold $EC_e$ beyond that $ET_a$ starts to be reduced (dS $m^{-1}$), $b$ is the slope parameter (m $dS^{-1}$), and $EC_{eo}$ is the critical $EC_e$ beyond which $ET_a = 0$, $EC_{e50}$ shows the $EC_e$ when $ET_a/ET_m = 0.5$, and $\alpha$ is an empirical variable. The common factor used in the above functions is $EC_e$ but it could also be set to $EC_{iw}$ or drainage water salinity (Qiu et al., 2017).

The linear salinity response function for total growing–season $ET_a$ have been reported in young pomegranates and hot pepper (Bhantana & Lazarovitch, 2010; Qiu et al., 2017), and the sigmoidal logistic response function have been successfully applied in hot pepper, date palms and leeks (Kiremit & Arslan, 2016; Qiu et al., 2017; Tripler et al., 2011).

The effect of salinity on crop $ET_a$ can also be estimated by the FAO 56 single (Equation 19a) or dual crop coefficient (Equation 19b) methods by considering a stress coefficient due to osmotic stress induced by salinity and water deficit ($K_{EC}$)

$$ET_a = K_{EC}K_cET_o, \tag{19a}$$

$$ET_a = T_r + E_s = (K_{EC}K_{cb} + K_e)ET_o. \tag{19b}$$

The different versions of $K_{EC}$ are summarized in Table 5. This model has been tested for many crops such as maize, wheat, sweet sorghum, and sugarbeet (M. Liu, Shi, et al., 2022; Pereira et al., 2007; Rosa et al., 2016; Sepaskhah et al., 2006).

### 3.2.3. Heat Stress

Heat stress is defined as the temperatures above the threshold level (usually the normal optimum) lasting for varying duration (several days or weeks) and intensities (Kotak et al., 2007; Z. Q. Yang et al., 2023). Projected warming and climatic variability will cause more frequent and intense heat stress events. Such projections will carry adverse effect on overall crop production (B. Liu et al., 2016). Frequency of extreme temperature event that occurred once in 50 years on average are likely to occur 8.6 times for a future +1.5°C warming level than in 1850–1900, and increase in intensity to +2.0°C (IPCC, 2021).

There are limited studies investigating the effect of heat stress on crop $ET_a$ in open fields because of setup difficulties and other experimental challenges in maintaining controlled heating increments. Hence, the heat stress studies are mainly conducted in phytotrons or artificial climate chambers with potted plants (B. Liu et al., 2016). Recent efforts to experimentally assess heat stress, water stress, and their joint effects on two woody species in

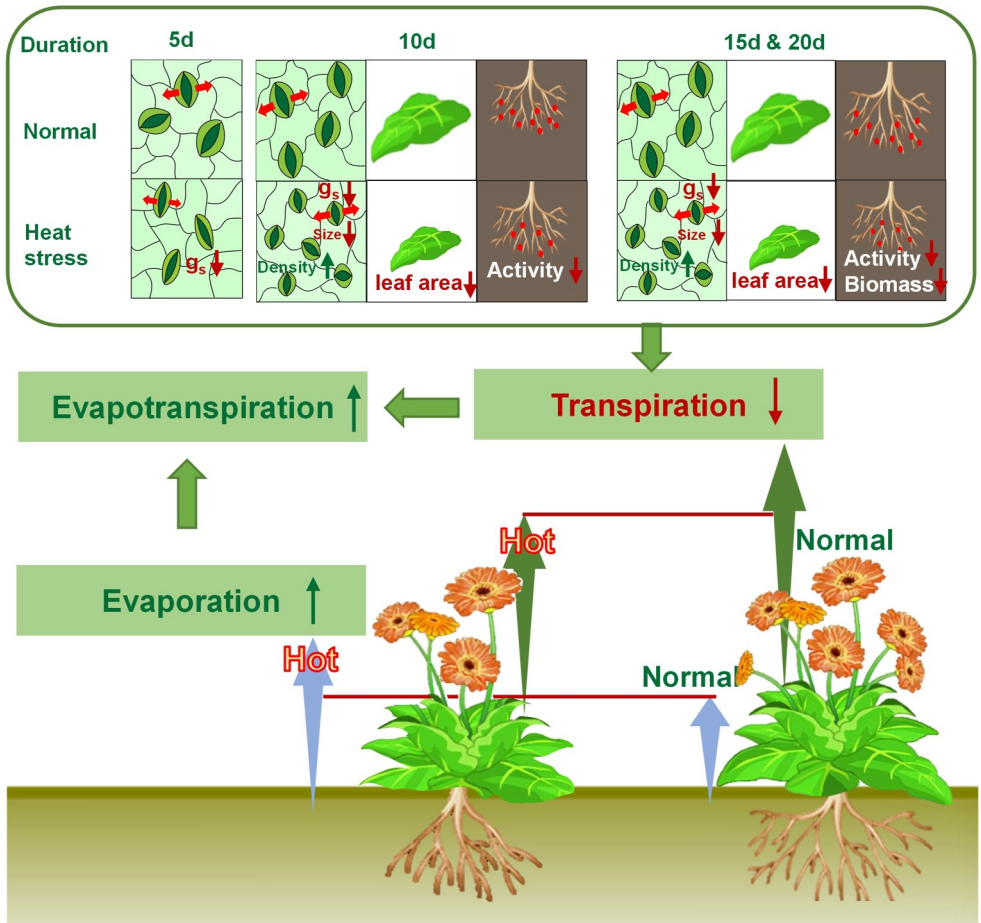


**Figure 7.** Effect of heat stress on evapotranspiration of gerbera during the vegetative growing stage. The $g_s$ is the stomatal conductance. Upper and lower arrows show increasement and decline. The figure was drawn based on the description in Z. Q. Yang et al. (2023).

chambers are underway (Grossiord et al., 2017) with interesting results on plant hydraulic adjustments and stomatal sensitivity to VPD.

The impact of heat stress on $ET_a$ is viewed as a compromise between its effect on reduced $T_r$ and enhanced $E_s$, along with a shortened growth period. Heat stress has adverse effects on $T_r$ and growth, whereas it has a positive effect on $E_s$ due to increased VPD under sufficient watered conditions (Figure 7). Daily $ET_a$ of soybean during the middle season have been shown to increase from 4.7 mm $d^{-1}$ at 28/18°C (day/night temperature) to 11.9 mm $d^{-1}$ at 44/34°C (L. H. Allen et al., 2003). Pot experiments also showed that daily $ET_a$ of gerbera was significantly increased (8.4%–24.5%) due to increased daily $E_s$ (100%–115%) than decreased daily $T_r$ (12.1%–31.8%) during heat stress period (38/28°C), while markedly reduced (11.1%–22.7%) after the end of heat stress (Z. Q. Yang et al., 2023). In addition, longer heat stress durations lead to greater reduction in daily $T_r$. This reduction of daily $T_r$ occurs near noon at the beginning of heat stress and extends to other daylight time as heat stress progresses (Z. Q. Yang et al., 2023). This is because short–term heat stress mainly limits $g_s$ (Green & Weedon, 2012; Tan et al., 2011), affecting the hourly $T_r$ during the period of heat stress. As heat stress progress, stomatal size, leaf area, and root actively start to be suppressed (B. Liu et al., 2017; C. Xu & Huang, 2008; Z. Q. Yang et al., 2023). These suppressions translate to reductions in hourly $T_r$ during other daylight hours. When heat stress is further maintained, root biomass begins to decline (Chavan et al., 2019; Khanna et al., 2017), further limiting water and nutrient access and transport in plants. After 15 days of heat stress during the vegetative growing stage of gerbera, reduction of hourly $T_r$ appeared for the entire daytime period as a result of restricted development of stomata, leaves, and roots (Z. Q. Yang et al., 2023). Additionally, the adverse effect of heat stress on $T_r$ weakened during

the middle and late stages than the early stage. More marked reduction of $T_r$ was observed during vegetative growth stage (19%–32%) than during the flowering bud differentiation stage (12%–20%) (Z. Q. Yang et al., 2023). Heat stress has been shown to accelerate phenology. For instance, the period from anthesis to maturity in rice is linearly decreased as post–anthesis heat degree–days increased (Shi et al., 2015). This leads to a low total growing–season $ET_a$ under heat stress.

Until now, several modeling studies evaluated the effect of heat stress on biomass, yield, and phenology (B. Liu et al., 2016, 2017; Shi et al., 2015; T. Sun et al., 2021). In these models, the effect of heat stress can be quantified by accumulated daily heat degree days (AHDD, °C d), using

$$\mathrm{AHDD}_i = \sum_{j=1}^{i} \mathrm{HDD}_j, \tag{20a}$$

where the $\mathrm{HDD}_j$ (°C) is the accumulation of hourly temperature ($T_i$) over the threshold temperature ($T_h$) on the $j$th day, which can be calculated as

$$\mathrm{HDD}_j = \frac{1}{24}\sum_{i=1}^{24} \mathrm{HD}_i, \tag{20b}$$

$$\mathrm{HD}_i = \begin{cases} 0 & T_i < T_h \\ T_i - T_h & T_i \geq T_h \end{cases}. \tag{20c}$$

While the effect of heat stress on $ET_a$ has been overlooked, this AHDD formulation may be incorporated into $ET_a$ models such as the Penman–Monteith, Priestley–Taylor, or crop coefficient schemes that seek to estimate heat stress effects on $ET_a$. In addition, the modified Priestley–Taylor model adopting temperature response function for estimating warming effect may be adopted for modeling crop $ET_a$ under heat stress (Qiu et al., 2021). These lines of inquiry deserve further investigation given the availability of $ET_a$ measurements and models.

### 3.3. Effects of Management Practices

#### 3.3.1. Planting Density

Appropriate planting density can minimize plant competition thereby increasing crop production and water use efficiency (Ahmadi et al., 2019). Planting density is also one of management factors affecting water consumption (R. G. Allen et al., 1998; R. G. Allen & Pereira, 2009). Although some studies show that planting density have no significant effect on total growing–season $ET_a$ for winter wheat in four of five growing seasons (S. Chen et al., 2010), maize (Jia et al., 2018; F. Zhang et al., 2019), and sunflower (Echarte et al., 2020), the majority of studies indicate that planting density had appreciable effect on total growing–season $ET_a$ for maize (Dai et al., 2022; Gardiol et al., 2003; Jiang et al., 2014; Y. E. Liu et al., 2021; Sandhu & Irmak, 2019; Y. Zhang et al., 2019; J. Zhao et al., 2019), potato (Hou et al., 2020), Quinoa (Ahmadi et al., 2019), sugar beet (Khozaei et al., 2020), winter wheat (Eberbach & Pala, 2005), and bean (de Medeiros et al., 2001). It is to be noted that an analysis of Variance (ANOVA) was not presented in some of these studies to detect significance or lack thereof (Ahmadi et al., 2019; de Medeiros et al., 2001; Eberbach & Pala, 2005; Gardiol et al., 2003; Khozaei et al., 2020; Sandhu & Irmak, 2019).

Increasing planting density have been reported to increase total growing–season $ET_a$ of maize (Dai et al., 2022; Y. E. Liu et al., 2021). In addition, even when total growing–season $ET_a$ increased, total growing–season $ET_a$ per plant decreased (roughly linear) as planting density increased for maize and greenhouse–grown tomato under a range of experimental planting density (Jiang et al., 2014; Qiu et al., 2013; Y. Zhang et al., 2019). However, the highest total growing–season $ET_a$ of crops is not always observed at the highest planting density as a result of intense crop–crop competition for light, water, and nutrients (de Medeiros et al., 2001; Y. Zhang et al., 2019; J. Zhao et al., 2019). To be clear, plant–plant competition is expected to be highest in mono–cultured crops because of lack of separated ecological niches that can utilize varying resources. Such intense competition has been studied and several theories offered that successfully describe the "emergent power–law relation between mean biomass and planting density. Such power–law relations are termed the constant final yield and Yoda's self–

thinning rules, but those theories are reviewed elsewhere (Mrad et al., 2020) and not covered here. It suffices to state that planting density alters water consumption because of areal and sub–areal competition for light and water (Manoli et al., 2017).

The differences in daily $ET_a$ among planting density treatments mainly occurred at the initial and crop development stages for greenhouse–grown tomato and at the crop development and middle stages for maize (Jiang et al., 2014; Qiu et al., 2013). Jia et al. (2018) found that increasing planting density increased daily $ET_a$ during the early growing stages, while it decreased it in the late growing stages.

Some studies reported that differences in crop $ET_a$ result from varying planting density and can be explained by their differences in LAI or canopy coverage. This finding hint that the surface energy partitioning between soil and plants is the primary factor (Jiang et al., 2014). Although high planting density reduces the $R_n$ arriving at the soil surface thereby decreasing $E_s$ rate (S. Chen et al., 2010; Y. E. Liu et al., 2021), it increases the radiation energy intercepted by the crop canopy even before the crop canopy is fully covered (Francescangeli et al., 2006; Papadopoulos & Ormrod, 1988). More radiation load in the crop canopy accelerates soil moisture depletion (Dai et al., 2022; Hou et al., 2020; Y. Zhang et al., 2019) and increases $T_r$ (S. Chen et al., 2010; Eberbach & Pala, 2005; Jiang et al., 2014). However, after LAI reaches a threshold value (usually near fully covered crop canopy), further increases in LAI do not markedly increase the energy intercepted by the canopy. Radiation use efficiency has been found to be no longer increasing when LAI > 3 for cucumber and broccoli (Francescangeli et al., 2006). Therefore, further increases in LAI beyond some threshold will not significantly affect $ET_a$.

Increases in planting density accelerates leaf senescence, especially the lower leaves because of low radiation intercepted by the lower strata leaves (Djaman et al., 2022). This is particularly true for leaf senescence rate of maize (cultivar DK696) described elsewhere (Borrás et al., 2003). This accelerated senescence will lead to a low $T_r$ rate in high planting density during the late stage.

Translating these effects into models is the next step, and the concept of crop coefficients is, once again, a logical starting point. That is, planting density effects on $ET_a$ can be quantified by a density coefficient ($K_d$) in the single or dual crop coefficient models (R. G. Allen & Pereira, 2009; Rosa, Paredes, Rodrigues, Alves, et al., 2012). This $K_d$ is a function of LAI or effective fraction of ground cover ($f_{c\ \mathrm{eff}}$) and crop height ($h_c$), and is given by

$$K_d = \left(1 - \exp^{[-0.7\mathrm{LAI}]}\right), \tag{21a}$$

$$K_d = \min\left(1, M_c f_{c\,eff}, f_{c\ eff}^{1/(1+h_c)}\right), \tag{21b}$$

where $M_c$ is a multiplier of $f_{c\ \mathrm{eff}}$ [1.5, 2.0]. This $K_d$ can then be incorporated into the single or dual crop coefficient methods to estimate crop $ET_a$ as

$$\mathrm{ET_a} = K_s(K_{\mathrm{soil}} + K_d(K_{c\,\mathrm{full}} - K_{\mathrm{soil}}))\,\mathrm{ET_o}, \tag{22a}$$

$$\mathrm{ET_a} = (K_s(K_{c\mathrm{min}} + K_d(K_{cb\mathrm{full}} - K_{c\mathrm{min}})) + K_e)\,\mathrm{ET_o}, \tag{22b}$$

where $K_{\mathrm{soil}}$ is the mean $K_c$ from the exposed soil surface, $K_{c\,\mathrm{full}}$ and $K_{cb\,\mathrm{full}}$ are $K_c$ and $K_{cb}$ when the crop almost fully covers the ground (R. G. Allen & Pereira, 2009).

The above methods have been successfully applied for many crops such as artichoke, beans, broccoli, lettuce, cantaloupe/honeydew, onion, strawberry, tomato, hot pepper, maize, winter wheat, cotton, barley, sunflower, canola, soybean, cucumber, eggplant, watermelon, zucchini, and strawberry (R. G. Allen & Pereira, 2009; Jiang et al., 2014; Pereira et al., 2020, 2021; Qiu et al., 2015a; Rosa, Paredes, Rodrigues, Fernando, et al., 2012; B. Z. Zhang et al., 2013; N. Zhao et al., 2013).

### 3.3.2. Irrigation Methods

Irrigation plays a first–order role in maintaining and increasing grain production worldwide, especially in arid and semi–arid regions. The total irrigated area in China, India, USA, Pakistan, and Iran (top five countries) reached 65.9, 62.0, 23.5, 19.1, and 8.46 million ha, respectively, accounting for 54%, 18%, 37%, 61%, and 61% of total cultivated area of the corresponding country (ICID, 2021). Compared to rain–fed agriculture, irrigated agriculture

**Table 6**
*The Effect of Irrigation Methods on Total Growing–Season Evapotranspiration ($ET_a$) Under Sufficient Water Condition*

| Crop | Reference irrigation | Irrigation method | Percentage change relative to reference (%) | Reference |
|---|---|---|---|---|
| Maize ($C_4$) | Sprinkler | Drip (surface) | −25 | Valentín et al. (2020) |
| | Sprinkler | Drip (subsurface) | −39 | |
| | Border | Furrow | −4 | T. Zhang et al. (2021) |
| | Border | Drip (surface) | −8 | |
| | Center pivot | Furrow | −4 | Mohammed and Irmak (2022) |
| | Center pivot | Drip (subsurface) | −8 | |
| | Border | Drip | −7[a] | Y. Wang et al. (2020) |
| | Flood | Drip | −9 | X. Wang et al. (2018) |
| | Porous capsule | Drip (surface) | −2 | Kanani et al. (2022) |
| | Porous capsule | Drip (subsurface) | −3 | |
| Okra ($C_3$) | Surface | Drip (surface) | −11 to 22 | Patra et al. (2023) |
| Spring wheat ($C_3$) | Border | Drip (surface) | −4 to 6[b] | D. Yang et al. (2020) |
| Tomato ($C_3$)[c] | Furrow | Drip (surface) | −10 to 12 | B. Li et al. (2021) |
| Sugar beet ($C_3$) | Furrow | Drip (surface) | −43 | Sugita et al. (2017) |

[a]The value is the mean based on 5 years experiment measured using two eddy covariance systems. [b]The values are measured using two Bowen–ratio Energy Balance systems. [c]The tomato plants are grown under greenhouse.

yielded 40%–45% of the total food production using only one–fifth of the total cultivated area (Döll & Siebert, 2002). However, conventional irrigation methods such as flooding irrigation are deemed wasteful. With increasing water scarcity, there is increasing competition for water resources between the agricultural sector and other sectors. This will inevitably translate to less water being available to maintain or expand irrigated agriculture in the future. Hence, water saving technologies such as sprinkle and micro irrigation have been widely adopted to save irrigation water and improve water productivity. The total area of sprinkle plus micro irrigation is now 16, 9.0, 5, 5, and 3 million ha, respectively, for the USA, China, India, Brazil, and Spain (top five countries), accounting for 69%,14%, 8%, 77%, and 74% of total irrigated area of the corresponding country (ICID, 2021).

Compared to other traditional irrigation methods, total growing–season $ET_a$ under drip irrigation was reduced by 2%–39% for maize, 11%–22% for okra, 4%–6% for spring wheat, 10%–12% for tomato, and 43% for sugar beet (Table 6). This reduction under drip irrigation was influenced by lower soil wetting area, shortened growing season, less energy partitioning to $\lambda ET_a$, increased VPD, and altered crop characteristics. (a) Drip irrigation has a lower irrigation amount and wetting area, leading to a lower $E_s$ rate than traditional irrigation methods. Compared to border irrigation, drip irrigation decreased total growing–season $E_s$ by an average of 23% for maize under a transparent plastic film mulch (Guo et al., 2022; S. Qin et al., 2016; Y. Wang et al., 2020), and by 4% for spring wheat (D. Yang et al., 2020). (b) The phenology under drip irrigation have been reported to be ahead by 5–23 days for maize under transparent plastic film mulch, and by 7 days for spring wheat relative to border irrigation, which reduced total growing–season $ET_a$ (Guo et al., 2022; D. Yang et al., 2020; Y. Zhao et al., 2021). This shortened phenology induced by drip irrigation also affected total growing–season $T_r$, which was reduced by 1%–14% in four of five seasons of maize and by 5% for spring wheat than border irrigation. However, a larger daily average growing–season $T_r$ rate was also observed for maize and wheat (increased by 7% and 1%, respectively) under drip irrigation (S. Qin et al., 2016; Y. Wang et al., 2020; D. Yang et al., 2020). (c) LAI affecting the canopy transpiration shows inconsistent results for varying crop species under different irrigation methods. Drip irrigation increased LAI for maize (S. Qin, Fan, et al., 2023; Y. Wang et al., 2020) and okra (Patra et al., 2023) relative to border irrigation and surface irrigation, respectively, while it reduced it by 16.9% for spring wheat when compared to border irrigation (D. Yang et al., 2023), and decreased it by 7%–13% for greenhouse–grown tomato compared to furrow irrigation (B. Li et al., 2020). In addition, drip irrigation supply water and fertilizers directly to crop root zone using high-frequency irrigation with elevated irrigation efficiency and low irrigation amount based on crop water demand, thereby promoting root growth and root water uptake (Mahajan & Singh, 2006; P. Yang et al., 2023). (d) Drip irrigation also resulted in warmer canopies and low humidity, in turn potentially

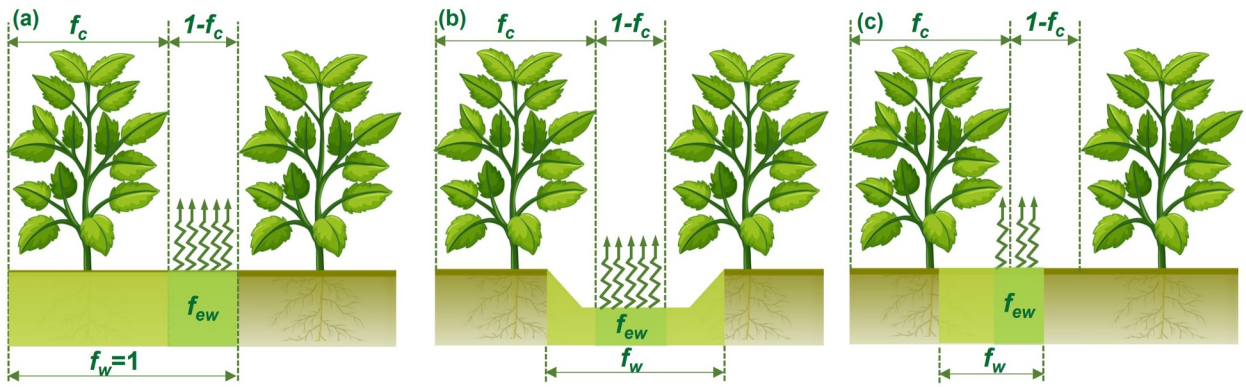


**Figure 8.** Estimation of the fraction of the soil both exposed and wetted ($f_{ew}$) based on fractions of canopy coverage ($f_c$) and the wetted surface ($f_w$) for non–fully covered crops when the wetting comes from precipitation, basin, border or sprinkler irrigations that fully wets the soil surface (a) or from furrow (b) and drip irrigation (c) that partially wets the soil surface.

enhancing daily $ET_a$. Drip irrigation increased the mean seasonal canopy temperature by 0.52 and 1.11°C, respectively, for maize and spring wheat when compared to border irrigation (S. Qin, Fan, et al., 2023; D. Yang et al., 2023). It also increased mean seasonal $T_a$ by 0.28–0.61°C and reduced mean seasonal RH from 77% to 74% for greenhouse–grown tomato relative to furrow irrigation, resulting in an increasement of VPD by 0.1–0.2 kPa (B. Li et al., 2020). This increased $T_a$ incorporating great soil temperature induced by drip irrigation is also one of the reasons for advancing the phenology and accelerating crop growth as discussed earlier. (e) Drip irrigation altered the energy balance components as expected. Drip irrigation increased the overall available energy by 3% for a maize field (mainly at initial stage of 10%), and by 7.48 W $m^{-2}$ for spring wheat relative to border irrigation, and increased by 1% during winter season, while reduced by 6% during the summer season for greenhouse–grown tomato (B. Li et al., 2020; S. Qin, Fan, et al., 2023; D. Yang et al., 2023). However, the energy was partitioned less to $\lambda ET_a$ under drip irrigation than other irrigation methods that more energy was used to warm canopy as earlier discussed. Drip irrigation decreased growing–season $\lambda ET_a/R_n$ by 6%–12% for greenhouse–grown tomato compared to furrow irrigation, and by 11% for spring wheat than border irrigation, and reduced growing–season $\lambda ET_a/(R_n–G_0)$ by 7% for maize relative to border irrigation.

The effect of irrigation methods on $ET_a$ have been considerate in the modified dual crop coefficient method and incorporated into its interactive software, SIMDualKc (Rosa, Paredes, Rodrigues, Alves, et al., 2012). Some studies (R. G. Allen et al., 2005) modified the $E_s$ estimation procedure to calculate daily $K_e$ when irrigation partially wets the soil (such as drip and furrow irrigations) and canopy cover is not full (Figure 8b), which is different from the condition for full wetted soil surface (Figure 8a). In this modification, $K_e$ was divided into two parts. One part ($K_{ep}$) was for the exposed fraction of wetted soil only by precipitation ($f_{ewp}$), and another ($K_{ei}$) was for the exposed fraction of wetted soil by both irrigation and precipitation ($f_{ewi}$). Thus,

$$K_e = K_{ep} + K_{ei}, \tag{23}$$

where $K_{ep}$ is the $K_e$ for $f_{ewp}$, and $K_{ei}$ is the $K_e$ for $f_{ewi}$. $K_{ep}$ and $K_{ei}$ can be calculated as

$$K_{ep} = K_{rp}(1 - W)(K_{c\max} - K_{cb}) \le f_{ewp}K_{c\max}, \tag{24a}$$

$$K_{ei} = K_{ri}W(K_{c\max} - K_{cb}) \le f_{ewi}K_{c\max}, \tag{24b}$$

where $K_{rp}$ and $K_{ri}$ is the evaporation reduction coefficient for $f_{ewp}$ and $f_{ewi}$ fractions. Here, $W$ is a weighting factor for partitioning the available energy into $f_{ewi}$ and $f_{ewp}$ fractions, $K_{c\max}$ is the maximum value of $K_c$. The $f_{ewp}$ and $f_{ewi}$ can be determined as

$$f_{ewp} = 1 - f_c - f_{ewi}, \tag{25a}$$

$$f_{ewi} = \min(1 - f_c, f_w), \tag{25b}$$

where $f_c$ is the fraction of canopy cover, and $f_w$ is the fraction of the wetted soil surface by irrigation. For drip irrigation, multiplying $f_w$ by $[1-2/3f_c]$ in Equation 25b is recommended (R. G. Allen et al., 1998). The detailed calculation procedure can be found elsewhere (R. G. Allen et al., 2005; Rosa, Paredes, Rodrigues, Alves, et al., 2012). The method has been used for many irrigation practices such as surface, basin, sprinkler, furrow and drip irrigations (R. G. Allen et al., 2005; Martins et al., 2013; Qiu et al., 2015a; Rosa, Paredes, Rodrigues, Fernando, et al., 2012; B. Z. Zhang et al., 2013).

#### 3.3.3. Mulching

Mulching is a widely adopted agricultural practice to increase crop production and leaf water use efficiency (i.e., WUE = $A_n/T_{r-\text{leaf}}$), including plastic film, straw, and degradable film mulching, among others. Among these methods, plastic film mulching is the dominant type until now and degradable film mulching is the most prospective type to avoid film residuals. In China, the total amount of plastic film in agricultural land reached 2.4 million tons in 2019, covering 11% (17.6 million ha) of cropland (National Bureau of Statistics of China, 2023), although no further increase or even a slight decline was reported in recent years.

The effect of mulching on total growing–season $ET_a$ shows inconsistent results, varying from negative (N. Chen et al., 2021; S. Qin et al., 2014; Y. Zhang et al., 2018; Y. Zhao et al., 2021) to no change (Chai et al., 2022; Fan et al., 2017), and to positive (G. Liu et al., 2018; D. Sun et al., 2020; Xie et al., 2005), depending on the crop, mulching type, region, and soil characteristics. A meta–analysis showed that total growing–season $ET_a$ under plastic film mulching was not affected for corn, but increased for wheat, and decreased for potato (L. Xiao et al., 2023). In addition, the overall results by the same study showed that total growing–season $ET_a$ was significantly reduced in subgroups with black plastic film and regions in Northeast China. However, total growing–season $ET_a$ increased in areas with mean annual precipitation of 400–600 mm and soil organic carbon concentration of 10 g $kg^{-1}$. Another meta–analysis showed that plastic film, straw, and degradable film mulching significantly decreased total growing–season $ET_a$ of maize by 5%, 3%, and 8%, respectively, and the reduction occurred in areas with altitude of 500–1,500 m, >1,500 m, 500–1,000 m, respectively, with mean annual rainfall of <500, <500, 500–1,000 mm, respectively, and mean annual temperature of 10–15, 5–10, 10–15°C, respectively (W. Cai et al., 2022). The planting pattern in combination with mulching also affected total growing–season $ET_a$ of maize, where significant reduction was observed for plastic film mulching under both flat and ridge–furrow planting, and for both straw and degradable film mulching under flat planting (W. Cai et al., 2022). Generally, total growing–season $ET_a$ of potato was not affected by plastic film and straw mulching in subgroups of different regions in China, temperate zones, film colors, and mean annual precipitation. A notable exception is the significant increase (by 11%) in total growing–season $ET_a$ when the mean growth temperatures >20°C for straw mulching and modest reduction (by 2%) when mean annual precipitation <400 mm for plastic film mulching (Q. Li et al., 2018).

The effect of mulching on $ET_a$ rates also varied at different growth stages with different canopy coverage. Compared to non–mulching treatment, daily $ET_a$ of maize under transparent plastic film mulching was lower at the initial, development, and late season stages, but greater at the middle growing stages (Fan et al., 2017; Y. Zhang et al., 2018). Based on 24 field experiments, the $ET_a$ of winter wheat under transparent plastic film mulching in northwest China was not affected in the early and late stages, but was markedly increased by 30 mm in the middle stage (Chai et al., 2022).

The variability of responses of $ET_a$ to mulching can be attributed to the comprehensive effect of mulching on reduction in $E_s$ and increases in $T_r$, along with a shortened phenology. Applying mulching, especially when crop canopy coverage is small, can markedly prevent water loss from the soil surface through reductions in available energy (Rosa, Paredes, Rodrigues, Alves, et al., 2012). The total growing–season $E_s$ was reduced by 45%–55% under transparent plastic film mulching (Y. Zhang et al., 2018; Y. Zhao et al., 2021), by 18% under wheat straw mulch for maize (S. X. Li et al., 2013), and by 25%–30% under straw mulching for wheat (Balwinder-Singh et al., 2011; J. Wang et al., 2018). The $T_r$ rate can be enhanced under mulching because of improved soil hydrothermal conditions by decreasing nitrogen leaching and increasing soil temperature and maintaining good soil moisture content by inhibiting $E_s$. These conditions promote crop growth and development later, which in turn, increases $T_r$ (L. Xiao et al., 2023; Y. Zhang et al., 2018). A meta–analysis showed that plastic film mulching increases mean soil moisture by 9% across soil layers, with more increases in the topsoil (13%) than at the 80–100 cm soil layer (6%) (D. Ma et al., 2018). Greater $g_s$ (C. Li et al., 2023; X. Zhang et al., 2019), LAI (N. Chen et al., 2021; Y. Feng, Gong, et al., 2017; Xie et al., 2005; Y. Zhang et al., 2018), root length density and root dry biomass (Gao

et al., 2014; Thidar et al., 2020) were also observed under mulching conditions than non–mulched fields, which in turn further enhance the ability of root water uptake and $T_r$. Total growing–season $T_r$ has increased by 6%–18% under transparent plastic film mulching for maize (Y. Zhang et al., 2018; Y. Zhao et al., 2021), and by 15% under rice straw mulch for wheat (Balwinder-Singh et al., 2011). Plastic film mulching alters the available energy ($R_n$–$G_0$) by changing the surface reflectance, absorption, and soil temperature, which affect $ET_a$ (S. Qin, Li, et al., 2023). Transparent plastic film mulching has been reported to decrease daily $R_n$ by 3%–10%, and daily $G_0$ by 28% over the whole growing season of maize (Fan et al., 2017; Y. Feng, Gong, et al., 2017; Y. Zhang et al., 2018; Y. Zhao et al., 2021), leading to a reduction in growing–season available energy by 3%. This reduction in available energy mainly appeared in the initial stage of maize (24%) when canopy coverage was small. Clearly, the small canopy coverage resulted in more area affected by the plastic film mulching than crop canopy (Y. Zhao et al., 2021). However, the black plastic film mulching had the opposite effect, which has been reported to increase $R_n$ and $G_0$ over a potato field, especially during the initial stage (Y. L. Zhang et al., 2017). Mulching can also shorten the growth duration and terminate the growing season earlier. This reduced growing season results in a decline in total growing–season $ET_a$. Some four–five (Y. Zhang et al., 2018) and 9–12 (Y. Feng, Gong, et al., 2017) reduction days were reported for maize under transparent plastic film mulching.

To consider the effect of plastic mulching on field $ET_a$, previous studies generally introduced the fraction of soil covered by plastic mulching ($f_m$) into $ET_a$ models. An $f_m$ (S. Li et al., 2013) was introduced for mulching soil resistance ($r_s^m$) into the Shuttleworth–Wallace model, and practically ignored the mulched $E_s$ by treating $r_s^m$ as infinity (N. Chen et al., 2021). Others (S. Qin et al., 2018) further calibrated $r_s^m$ by using measured mulched $E_s$, and obtained a value of 1,280 s $m^{-1}$ for the transparent–mulched maize field in northwest China. On a similar line of reasoning (N. Chen et al., 2022), $f_m$ and $r_s^m$ can be included in a modified multi–source $ET_a$ model such as the one of Shuttleworth–Wallace. Such revision was evaluated in a corn/tomato inter–cropped ecosystem with plastic mulching with good agreement between models and data. In addition, $f_m$ was also introduced into the dynamic dual crop coefficient model through affecting $K_e$ (Ding, Kang, Zhang, et al., 2013) and a modified Priestley–Taylor model by including a soil evaporation coefficient (Ding, Kang, Li, et al., 2013) to improve their performance in mulched fields. In the dual crop coefficient model and its interactive software, SIMDualKc, the effect of mulching on $E_s$ can be considered in $K_e$ by changing $f_c$ of the soil surface shaded or not exposed to radiation (Rosa, Paredes, Rodrigues, Alves, et al., 2012), where the $f_c$ under plastic mulching condition ($f_{c\_m}$) in Equations 25a and 25b should be modified as

$$f_{c\_\mathrm{m}} = \max(f_c, f_m). \tag{26}$$

For organ mulching, the mulch density and depth, and $f_m$ control the amount of reduction in $E_s$, which is decreased by ~5% for every 10% of soil surface covered by organic mulching (R. G. Allen et al., 1998). Thus, the magnitudes of $K_{ei}$ and $K_{ep}$ are reduced by the same amount. Overall, the total reduction in $E_s$ under mulching in the dual crop coefficient model depends on $f_m$ and the percentage of reduction in $E_s$ (Rosa, Paredes, Rodrigues, Alves, et al., 2012).

In addition, mulching markedly changes surface albedo and inhibits vapor and $CO_2$ exchange between the soil and the atmosphere. This revision by mulching affects the energy balance, which was considered in some land surface models. For instance, a mulched soil surface reflectance scheme was proposed and integrated into the two–stream radiation transfer model (S. Qin, Li, et al., 2023). An increase of 11% of surface reflectance was found for mulched fields relative to non–mulched cases, and contribution of mulched soil surface to field surface reflectance was 42% over a transparent mulched maize field when $f_m$ was set to 0.75. A modified land surface model, Two–Big–Leaf–SHAW, was also developed and used to represent water, heat and $CO_2$ fluxes under plastic mulching conditions (Q. Yang et al., 2012). This model is now being tested across a variety of mulching practices and compared to other models.

#### 3.3.4. Nitrogen Application

Fertilizer application is an important source of nutrition for plant production, where N fertilizer is the most applied. Worldwide, fertilizer application increased by 8.7 times from 1961 to 2021 for N (from 7.54 to 65.45 kg $ha^{-1}$ $yr^{-1}$), by 3.9 times for $P_2O_5$ (from 7.45 to 28.75 kg $ha^{-1}$ $yr^{-1}$), and by 4.3 times for $K_2O$ (from 5.70 to 24.42 kg $ha^{-1}$ $yr^{-1}$) as reported by the Food and Agricultural Organization (FAO Statistics, 2024). In China,

**Table 7**
*The Effect of Nitrogen (N) Application on Total Growing–Season Crop Evapotranspiration Under Sufficient Water Condition*

| Crop type | Reference N (kg ha$^{-1}$) | N application (kg ha$^{-1}$) | Percentage change relative to reference (%) | Source |
|---|---|---|---|---|
| Wheat ($C_3$) | 70 | 350 | 28 | Hunsaker et al. (2000) |
| | 15 | 350 | 28 | |
| | 0 | 80 | 23 | Caviglia and Sadras (2001) |
| | 0 | 120 | 27 | |
| | 0 | 160 | 38 | |
| | 0 | 240 | 22–27 | L. Liu et al. (2016) |
| | 0 | 60 | 1 | N. K. Lenka et al. (2021) |
| | 0 | 120 | 2 | |
| | 0 | 180 | 3 | |
| | 0 | 90 | 9 | S. Lenka et al. (2009) |
| | 0 | 120 | 12 | |
| | 0 | 180 | 17 | |
| Maize ($C_4$) | 0 | 100 | 10 | Ogola et al. (2002) |
| | 0 | 120 | 5 | Hernández et al. (2015) |
| | 0 | 135 | 8 | Carlson et al. (1959) |
| | 0 | 180 | 4 | Barbieri et al. (2012) |
| | 0 | 84 | 6 | Rudnick and Irmak (2014) |
| | 0 | 140 | 7 | |
| | 0 | 196 | 6 | |
| | 0 | 252 | 10 | |
| | 0 | 75 | 5 | Srivastava et al. (2020) |
| | 0 | 100 | 8 | |
| | 0 | 125 | 10 | |
| | 0 | 90 | 7 | S. Lenka et al. (2009) |
| | 0 | 120 | 8 | |
| | 0 | 180 | 18 | |
| | 0 | 180 | 17 | Zhong and Shangguan (2014) |
| | 0 | 270 | 19 | |
| | 0 | 360 | 17 | |
| | 88 | 350 | 1 | Saeidi et al. (2021) |
| | 88 | 263 | 4 | |
| | 88 | 175 | 7 | |
| Potato ($C_3$) | 0 | 240 | 6[a] | Ferreira and Carr (2002) |
| Soybean ($C_3$) | 0 | 15 | NS | N. K. Lenka et al. (2020) |
| | 0 | 30 | NS | |
| | 0 | 45 | 3[b] | |
| | 0 | 75 | NS | L. Liu et al. (2016) |
| Cotton ($C_3$) | 100 | 150 | NS | Oweis et al. (2011) |
| | 100 | 200 | NS | |

[a]Data were for 1989 season. [b]Data were for 2016 season.

over–application of N fertilizer (305 kg ha$^{-1}$ yr$^{-1}$) does not appreciably enhance crop yield, and can lead to adverse environmental issues such as widespread water pollution, soil acidification, and excessive greenhouse gas emissions (Cui et al., 2018).

The effect of N application on crop $ET_a$ has been widely reported and summarized in Table 7. Although some studies show that N supplement had no significant effect on total growing–season $ET_a$ (N. K. Lenka et al., 2020; L. Liu et al., 2016), the majority of studies reported that appropriate N supplement can increase total growing–season crop $ET_a$. For instance, compared to no N treatment, the total growing–season $ET_a$ increased by 1%–38% for wheat when receiving 60–240 kg N $ha^{-1}$ (Caviglia & Sadras, 2001; N. K. Lenka et al., 2021; L. Liu et al., 2016), by 4%–10% for maize when applying 84–252 kg N $ha^{-1}$ (Hernández et al., 2015; Ogola et al., 2002; Rudnick & Irmak, 2014; Srivastava et al., 2020), and by 6% for potato with application of 240 kg N $ha^{-1}$ under sufficient water (Ferreira & Carr, 2002).

However, over–application of N fertilizer did not further increase total growing–season crop $ET_a$ (Zhong & Shangguan, 2014). For instance, there is no significant effect for total growing–season $ET_a$ of cotton among N levels of 100, 150, and 200 kg $ha^{-1}$ supplied with drip irrigation (Oweis et al., 2011). Total growing–season $ET_a$ of wheat increased with the increased N level from 0 to 337.5 kg N $ha^{-1}$ but decreased beyond 337.5 kg N $ha^{-1}$ (F. S. Li et al., 2004). In addition, N supplement methods had no significant effect on total growing–season $ET_a$. There are no significant differences for total growing–season $ET_a$ of maize among fixed rate, variable rate, and pre–plant N application methods (Sharma & Irmak, 2021).

The influence of N application on crop total growing–season $ET_a$ is viewed as a compromise between its effect on enhanced $T_r$ and reduced $E_s$. (a) The appropriate N application produces an increased photosynthetic capacity per unit leaf area, and thus a greater $g_s$ (Liao et al., 2022; Saeidi et al., 2021). These increases subsequently promote development of leaf area (N. K. Lenka et al., 2020; Srivastava et al., 2020) and possible root biomass, which in turn, enhance $T_r$. The mean mid–day $g_s$ (10:00–14:00) of wheat was increased by ~86% for 450 kg N $ha^{-1}$ relative to no N (F. S. Li et al., 2004). The LAI also increased by 23%–45% for maize with 100–450 kg N $ha^{-1}$ compared to no N (F. S. Li et al., 2004; Ogola et al., 2002). The root biomass was not affected by N application for maize, cotton, sorghum, and sunflower (T. Ma et al., 2017; Ogola et al., 2002; Sainju et al., 2005), but markedly increased for rice with 100–300 kg N $ha^{-1}$ compared to no N (Ju et al., 2015). Total growing–season $T_r$ was increased by 15%–26% for maize when applying 75–125 kg N $ha^{-1}$ (Ogola et al., 2002; Srivastava et al., 2020), by 29%–50% for wheat with 80–120 kg N $ha^{-1}$ (Caviglia & Sadras, 2001), and by 21%–46% for potato with 80–240 kg N $ha^{-1}$ when compared to no N treatment (Ferreira & Carr, 2002). (b) The increased LAI caused by N supplement leads to a low intercepted radiation at the soil (Hernández et al., 2015). This reduced radiation reduces $E_s$. Total growing–season $E_s$ decreased by 3%–22% for maize with 75–125 kg N $ha^{-1}$ (Ogola et al., 2002; Srivastava et al., 2020), by 31%–59% for wheat with 80–120 kg N $ha^{-1}$ (Caviglia & Sadras, 2001), and by 34%–57% for potato with 80–240 kg N $ha^{-1}$ with respect to no N treatment (Ferreira & Carr, 2002). More increased total growing–season $T_r$ than reduced $E_s$ leads to an increased total growing–season $ET_a$ with appropriate N application (Ferreira & Carr, 2002; Srivastava et al., 2020).

At present, the effect of N application on $ET_a$ was primarily modeled in some crop models such as in AquaCrop (H. Wu et al., 2022) and DSSAT (Irmak et al., 2024) indirectly through increased LAI or canopy coverage. A more physiologically based approach would track the effects of soil N on leaf–level N and subsequent enhancement in photosynthetic activities (Palmroth et al., 2013). When deriving empirical adjustments to stress coefficients, a polynomial function had the best performance in estimating stress that is induced by the combined salinity and N application (Saeidi et al., 2021), which may be further incorporated into crop coefficient and Priestley–Taylor models.

### 3.4. Other Considerations

Some studies have reported other factors that affect cropland $ET_a$. While these factors have been partially covered throughout the review, we flag them below for completeness.

1. Structural properties of the canopy: Differences in $g_s$, canopy height, roughness, surface reflection, LAI, and root systems lead to varying $ET_a$ magnitudes for different types of crops, varieties, and growing stages under the same environmental conditions (R. G. Allen et al., 1998). For instance, despite the nearly overlapping growing seasons of maize and vineyards (with similar climate conditions), closed maize ($C_4$) canopies have greater available energy and allocates more of this energy to $\lambda ET_a$ than canopies of sparse grapevines ($C_3$), resulting in a 58% higher growing–season mean $ET_a$ rate (Jiao et al., 2018).
2. Irrigation and rainfall: Both irrigation and rainfall affect $ET_a$ and energy partitioning by altering soil water content and VPD. Both $T_r$ and $E_s$ will increase as soil moisture increases following irrigation and rainfall,

especially for sparse canopies in arid or semi-arid regions. Daily $ET_a$ has been reported to increase by 38% after a 70 mm irrigation and by 175% after a 29 mm rainfall for a sparse vineyard in northeast China (B. Z. Zhang et al., 2010).

3. Frost damage: Frost damages cell membrane and leaf structure (Qu et al., 2007), which reduces stomatal opening and consequently leads to a reduction in $T_r$. Daily $ET_a$ of vineyard have been reported to be reduced by 32% after suffering from frost (B. Z. Zhang et al., 2010).
4. Waterlogging: Waterlogging inhibits leaf water potential, $g_s$, root biomass, and leaf area (Dickin & Wright, 2008; B. Huang et al., 1994; Malik et al., 2002), thereby negatively affecting $ET_a$. Root biomass of wheat was reduced by an average of 62% after waterlogging lasting 7–42 days (Herzog et al., 2016). Additionally, waterlogging lasting for 16 days also decreased $g_s$ of wheat by 35%–54%, leaf area by 49%–67%, root dry weight by 72%–74%, leaf water potential by 27%–48% (B. Huang et al., 1994). Leaf transpiration has been reported to be 3%–16% lower on the day following waterlogging during the tillering stage compared to the water-drained treatment (Shao et al., 2013). However, studies on the effect of waterlogging on $ET_a$ are rarely reported.
5. Harvesting: A variety of crops, such as alfalfa, are grown for forage or hay and are typically harvested multiple times during the growing season. Each harvest effectively concludes a "sub" growing season, allowing for regrowth. The impact of these harvests on alfalfa $ET_a$ is primarily influenced by varying meteorological conditions experienced during each cutting cycle under sufficient water conditions. The values of $K_c$ or $K_{cb}$ (removing the effect of climate conditions) for the initial, mid, and late season of each cutting cycle were similar (R. G. Allen et al., 1998; Benli et al., 2006).
6. Enclosed and semi-enclosed environments and ventilation: Ventilation modes have been reported to have no significant effect on total growing–season $ET_a$ of greenhouse–grown tomatoes (Gong et al., 2022), despite their impact the microclimate conditions in greenhouses. The average daily values of $T_a$ and RH between 10:00 and 14:00 were 5.0 % and 5.5 % lower, respectively, while VPD was 8.1% higher in the treatment with simultaneous opening of the roof and south vents compared to the treatment with only the roof vent open.

## 4. Conclusions and Outlook

Reported impacts of e[$CO_2$], e[$O_3$], global warming, water, salinity and heat stresses, planting density, irrigation methods, mulching, and N application on cropland $ET_a$ were reviewed, along with their possible causes and estimation. There is general agreement that e[$O_3$], water and salinity stresses, and adopting drip irrigation all lead to lower total growing–season $ET_a$ for almost all crops. However, total growing–season $ET_a$ in response to e[$CO_2$], warming, heat stress, planting density, and N application were inconsistent across studies.

The potential causes of 10 key factors affecting total growing-season $ET_a$ are summarized in Table 8. The impacts of e[$CO_2$] and e[$O_3$], water and salinity stresses on total growing–season $ET_a$ are mainly through $g_s$, the ability of soil to conduct water to roots, development of roots and LAI, microclimate, and possibly phenology. The effect of warming on total growing–season $ET_a$ can be largely explained by both variations in ambient growing–season mean $T_a$ and growing duration. When water is sufficient, total growing–season $ET_a$ in response to heat stress (or mulching and appropriate N supplement) is a compromise between reduced (or enhanced) $T_r$ and increased (or decreased) $E_s$, along with possibly a shortened growth period. Differences in $ET_a$ under varying planting densities can be explained by the direct and indirect effects of leaf area on the constitutive terms of $ET_a$. The variation of total growing–season $ET_a$ under drip irrigation compared to conventional irrigation was affected by smaller soil wetting area, shortened growing season, less energy partitioning to $ET_a$, and changes in crop characteristics and microclimate.

The effect of e[$CO_2$] and water stress on $g_s$ can be operationally described by Jarvis type functions, which can then be incorporated into a Penman–Monteith model to track their effects on $ET_a$. The effect of water and salinity stresses and planting density on crop $ET_a$ can also be estimated using the FAO 56 crop coefficient model when introducing revisions to $K_s$, $K_{EC}$, and $K_d$. The effect of varying types of warming on $ET_a$ can be assessed based on a simplified Priestley–Taylor formulation with a dynamic coefficient. The $ET_a$ responses to irrigation method can be estimated using a modified dual crop coefficient method by separating $K_e$ into computing $E_s$ by the fraction of soil wetted by precipitation only ($K_{ep}$) and the evaporation from the fraction of soil wetted by both irrigation and precipitation ($K_{ei}$). The impact of mulching on cropland $ET_a$ can be quantified by introducing the fraction of soil covered by mulching ($f_m$) into the Shuttleworth–Wallace, dual crop coefficient, or Priestley–Taylor models.

**Table 8**
*The Potential Causes of Ten Affecting Factors on Total Growing-Season Transpiration ($T_r$), Evaporation ($E_s$), and Evapotranspiration ($ET_a$)*

| Factors | $g_s$ | Root growth | Leaf growth | VPD | Phenology[a] | Total $T_r$ | Total $E_s$ | Total $ET_a$ |
|---|---|---|---|---|---|---|---|---|
| $CO_2$ | (−) | (+) | (+) | (+) | NS | (+/NS/−) | (−) | (+/NS/−) |
| $O_3$ | (−) | (−) | (−) | (+) | (−) | (−) | (−) | (−) |
| Global warming | NA | NA | (+/NS/−) | (+) | (−) | NA | NA | (+/NS/−) |
| Water stress[b] | (−) | (−) | (−) | (+) | NA | (−) | (−) | (−) |
| Salinity stress[c] | (−) | (−) | (−) | (+) | NA | (−) | (−) | (−) |
| Heat stress | (−) | (−) | (−) | (+) | (−) | (−) | (+) | (+/NS/−) |
| Planting density | NA | NA | (+) | NA | (−) | (+/NS) | (−) | (+/NS) |
| Drip irrigation[d] | NA | (+) | (+/−) | (+) | (−) | (−) | (−) | (−) |
| Mulching[e] | (+) | (+) | (+) | NA | (−) | (+) | (−) | (+/NS) |
| Appropriate N application | (+) | (+/NS) | (+) | NA | NA | (+) | (−) | (+/NS) |

*Note.* $g_s$ is the leaf stomatal conductance to $H_2O$. VPD is the vapor pressure deficit. NA is not reported. NS is no significant difference. (+) and (−) represent positive and negative effects on variables, and thereby $ET_a$. [a]Negative represents shorten the total growing season. [b]Limited root water uptake due to low soil water potential is also the reason affecting $ET_a$. [c]Limited root water uptake due to osmotic stress, iron imbalance and oxidative stress also affect $ET_a$. [d]Less available energy transferring to latent heat flux is also the reason affecting $ET_a$. [e]Altered available energy by changing the surface reflectance, absorption, and soil temperature is also the reason affecting $ET_a$.

Although the response of $ET_a$ to primary influencing factors has been reviewed, there are many aspects that deserve further inquiry:

1. The effect of e[$O_3$] on $g_s$ can be described by a modified Jarvis function. However, it is mainly used to calculate the stomatal $O_3$ flux. There is a lack of attempt to incorporate this response of $g_s$ to e[$O_3$] into the Penman–Monteith model to estimate $ET_a$.
2. Many controlled manipulation experiments such as FACE, OTC, and free air temperature increase facilities investigated varying types of warming on $A_n$, crop growth, grain yield, and quality. However, crop $ET_a$ under varying types of warming is under–reported. Water balance method, the residual in the energy balance method, sap flow plus micro–lysimeters, or even weighting lysimeters can be used to observe $ET_a$ under several warming scenarios, which is needed to link cropland $ET_a$ to productivity in response to warming.
3. At present, there are few studies on $ET_a$ responses to heat stress, and most are based on pot experiments in phytotrons or artificial climate chambers (Nakad et al., 2023). Obtaining larger–scale data of $ET_a$ under heat stress, such as data from tanks with an area of 1–4 $m^2$ in phytotrons, is beneficial to understand heat stresses on $ET_a$. In addition, there is a need to unify the accumulated daily heat degree days used to quantify the effect of heat stress on biomass, yield, and phenology in crop models with $ET_a$.
4. Models for e[$CO_2$] and e[$O_3$] on $ET_a$ using a simplified Priestley–Taylor and crop coefficient models are rarely reported. The key to establish a modified Priestley–Taylor model is to quantify the effect of e[$CO_2$] and e[$O_3$] on the Priestley–Taylor coefficient. For crop coefficient models, the challenge is to propose coefficients of e[$CO_2$] and e[$O_3$] on $K_c$ or $K_{cb}$ similar to $K_s$, $K_{EC}$, and $K_d$.
5. In practice, the cropland $ET_a$ is jointly affected by multiple factors, such as compound drought and heat stresses, e[$CO_2$] and warming, e[$O_3$] and warming, e[$CO_2$] and salinity stress. The impact of multiple factors on cropland $ET_a$ is a complex and multifaceted phenomenon that requires long–term consideration of many environmental stressors and their interactions.

## Data Availability Statement

Data supporting Tables are through the cited literature. Typical error data in Table 1 are from R. G. Allen et al. (2011b). Data in Table 3 are collected from Burkart et al. (2011), Bernacchi et al. (2006), Magliulo et al. (2003), Hussain et al. (2013), Kimball et al. (1999), Triggs et al. (2004), Yoshimoto et al. (2005), Kimball et al. (1994), N. K. Lenka et al. (2021), Kang, Zhang, Hu, and Zhang (2002), L. H. Allen et al. (2003), F. S. Li et al. (2004), Wei et al. (2021, 2022), and X. J. Li et al. (2018). Data in Table 6 are collected from Valentín

et al. (2020), T. Zhang et al. (2021), Mohammed and Irmak (2022), X. Wang et al. (2018), Y. Wang et al. (2020), Kanani et al. (2022), Patra et al. (2023), D. Yang et al. (2020), B. Li et al. (2021), Sugita et al. (2017). Data in Table 7 are obtained from Hunsaker et al. (2000), Caviglia and Sadras (2001), L. Liu et al. (2016), S. Lenka et al. (2009), N. K. Lenka et al. (2020, 2021), Ogola et al. (2002), Hernández et al. (2015), Carlson et al. (1959), Barbieri et al. (2012), Rudnick and Irmak (2014), Srivastava et al. (2020), Zhong and Shangguan (2014), Saeidi et al. (2021), Ferreira and Carr (2002), and Oweis et al. (2011).

**Acknowledgments**
We acknowledge support from the National Natural Science Foundation of China (52322904, 52179036), and the Fundamental Research Funds for the Central Universities.

## References

Ahmadi, S. H., Solgi, S., & Sepaskhah, A. R. (2019). Quinoa: A super or pseudo-super crop? Evidences from evapotranspiration, root growth, crop coefficients, and water productivity in a hot and semi-arid area under three planting densities. *Agricultural Water Management*, *225*, 105784. https://doi.org/10.1016/j.agwat.2019.105784

Ainsworth, E. A. (2008). Rice production in a changing climate: A meta-analysis of responses to elevated carbon dioxide and elevated ozone concentration. *Global Change Biology*, *14*(7), 1642–1650. https://doi.org/10.1111/j.1365-2486.2008.01594.x

Ainsworth, E. A., & Rogers, A. (2007). The response of photosynthesis and stomatal conductance to rising [$CO_2$]: Mechanisms and environmental interactions. *Plant, Cell & Environment*, *30*(3), 258–270. https://doi.org/10.1111/j.1365-3040.2007.01641.x

Alberto, M. C. R., Wassmann, R., Hirano, T., Miyata, A., Hatano, R., Kumar, A., et al. (2011). Comparisons of energy balance and evapotranspiration between flooded and aerobic rice fields in the Philippines. *Agricultural Water Management*, *98*(9), 1417–1430. https://doi.org/10.1016/j.agwat.2011.04.011

Alberto, M. C. R., Wassmann, R., Hirano, T., Miyata, A., Kumar, A., Padre, A., & Amante, M. (2009). $CO_2$/heat fluxes in rice fields: Comparative assessment of flooded and non-flooded fields in the Philippines. *Agricultural and Forest Meteorology*, *149*(10), 1737–1750. https://doi.org/10.1016/j.agrformet.2009.06.003

Albertson, J. D., Parlange, M. B., Katul, G. G., Chu, C., Stricker, H., & Tyler, S. (1995). Sensible heat flux from arid regions: A simple flux-variance method. *Water Resources Research*, *31*(4), 969–973. https://doi.org/10.1029/94wr02978

Alfieri, J. G., Kustas, W. P., Prueger, J. H., Hipps, L. E., Evett, S. R., Basara, J. B., et al. (2012). On the discrepancy between eddy covariance and lysimetry-based surface flux measurements under strongly advective conditions. *Advances in Water Resources*, *50*, 62–78. https://doi.org/10.1016/j.advwatres.2012.07.008

Allen, L. H., Pan, D., Boote, K. J., Pickering, N. B., & Jones, J. W. (2003). Carbon dioxide and temperature effects on evapotranspiration and water use efficiency of soybean. *Agronomy Journal*, *95*(4), 1071–1081. https://doi.org/10.2134/agronj2003.1071

Allen, R. G., & Pereira, L. S. (2009). Estimating crop coefficients from fraction of ground cover and height. *Irrigation Science*, *28*(1), 17–34. https://doi.org/10.1007/s00271-009-0182-z

Allen, R. G., Pereira, L. S., Howell, T. A., & Jensen, M. E. (2011a). Evapotranspiration information reporting: I. Factors governing measurement accuracy. *Agricultural Water Management*, *98*(6), 899–920. https://doi.org/10.1016/j.agwat.2010.12.015

Allen, R. G., Pereira, L. S., Howell, T. A., & Jensen, M. E. (2011b). Evapotranspiration information reporting: II. Recommended documentation. *Agricultural Water Management*, *98*(6), 921–929. https://doi.org/10.1016/j.agwat.2010.12.016

Allen, R. G., Pereira, L. S., Raes, D., & Smith, M. (1998). *Crop evapotranspiration: Guidelines for computing crop water requirements*, *FAO Irrigation and Drainage Paper 56*. FAO.

Allen, R. G., Pereira, L. S., Smith, M., Raes, D., & Wright, J. L. (2005). FAO56 dual crop coefficient method for estimating evaporation from soil and application extensions. *Journal of Irrigation and Drainage Engineering*, *131*(1), 2–13. https://doi.org/10.1061/(asce)0733-9437(2005)131:1(2)

Asseng, S., Jamieson, P. D., Kimball, B., Pinter, P., Sayre, K., Bowden, J. W., & Howden, S. M. (2004). Simulated wheat growth affected by rising temperature, increased water deficit and elevated atmospheric $CO_2$. *Field Crops Research*, *85*(2), 85–102. https://doi.org/10.1016/s0378-4290(03)00154-0

Assouline, S., Möller, M., Cohen, S., Ben-Hur, M., Grava, A., Narkis, K., & Silber, A. (2006). Soil-Plant system response to pulsed drip irrigation and salinity. *Soil Science Society of America Journal*, *70*(5), 35–42. https://doi.org/10.2136/sssaj2005.0365

Azuchi, F., Kinose, Y., Matsumura, T., Kanomata, T., Uehara, Y., Kobayashi, A., et al. (2014). Modeling stomatal conductance and ozone uptake of *Fagus crenata* grown under different nitrogen loads. *Environmental Pollution*, *184*, 481–487. https://doi.org/10.1016/j.envpol.2013.09.025

Balwinder-Singh, Eberbach, P. L., Humphreys, E., & Kukal, S. S. (2011). The effect of rice straw mulch on evapotranspiration, transpiration and soil evaporation of irrigated wheat in Punjab, India. *Agricultural Water Management*, *98*(12), 1847–1855. https://doi.org/10.1016/j.agwat.2011.07.002

Barbieri, P., Echarte, L., Della Maggiora, A., Sadras, V. O., Echeverria, H., & Andrade, F. H. (2012). Maize evapotranspiration and water-use efficiency in response to row spacing. *Agronomy Journal*, *104*(4), 939–944. https://doi.org/10.2134/agronj2012.0014

Barrett, E. W., & Suomi, V. E. (1949). Preliminary report on temperature measurement by sonic means. *Journal of Atmospheric Sciences*, *6*(4), 273–276. https://doi.org/10.1175/1520-0469(1949)006<0273:protmb>2.0.co;2

Ben-Gal, A., Ityel, E., Dudley, L., Cohen, S., Yermiyahu, U., Presnov, E., et al. (2008). Effect of irrigation water salinity on transpiration and on leaching requirements: A case study for bell peppers. *Agricultural Water Management*, *95*(5), 587–597. https://doi.org/10.1016/j.agwat.2007.12.008

Ben-Gal, A., Karlberg, L., Jansson, P., & Shani, U. (2003). Temporal robustness of linear relationships between production and transpiration. *Plant and Soil*, *251*(2), 211–218. https://doi.org/10.1023/a:1023004024653

Benli, B., Kodal, S., Ilbeyi, A., & Ustun, H. (2006). Determination of evapotranspiration and basal crop coefficient of alfalfa with a weighing lysimeter. *Agricultural Water Management*, *81*(3), 358–370. https://doi.org/10.1016/j.agwat.2005.05.003

Bernacchi, C. J., Kimball, B. A., Quarles, D. R., Long, S. P., & Ort, D. R. (2006). Decreases in stomatal conductance of soybean under open-air elevation of [$CO_2$] are closely coupled with decreases in ecosystem evapotranspiration. *Plant Physiology*, *143*(1), 134–144. https://doi.org/10.1104/pp.106.089557

Bernacchi, C. J., Leakey, A. D. B., Kimball, B. A., & Ort, D. R. (2011). Growth of soybean at future tropospheric ozone concentrations decreases canopy evapotranspiration and soil water depletion. *Environmental Pollution*, *159*(6), 1464–1472. https://doi.org/10.1016/j.envpol.2011.03.011

Bhantana, P., & Lazarovitch, N. (2010). Evapotranspiration, crop coefficient and growth of two young pomegranate (*Punica granatum* L.) varieties under salt stress. *Agricultural Water Management*, *97*(5), 715–722. https://doi.org/10.1016/j.agwat.2009.12.016

Bolton, D. (1980). The computation of equivalent potential temperature. *Monthly Weather Review*, *108*(7), 1046–1053. https://doi.org/10.1175/1520-0493(1980)108<1046:tcoept>2.0.co;2

Bonner, J. (1959). Water Transport: This classical problem in plant physiology is becoming increasingly amenable to mathematical analysis. *Science*, *129*(3347), 447–450. https://doi.org/10.1126/science.129.3347.447

Booker, F. L. (2004). Influence of ozone on ribonuclease activity in wheat (*Triticum aestivum*) leaves. *Physiologia Plantarum*, *120*(2), 249–255. https://doi.org/10.1111/j.0031-9317.2004.0238.x

Booker, F. L., Fiscus, E. L., & Miller, J. E. (2004). Combined effects of elevated atmospheric carbon dioxide and ozone on soybean whole-plant water use. *Environmental Management*, *33*(1), S355–S362. https://doi.org/10.1007/s00267-003-9144-z

Borrás, L., Maddonni, G. A., & Otegui, M. E. (2003). Leaf senescence in maize hybrids: Plant population, row spacing and kernel set effects. *Field Crops Research*, *82*(1), 13–26. https://doi.org/10.1016/s0378-4290(03)00002-9

Bou Jaudé, M., Katerji, N., Mastrorilli, M., & Rana, G. (2008). Analysis of the effect of ozone on soybean in the Mediterranean region: I. The consequences on crop-water status. *European Journal of Agronomy*, *28*(4), 508–518. https://doi.org/10.1016/j.eja.2007.09.002

Bowen, I. S. (1926). The ratio of heat losses by conduction and by evaporation from any water surface. *Physical Review*, *27*(6), 779–787. https://doi.org/10.1103/physrev.27.779

Brutsaert, W. (1965). A model for evaporation as a molecular diffusion process into a turbulent atmosphere. *Journal of Geophysical Research*, *70*(20), 5017–5024. https://doi.org/10.1029/jz070i020p05017

Brutsaert, W. (1982). *Evaporation into the atmosphere: Theory, history, and applications*. Springer.

Brutsaert, W. (2014). Daily evaporation from drying soil: Universal parameterization with similarity. *Water Resources Research*, *50*(4), 3206–3215. https://doi.org/10.1002/2013wr014872

Burkart, S., Manderscheid, R., Wittich, K. P., Löpmeier, F. J., & Weigel, H. J. (2011). Elevated $CO_2$ effects on canopy and soil water flux parameters measured using a large chamber in crops grown with free-air $CO_2$ enrichment. *Plant Biology*, *13*(2), 258–269. https://doi.org/10.1111/j.1438-8677.2010.00360.x

Cai, C., Yin, X., He, S., Jiang, W., Si, C., Struik, P. C., et al. (2016). Responses of wheat and rice to factorial combinations of ambient and elevated $CO_2$ and temperature in FACE experiments. *Global Change Biology*, *22*(2), 856–874. https://doi.org/10.1111/gcb.13065

Cai, W., Gu, X., Du, Y., Chang, T., Lu, S., Zheng, X., et al. (2022). Effects of mulching on water saving, yield increase and emission reduction for maize in China. *Agricultural Water Management*, *274*, 107954. https://doi.org/10.1016/j.agwat.2022.107954

Cammalleri, C., Rallo, G., Agnese, C., Ciraolo, G., Minacapilli, M., & Provenzano, G. (2013). Combined use of eddy covariance and sap flow techniques for partition of ET fluxes and water stress assessment in an irrigated olive orchard. *Agricultural Water Management*, *120*, 89–97. https://doi.org/10.1016/j.agwat.2012.10.003

Campbell, G. S., & Norman, J. M. (1998). *An introduction to environmental biophysics*. Springer Verlag.

Carlson, C. W., Alessi, J., & Mickelson, R. H. (1959). Evapotranspiration and yield of corn as influenced by moisture level, nitrogen fertilization, and plant density. *Soil Science Society of America Journal*, *23*(3), 242–245. https://doi.org/10.2136/sssaj1959.03615995002300030026x

Caviglia, O. P., & Sadras, V. O. (2001). Effect of nitrogen supply on crop conductance, water- and radiation-use efficiency of wheat. *Field Crops Research*, *69*(3), 259–266. https://doi.org/10.1016/s0378-4290(00)00149-0

Čermák, J., Deml, M., & Penka, M. (1973). A new method of sap flow rate determination in trees. *Biologia Plantarum*, *15*(3), 171–178. https://doi.org/10.1007/bf02922390

Čermák, J., Kučera, J., & Penka, M. (1976). Improvement of the method of sap flow rate determination in full-grown trees based on heat balance with direct electric heating of xylem. *Biologia Plantarum*, *18*(2), 105–110. https://doi.org/10.1007/bf02923147

Chai, Y., Chai, Q., Yang, C., Chen, Y., Li, R., Li, Y., et al. (2022). Plastic film mulching increases yield, water productivity, and net income of rain-fed winter wheat compared with no mulching in semiarid Northwest China. *Agricultural Water Management*, *262*, 107420. https://doi.org/10.1016/j.agwat.2021.107420

Chameides, W. L., Kasibhatla, P. S., Yienger, J., & Levy, H. (1994). Growth of continental-scale metro-agro-plexes, regional ozone pollution, and world food production. *Science*, *264*(5155), 74–77. https://doi.org/10.1126/science.264.5155.74

Chavan, S. G., Duursma, R. A., Tausz, M., & Ghannoum, O. (2019). Elevated $CO_2$ alleviates the negative impact of heat stress on wheat physiology but not on grain yield. *Journal of Experimental Botany*, *70*(21), 6447–6459. https://doi.org/10.1093/jxb/erz386

Chen, J., Chen, C. G., Tian, Y. L., Zhang, X., Dong, W. J., Zhang, B., et al. (2017). Differences in the impacts of nighttime warming on crop growth of rice-based cropping systems under field conditions. *European Journal of Agronomy*, *82*, 80–92. https://doi.org/10.1016/j.eja.2016.10.006

Chen, J. L., Kang, S. Z., Du, T. S., Guo, P., Qiu, R. J., Chen, R. Q., & Gu, F. (2014). Modeling relations of tomato yield and fruit quality with water deficit at different growth stages under greenhouse condition. *Agricultural Water Management*, *146*, 131–148. https://doi.org/10.1016/j.agwat.2014.07.026

Chen, N., Li, X., Shi, H., Hu, Q., Zhang, Y., Hou, C., & Liu, Y. (2022). Modeling evapotranspiration and evaporation in corn/tomato intercropping ecosystem using a modified ERIN model considering plastic film mulching. *Agricultural Water Management*, *260*, 107286. https://doi.org/10.1016/j.agwat.2021.107286

Chen, N., Li, X., Shi, H., Yan, J., Hu, Q., & Zhang, Y. (2021). Assessment and modeling of maize evapotranspiration and yield with plastic and biodegradable film mulch. *Agricultural and Forest Meteorology*, *307*, 108474. https://doi.org/10.1016/j.agrformet.2021.108474

Chen, S., Zhang, X., Sun, H., Ren, T., & Wang, Y. (2010). Effects of winter wheat row spacing on evapotranspiration, grain yield and water use efficiency. *Agricultural Water Management*, *97*(8), 1126–1132. https://doi.org/10.1016/j.agwat.2009.09.005

Chen, S., Zhang, Z. Y., Wang, Z. C., Guo, X. P., Liu, M. H., Hamoud, Y. A., et al. (2016). Effects of uneven vertical distribution of soil salinity under a buried straw layer on the growth, fruit yield, and fruit quality of tomato plants. *Scientia Horticulturae*, *203*, 131–142. https://doi.org/10.1016/j.scienta.2016.03.024

Cooper, O. R., Parrish, D. D., Ziemke, J., Balashov, N. V., Cupeiro, M., Galbally, I. E., et al. (2014). Global distribution and trends of tropospheric ozone: An observation-based review. *Elementa: Science of the Anthropocene*, *2*, 000029. https://doi.org/10.12952/journal.elementa.000029

Corwin, D. L., Rhoades, J. D., & Šimůnek, J. (2007). Leaching requirement for soil salinity control: Steady-state versus transient models. *Agricultural Water Management*, *90*(3), 165–180. https://doi.org/10.1016/j.agwat.2007.02.007

Cowan, I. R., & Farquhar, G. D. (1977). Stomatal function in relation to leaf metabolism and environment, *Symposia of the Society for Experimental Biology* (Vol. *31*, pp. 471–505).

Cowan, I. R., & Troughton, J. H. (1971). The relative role of stomata in transpiration and assimilation. *Planta*, *97*(4), 325–336. https://doi.org/10.1007/bf00390212

Cui, Z., Zhang, H., Chen, X., Zhang, C., Ma, W., Huang, C., et al. (2018). Pursuing sustainable productivity with millions of smallholder farmers. *Nature*, *555*(7696), 363–366. https://doi.org/10.1038/nature25785

Cuxart, J., & Boone, A. A. (2020). Evapotranspiration over land from a boundary-layer meteorology perspective. *Boundary-Layer Meteorology*, *177*(2), 427–459. https://doi.org/10.1007/s10546-020-00550-9

Dai, Y., Fan, J., Liao, Z., Zhang, C., Yu, J., Feng, H., et al. (2022). Supplemental irrigation and modified plant density improved photosynthesis, grain yield and water productivity of winter wheat under ridge-furrow mulching. *Agricultural Water Management*, *274*, 107985. https://doi.org/10.1016/j.agwat.2022.107985

Dalton, J. (1802). Experimental essays on the constitution of mixed gases; on the force of steam of vapor from waters and other liquids in different temperatures, both in a Torricellian vacuum and in air on evaporation and on the expansion of gases by heat. *Memoirs and Proceedings - Manchester Literary and Philosophical Society*, *5*, 535–602.

Damour, G., Simonneau, T., Cochard, H., & Urban, L. (2010). An overview of models of stomatal conductance at the leaf level. *Plant, Cell & Environment*, *33*(9), 1419–1438. https://doi.org/10.1111/j.1365-3040.2010.02181.x

Darwin, F. (1898). IX. Observations on stomata. *Philosophical Transactions of the Royal Society of London. Series B, Containing Papers of a Biological Character*, *190*, 531–621.

de Medeiros, G. A., Arruda, F. B., Sakai, E., & Fujiwara, M. (2001). The influence of crop canopy on evapotranspiration and crop coefficient of beans (*Phaseolus vulgaris* L.). *Agricultural Water Management*, *49*(3), 211–224. https://doi.org/10.1016/s0378-3774(00)00150-5

Dewar, R., Mauranen, A., Mäkelä, A., Hölttä, T., Medlyn, B., & Vesala, T. (2018). New insights into the covariation of stomatal, mesophyll and hydraulic conductances from optimization models incorporating nonstomatal limitations to photosynthesis. *New Phytologist*, *217*(2), 571–585. https://doi.org/10.1111/nph.14848

Dickin, E., & Wright, D. (2008). The effects of winter waterlogging and summer drought on the growth and yield of winter wheat (*Triticum aestivum* L.). *European Journal of Agronomy*, *28*(3), 234–244. https://doi.org/10.1016/j.eja.2007.07.010

Ding, R. S., Kang, S. Z., Li, F. S., Zhang, Y. Q., & Tong, L. (2013). Evapotranspiration measurement and estimation using modified Priestley–Taylor model in an irrigated maize field with mulching. *Agricultural and Forest Meteorology*, *168*, 140–148. https://doi.org/10.1016/j.agrformet.2012.08.003

Ding, R. S., Kang, S. Z., Li, F. S., Zhang, Y. Q., Tong, L., & Sun, Q. Y. (2010). Evaluating eddy covariance method by large-scale weighing lysimeter in a maize field of northwest China. *Agricultural Water Management*, *98*(1), 87–95. https://doi.org/10.1016/j.agwat.2010.08.001

Ding, R. S., Kang, S. Z., Zhang, Y. Q., Hao, X. M., Tong, L., & Du, T. S. (2013). Partitioning evapotranspiration into soil evaporation and transpiration using a modified dual crop coefficient model in irrigated maize field with ground-mulching. *Agricultural Water Management*, *127*, 85–96. https://doi.org/10.1016/j.agwat.2013.05.018

Ding, R. S., Tong, L., Li, F. S., Zhang, Y. Q., Hao, X. M., & Kang, S. Z. (2015). Variations of crop coefficient and its influencing factors in an arid advective cropland of northwest China. *Hydrological Processes*, *29*(2), 239–249. https://doi.org/10.1002/hyp.10146

Dixon, H. H., & Joly, J. (1894). On the ascent of sap. *Annals of Botany*, *8*, 468–470.

Djaman, K., Allen, S., Djaman, D. S., Koudahe, K., Irmak, S., Puppala, N., et al. (2022). Planting date and plant density effects on maize growth, yield and water use efficiency. *Environmental Challenges*, *6*, 100417. https://doi.org/10.1016/j.envc.2021.100417

Döll, P., & Siebert, S. (2002). Global modeling of irrigation water requirements. *Water Resources Research*, *38*(4), 1037. https://doi.org/10.1029/2001wr000355

Dong, W. J., Chen, J., Zhang, B., Tian, Y. L., & Zhang, W. J. (2011). Responses of biomass growth and grain yield of midseason rice to the anticipated warming with FATI facility in East China. *Field Crops Research*, *123*(3), 259–265. https://doi.org/10.1016/j.fcr.2011.05.024

Easterling, W. E., Rosenberg, N. J., McKenney, M. S., Allan Jones, C., Dyke, P. T., & Williams, J. R. (1992). Preparing the erosion productivity impact calculator (EPIC) model to simulate crop response to climate change and the direct effects of $CO_2$. *Agricultural and Forest Meteorology*, *59*(1), 17–34. https://doi.org/10.1016/0168-1923(92)90084-h

Eberbach, P., & Pala, M. (2005). Crop row spacing and its influence on the partitioning of evapotranspiration by winter-grown wheat in Northern Syria. *Plant and Soil*, *268*(1), 195–208. https://doi.org/10.1007/s11104-004-0271-y

Echarte, L., Echarte, M. M., Cerrudo, D., Gonzalez, V. H., Alfonso, C., Cambareri, M., et al. (2020). Sunflower evapotranspiration and water use efficiency in response to plant density. *Crop Science*, *60*(1), 357–366. https://doi.org/10.1002/csc2.20001

Ewers, B. E., & Oren, R. (2000). Analyses of assumptions and errors in the calculation of stomatal conductance from sap flux measurements. *Tree Physiology*, *20*(9), 579–589. https://doi.org/10.1093/treephys/20.9.579

Fan, Y., Ding, R., Kang, S., Hao, X., Du, T., Tong, L., & Li, S. (2017). Plastic mulch decreases available energy and evapotranspiration and improves yield and water use efficiency in an irrigated maize cropland. *Agricultural Water Management*, *179*, 122–131. https://doi.org/10.1016/j.agwat.2016.08.019

FAO Statistics. (2024). Food and Agricultural Organization: FAOSTAT Section. Retrieved from www.fao.org/faostat/en/#data/QCL

Farooq, M., Wahid, A., Kobayashi, N., Fujita, D., & Basra, S. M. A. (2009). *Plant drought stress: Effects, mechanisms and management*, *Sustainable Agriculture* (pp. 153–188). Springer.

Feng, X. Y., Liu, H. J., Feng, D. X., Tang, X. P., Li, L., Chang, J., et al. (2023). Quantifying winter wheat evapotranspiration and crop coefficients under sprinkler irrigation using eddy covariance technology in the North China Plain. *Agricultural Water Management*, *277*, 108131. https://doi.org/10.1016/j.agwat.2022.108131

Feng, Y., Cui, N., Du, T., Gong, D., Hu, X., & Zhao, L. (2017). Response of sap flux and evapotranspiration to deficit irrigation of greenhouse pear-jujube trees in semi-arid northwest China. *Agricultural Water Management*, *194*, 1–12. https://doi.org/10.1016/j.agwat.2017.08.019

Feng, Y., Gong, D., Mei, X., Hao, W., Tang, D., & Cui, N. (2017). Energy balance and partitioning in partial plastic mulched and non-mulched maize fields on the Loess Plateau of China. *Agricultural Water Management*, *191*, 193–206. https://doi.org/10.1016/j.agwat.2017.06.009

Feng, Z. Z., & Kobayashi, K. (2009). Assessing the impacts of current and future concentrations of surface ozone on crop yield with meta-analysis. *Atmospheric Environment*, *43*(8), 1510–1519. https://doi.org/10.1016/j.atmosenv.2008.11.033

Feng, Z. Z., Kobayashi, K., & Ainsworth, E. A. (2008). Impact of elevated ozone concentration on growth, physiology, and yield of wheat (*Triticum aestivum* L.): A meta-analysis. *Global Change Biology*, *14*(11), 2696–2708. https://doi.org/10.1111/j.1365-2486.2008.01673.x

Feng, Z. Z., Xu, Y. S., Kobayashi, K., Dai, L. L., Zhang, T. Y., Agathokleous, E., et al. (2022). Ozone pollution threatens the production of major staple crops in East Asia. *Nature Food*, *3*(1), 47–56. https://doi.org/10.1038/s43016-021-00422-6

Ferreira, T. C., & Carr, M. K. V. (2002). Responses of potatoes (*Solanum tuberosum* L.) to irrigation and nitrogen in a hot, dry climate: I. Water use. *Field Crops Research*, *78*(1), 51–64. https://doi.org/10.1016/s0378-4290(02)00089-8

Fischer, M., Katul, G., Noormets, A., Pozníková, G., Domec, J., Orság, M., et al. (2023). Merging flux-variance with surface renewal methods in the roughness sublayer and the atmospheric surface layer. *Agricultural and Forest Meteorology*, *342*, 109692. https://doi.org/10.1016/j.agrformet.2023.109692

Flumignan, D. L., de Faria, R. T., & Prete, C. E. C. (2011). Evapotranspiration components and dual crop coefficients of coffee trees during crop production. *Agricultural Water Management*, *98*(5), 791–800. https://doi.org/10.1016/j.agwat.2010.12.002

Francescangeli, N., Sangiacomo, M. A., & Martí, H. (2006). Effects of plant density in broccoli on yield and radiation use efficiency. *Scientia Horticulturae*, *110*(2), 135–143. https://doi.org/10.1016/j.scienta.2006.06.025

Gao, Y., Xie, Y., Jiang, H., Wu, B., & Niu, J. (2014). Soil water status and root distribution across the rooting zone in maize with plastic film mulching. *Field Crops Research*, *156*, 40–47. https://doi.org/10.1016/j.fcr.2013.10.016

Gardiol, J. M., Serio, L. A., & Della Maggiora, A. I. (2003). Modelling evapotranspiration of corn (*Zea mays*) under different plant densities. *Journal of Hydrology*, *271*(1), 188–196. https://doi.org/10.1016/s0022-1694(02)00347-5

Gardner, H. R., & Gardner, W. R. (1969). Relation of water application to evaporation and storage of soil water. *Soil Science Society of America Journal*, *33*(2), 192–196. https://doi.org/10.2136/sssaj1969.03615995003300020012x

Gardner, W. R. (1959). Solutions of the flow equation for the drying of soils and other porous media. *Soil Science Society of America Journal*, *23*(3), 183–187. https://doi.org/10.2136/sssaj1959.03615995002300030010x

Garratt, J. R., & Hicks, B. B. (1973). Momentum, heat and water vapour transfer to and from natural and artificial surfaces. *Quarterly Journal of the Royal Meteorological Society*, *99*(422), 680–687. https://doi.org/10.1002/qj.49709942209

Göksoy, A. T., Demir, A. O., Turan, Z. M., & Dağüstü, N. (2004). Responses of sunflower (*Helianthus annuus* L.) to full and limited irrigation at different growth stages. *Field Crops Research*, *87*(2), 167–178. https://doi.org/10.1016/j.fcr.2003.11.004

Gong, X. W., Li, X. M., Qiu, R. J., Bo, G. K., Ping, Y. L., Xin, Q. S., & Ge, J. K. (2022). Ventilation and irrigation management strategy for tomato cultivated in greenhouses. *Agricultural Water Management*, *273*, 107908. https://doi.org/10.1016/j.agwat.2022.107908

Gong, X. W., Qiu, R. J., Sun, J. S., Ge, J. K., Li, Y. B., & Wang, S. S. (2020). Evapotranspiration and crop coefficient of tomato grown in a solar greenhouse under full and deficit irrigation. *Agricultural Water Management*, *235*, 106154. https://doi.org/10.1016/j.agwat.2020.106154

Granier, A. (1987). Evaluation of transpiration in a Douglas-fir stand by means of sap flow measurements. *Tree Physiology*, *3*(4), 309–320. https://doi.org/10.1093/treephys/3.4.309

Green, D. H., & Weedon, M. M. (2012). Modelling photosynthetic responses to temperature of grapevine (*Vitis vinifera* cv. Semillon) leaves on vines grown in a hot climate. *Plant, Cell & Environment*, *35*(6), 1050–1064. https://doi.org/10.1111/j.1365-3040.2011.02471.x

Grime, V. L., Morison, J. I., & Simmonds, L. P. (1995). Including the heat storage term in sap flow measurements with the stem heat balance method. *Agricultural and Forest Meteorology*, *74*(1–2), 1–25. https://doi.org/10.1016/0168-1923(94)02187-o

Grossiord, C., Sevanto, S., Borrego, I., Chan, A. M., Collins, A. D., Dickman, L. T., et al. (2017). Tree water dynamics in a drying and warming world. *Plant, Cell & Environment*, *40*(9), 1861–1873. https://doi.org/10.1111/pce.12991

Guo, H., Li, S., Kang, S., Du, T., Liu, W., Tong, L., et al. (2022). The controlling factors of ecosystem water use efficiency in maize fields under drip and border irrigation systems in Northwest China. *Agricultural Water Management*, *272*, 107839. https://doi.org/10.1016/j.agwat.2022.107839

Guswa, A. J. (2008). The influence of climate on root depth: A carbon cost-benefit analysis. *Water Resources Research*, *44*(2), W02427. https://doi.org/10.1029/2007wr006384

Guswa, A. J. (2010). Effect of plant uptake strategy on the water– optimal root depth. *Water Resources Research*, *46*(9), W09601. https://doi.org/10.1029/2010wr009122

Halley, E. (1687). An estimate of the quantity of vapour raised out of the sea by the warmth of the sun; derived from an experiment shown before the Royal Society, at one of their late meetings. *Philosophical Transactions of the Royal Society of London*, *16*(189), 366–370. https://doi.org/10.1098/rstl.1686.0067

Hari, P., Mäkelä, A., Korpilahti, E., & Holmberg, M. (1986). Optimal control of gas exchange. *Tree Physiology*, *2*(1–2-3), 169–175. https://doi.org/10.1093/treephys/2.1-2-3.169

Harman, I. N., & Finnigan, J. J. (2008). Scalar concentration profiles in the canopy and roughness sublayer. *Boundary-Layer Meteorology*, *129*(3), 323–351. https://doi.org/10.1007/s10546-008-9328-4

Hatamnia, A. A., Abbaspour, N., Darvishzadeh, R., Rahmani, F., & Heidari, R. (2013). Effect of salt stress on growth, ion content and photosynthesis of two oriental Tobacco (*Nicotiana tabacum*) cultivars. *International Journal of Agriculture and Crop Sciences*, *6*(11), 757–761.

Hernández, M., Echarte, L., Della Maggiora, A., Cambareri, M., Barbieri, P., & Cerrudo, D. (2015). Maize water use efficiency and evapotranspiration response to N supply under contrasting soil water availability. *Field Crops Research*, *178*, 8–15. https://doi.org/10.1016/j.fcr.2015.03.017

Herzog, M., Striker, G. G., Colmer, T. D., & Pedersen, O. (2016). Mechanisms of waterlogging tolerance in wheat – A review of root and shoot physiology. *Plant, Cell & Environment*, *39*(5), 1068–1086. https://doi.org/10.1111/pce.12676

Homaee, M., Dirksen, C., & Feddes, R. A. (2002). Simulation of root water uptake: I. Non-uniform transient salinity using different macroscopic reduction functions. *Agricultural Water Management*, *57*(2), 89–109. https://doi.org/10.1016/s0378-3774(02)00072-0

Homaee, M., & Schmidhalter, U. (2008). Water integration by plants root under non-uniform soil salinity. *Irrigation Science*, *27*(1), 83–95. https://doi.org/10.1007/s00271-008-0123-2

Hou, X., Li, R., He, W., & Ma, K. (2020). Effects of planting density on potato growth, yield, and water use efficiency during years with variable rainfall on the Loess Plateau, China. *Agricultural Water Management*, *230*, 105982. https://doi.org/10.1016/j.agwat.2019.105982

Hsiao, T. C. (1973). Plant responses to water stress. *Annual Review of Plant Physiology*, *24*(1), 519–570. https://doi.org/10.1146/annurev.pp.24.060173.002511

Hu, E. Z., Gao, F., Xin, Y., Jia, H. X., Li, K. H., Hu, J. J., & Feng, Z. Z. (2015). Concentration- and flux-based ozone dose–response relationships for five poplar clones grown in North China. *Environmental Pollution*, *207*, 21–30. https://doi.org/10.1016/j.envpol.2015.08.034

Hu, Y., Buttar, N. A., Tanny, J., Snyder, R. L., Savage, M. J., & Lakhiar, I. A. (2018). Surface renewal application for estimating evapotranspiration: A review. *Advances in Meteorology*, *2018*(1), 1690714. https://doi.org/10.1155/2018/1690714

Hu, Z., Yu, G., Zhou, Y., Sun, X., Li, Y., Shi, P., et al. (2009). Partitioning of evapotranspiration and its controls in four grassland ecosystems: Application of a two-source model. *Agricultural and Forest Meteorology*, *149*(9), 1410–1420. https://doi.org/10.1016/j.agrformet.2009.03.014

Huang, B., Johnson, J. W., Nesmith, S., & Bridges, D. C. (1994). Growth, physiological and anatomical responses of two wheat genotypes to waterlogging and nutrient supply. *Journal of Experimental Botany*, *45*(2), 193–202. https://doi.org/10.1093/jxb/45.2.193

Huang, C., Chu, C., Hsieh, C., Palmroth, S., & Katul, G. G. (2015). Wind-induced leaf transpiration. *Advances in Water Resources*, *86*, 240–255. https://doi.org/10.1016/j.advwatres.2015.10.009

Hunsaker, D. J., Kimball, B. A., Pinter, P. J., Wall, G. W., LaMorte, R. L., Adamsen, F. J., et al. (2000). $CO_2$ enrichment and soil nitrogen effects on wheat evapotranspiration and water use efficiency. *Agricultural and Forest Meteorology*, *104*(2), 85–105. https://doi.org/10.1016/s0168-1923(00)00157-x

Hussain, M. Z., VanLoocke, A., Siebers, M. H., Ruiz-Vera, U. M., Cody Markelz, R. J., Leakey, A. D. B., et al. (2013). Future carbon dioxide concentration decreases canopy evapotranspiration and soil water depletion by field-grown maize. *Global Change Biology*, *19*(5), 1572–1584. https://doi.org/10.1111/gcb.12155

ICID. (2021). International Commission on Irrigation and Drainage (ICID) Database. Retrieved from https://icid-ciid.org/knowledge/icid_database

IPCC. (2021). Summary for Policymakers. In V. Masson-Delmotte, P. Zhai, A. Pirani, S. L. Connors, C. Péan, S. Berger, et al. (Eds.), *Climate Change 2021: The Physical Science Basis. Contribution of Working Group I to the Sixth Assessment Report of the Intergovernmental Panel on Climate Change*. Cambridge University Press.

Irmak, S., Amiri, E., Bazkiaee, P. A., & Araji, H. A. (2024). Evaluation of CERES-Maize model for simulating maize phenology, grain yield, soil–water, evapotranspiration, and water productivity under different nitrogen levels and rainfed, limited, and full irrigation conditions. *Irrigation Science*, *42*(3), 551–573. https://doi.org/10.1007/s00271-023-00909-z

Jarvis, P. G. (1976). The interpretation of the variations in leaf water potential and stomatal conductance found in canopies in the field. *Biological Sciences*, *273*(927), 593–610.

Jensen, K. H., Berg-Sørensen, K., Bruus, H., Holbrook, N. M., Liesche, J., Schulz, A., et al. (2016). Sap flow and sugar transport in plants. *Reviews of Modern Physics*, *88*(3), 035007. https://doi.org/10.1103/revmodphys.88.035007

Jia, Q., Sun, L., Ali, S., Zhang, Y., Liu, D., Kamran, M., et al. (2018). Effect of planting density and pattern on maize yield and rainwater use efficiency in the Loess Plateau in China. *Agricultural Water Management*, *202*, 19–32. https://doi.org/10.1016/j.agwat.2018.02.011

Jiang, X., Kang, S., Li, F., Du, T., Tong, L., & Comas, L. (2016). Evapotranspiration partitioning and variation of sap flow in female and male parents of maize for hybrid seed production in arid region. *Agricultural Water Management*, *176*, 132–141. https://doi.org/10.1016/j.agwat.2016.05.022

Jiang, X., Kang, S., Tong, L., Li, F., Li, D., Ding, R., & Qiu, R. (2014). Crop coefficient and evapotranspiration of grain maize modified by planting density in an arid region of northwest China. *Agricultural Water Management*, *142*, 135–143. https://doi.org/10.1016/j.agwat.2014.05.006

Jiao, L. J., Ding, R. S., Kang, S. Z., Du, T. S., Tong, L., & Li, S. E. (2018). A comparison of energy partitioning and evapotranspiration over closed maize and sparse grapevine canopies in northwest China. *Agricultural Water Management*, *203*, 251–260. https://doi.org/10.1016/j.agwat.2018.03.019

Johnson, D. M., Katul, G., & Domec, J. C. (2022). Catastrophic hydraulic failure and tipping points in plants. *Plant, Cell & Environment*, *45*(8), 2231–2266. https://doi.org/10.1111/pce.14327

Ju, C., Buresh, R. J., Wang, Z., Zhang, H., Liu, L., Yang, J., & Zhang, J. (2015). Root and shoot traits for rice varieties with higher grain yield and higher nitrogen use efficiency at lower nitrogen rates application. *Field Crops Research*, *175*, 47–55. https://doi.org/10.1016/j.fcr.2015.02.007

Jung, M., Reichstein, M., Ciais, P., Seneviratne, S. I., Sheffield, J., Goulden, M. L., et al. (2010). Recent decline in the global land evapotranspiration trend due to limited moisture supply. *Nature*, *467*(7318), 951–954. https://doi.org/10.1038/nature09396

Jury, W. A., & Horton, R. (2004). *Soil physics* (6th ed.). John Wiley & Sons.

Kaimal, J. C., & Wyngaard, J. C. (1990). The Kansas and Minnesota experiments. *Boundary-Layer Meteorology*, *50*(1), 31–47. https://doi.org/10.1007/bf00120517

Kanani, E., Dehghanisanij, H., & Akhavan, S. (2022). Variation in actual corn (*Zea mays* L.) evapotranspiration, single, and dual crop coefficient under different point source irrigation systems in a semiarid region. *Theoretical and Applied Climatology*, *148*(1), 303–315. https://doi.org/10.1007/s00704-022-03932-w

Kang, S., Hao, X., Du, T., Tong, L., Su, X., Lu, H., et al. (2017). Improving agricultural water productivity to ensure food security in China under changing environment: From research to practice. *Agricultural Water Management*, *179*, 5–17. https://doi.org/10.1016/j.agwat.2016.05.007

Kang, S., Zhang, F., Hu, X., & Zhang, J. (2002). Benefits of $CO_2$ enrichment on crop plants are modified by soil water status. *Plant and Soil*, *238*(1), 69–77. https://doi.org/10.1023/a:1014244413067

Kang, S., Zhang, L., Liang, Y., Hu, X., Cai, H., & Gu, B. (2002). Effects of limited irrigation on yield and water use efficiency of winter wheat in the Loess Plateau of China. *Agricultural Water Management*, *55*(3), 203–216. https://doi.org/10.1016/s0378-3774(01)00180-9

Karam, F., Breidy, J., Stephan, C., & Rouphael, J. (2003). Evapotranspiration, yield and water use efficiency of drip irrigated corn in the Bekaa Valley of Lebanon. *Agricultural Water Management*, *63*(2), 125–137. https://doi.org/10.1016/s0378-3774(03)00179-3

Karam, F., Lahoud, R., Masaad, R., Kabalan, R., Breidi, J., Chalita, C., & Rouphael, Y. (2007). Evapotranspiration, seed yield and water use efficiency of drip irrigated sunflower under full and deficit irrigation conditions. *Agricultural Water Management*, *90*(3), 213–223. https://doi.org/10.1016/j.agwat.2007.03.009

Katerji, N., Van Hoorn, J. W., Hamdy, A., & Mastrorilli, M. (2003). Salinity effect on crop development and yield, analysis of salt tolerance according to several classification methods. *Agricultural Water Management*, *62*(1), 37–66. https://doi.org/10.1016/s0378-3774(03)00005-2

Katul, G., Hsieh, C., Oren, R., Ellsworth, D., & Phillips, N. (1996). Latent and sensible heat flux predictions from a uniform pine forest using surface renewal and flux variance methods. *Boundary-Layer Meteorology*, *80*(3), 249–282. https://doi.org/10.1007/bf00119545

Katul, G., & Liu, H. (2017). A Kolmogorov-Brutsaert structure function model for evaporation into a turbulent atmosphere. *Water Resources Research*, *53*(5), 3635–3644. https://doi.org/10.1002/2016wr020006

Katul, G. G., Oren, R., Manzoni, S., Higgins, C., & Parlange, M. B. (2012). Evapotranspiration: A process driving mass transport and energy exchange in the soil-plant-atmosphere-climate system. *Reviews of Geophysics*, *50*(3), RG3002. https://doi.org/10.1029/2011rg000366

Katul, G. G., Palmroth, S., & Oren, R. (2009). Leaf stomatal responses to vapour pressure deficit under current and $CO_2$-enriched atmosphere explained by the economics of gas exchange. *Plant, Cell & Environment*, *32*(8), 968–979. https://doi.org/10.1111/j.1365-3040.2009.01977.x

Katul, G. G., & Parlange, M. B. (1992). A Penman-Brutsaert model for wet surface evaporation. *Water Resources Research*, *28*(1), 121–126. https://doi.org/10.1029/91wr02324

Khanna, P., Kaur, K., & Gupta, A. K. (2017). Root biomass partitioning, differential antioxidant system and thiourea spray are responsible for heat tolerance in spring maize. *Proceedings of the National Academy of Sciences, India Section B: Biological Sciences*, *87*(2), 351–359. https://doi.org/10.1007/s40011-015-0575-0

Khozaei, M., Kamgar Haghighi, A. A., Zand Parsa, S., Sepaskhah, A. R., Razzaghi, F., Yousefabadi, V., & Emam, Y. (2020). Evaluation of direct seeding and transplanting in sugar beet for water productivity, yield and quality under different irrigation regimes and planting densities. *Agricultural Water Management*, *238*, 106230. https://doi.org/10.1016/j.agwat.2020.106230

Kim, H., Ko, J., Kang, S., & Tenhunen, J. (2013). Impacts of climate change on paddy rice yield in a temperate climate. *Global Change Biology*, *19*(2), 548–562. https://doi.org/10.1111/gcb.12047

Kimball, B. A., LaMorte, R. L., Pinter, P. J., Jr., Wall, G. W., Hunsaker, D. J., Adamsen, F. J., et al. (1999). Free-air $CO_2$ enrichment and soil nitrogen effects on energy balance and evapotranspiration of wheat. *Water Resources Research*, *35*(4), 1179–1190. https://doi.org/10.1029/1998wr900115

Kimball, B. A., LaMorte, R. L., Seay, R. S., Pinter, P. J., Rokey, R. R., Hunsaker, D. J., et al. (1994). Effects of free-air $CO_2$ enrichment on energy balance and evapotranspiration of cotton. *Agricultural and Forest Meteorology*, *70*(1), 259–278. https://doi.org/10.1016/0168-1923(94)90062-0

Kiremit, M. S., & Arslan, H. (2016). Effects of irrigation water salinity on drainage water salinity, evapotranspiration and other leek (*Allium porrum* L.) plant parameters. *Scientia Horticulturae*, *201*, 211–217. https://doi.org/10.1016/j.scienta.2016.02.001

Kjelgaard, J. F., Stockle, C. O., Black, R. A., & Campbell, G. S. (1997). Measuring sap flow with the heat balance approach using constant and variable heat inputs. *Agricultural and Forest Meteorology*, *85*(3–4), 239–250. https://doi.org/10.1016/s0168-1923(96)02397-0

Konrad, W., Katul, G., & Roth Nebelsick, A. (2021). Leaf temperature and its dependence on atmospheric $CO_2$ and leaf size. *Geological Journal*, *56*(2), 866–885. https://doi.org/10.1002/gj.3757

Konrad, W., Katul, G., Roth-Nebelsick, A., & Jensen, K. H. (2019). Xylem functioning, dysfunction and repair: A physical perspective and implications for phloem transport. *Tree Physiology*, *39*(2), 243–261. https://doi.org/10.1093/treephys/tpy097

Kool, D., Agam, N., Lazarovitch, N., Heitman, J. L., Sauer, T. J., & Ben-Gal, A. (2014). A review of approaches for evapotranspiration partitioning. *Agricultural and Forest Meteorology*, *184*, 56–70. https://doi.org/10.1016/j.agrformet.2013.09.003

Kool, D., Ben-Gal, A., & Agam, N. (2018). Within-field advection enhances evaporation and transpiration in a vineyard in an arid environment. *Agricultural and Forest Meteorology*, *255*, 104–113. https://doi.org/10.1016/j.agrformet.2017.10.018

Köstner, B., Granier, A., & Cermák, J. (1998). Sapflow measurements in forest stands: Methods and uncertainties. *Annals of Forest Science*, *55*(1–2), 13–27. https://doi.org/10.1051/forest:19980102

Kotak, S., Larkindale, J., Lee, U., von Koskull-Döring, P., Vierling, E., & Scharf, K. (2007). Complexity of the heat stress response in plants. *Current Opinion in Plant Biology*, *10*(3), 310–316. https://doi.org/10.1016/j.pbi.2007.04.011

Kou, X., Han, W., & Kang, J. (2022). Responses of root system architecture to water stress at multiple levels: A meta-analysis of trials under controlled conditions. *Frontiers in Plant Science*, *13*, 1085409. https://doi.org/10.3389/fpls.2022.1085409

Larcher, W. (2003). *Physiological plant ecology: Ecophysiology and stress physiology of functional groups*. Springer-Verlag.

Lei, H., & Yang, D. (2010). Interannual and seasonal variability in evapotranspiration and energy partitioning over an irrigated cropland in the North China Plain. *Agricultural and Forest Meteorology*, *150*(4), 581–589. https://doi.org/10.1016/j.agrformet.2010.01.022

Lenka, N. K., Lenka, S., Thakur, J. K., Yashona, D. S., Shukla, A. K., Elanchezhian, R., et al. (2020). Carbon dioxide and temperature elevation effects on crop evapotranspiration and water use efficiency in soybean as affected by different nitrogen levels. *Agricultural Water Management*, *230*, 105936. https://doi.org/10.1016/j.agwat.2019.105936

Lenka, N. K., Lenka, S., Yashona, D. S., & Jat, D. (2021). Elevated temperature and low nitrogen partially offset the yield, evapotranspiration, and water use efficiency of winter wheat under carbon dioxide enrichment. *Agricultural Water Management*, *250*, 106856. https://doi.org/10.1016/j.agwat.2021.106856

Lenka, S., Singh, A. K., & Lenka, N. K. (2009). Water and nitrogen interaction on soil profile water extraction and ET in maize–wheat cropping system. *Agricultural Water Management*, *96*(2), 195–207. https://doi.org/10.1016/j.agwat.2008.06.014

Letey, J., & Feng, G. L. (2007). Dynamic versus steady-state approaches to evaluate irrigation management of saline waters. *Agricultural Water Management*, *91*(1–3), 1–10. https://doi.org/10.1016/j.agwat.2007.02.014

Lewis, J. M. (1995). The story behind the Bowen ratio. *Bulletin of the American Meteorological Society*, *76*(12), 2433–2444. https://doi.org/10.1175/1520-0477(1995)076<2433:tsbtbr>2.0.co;2

Li, B., Shi, B., Yao, Z., Kumar Shukla, M., & Du, T. (2020). Energy partitioning and microclimate of solar greenhouse under drip and furrow irrigation systems. *Agricultural Water Management*, *234*, 106096. https://doi.org/10.1016/j.agwat.2020.106096

Li, B., Wim, V., Shukla, M. K., & Du, T. (2021). Drip irrigation provides a trade-off between yield and nutritional quality of tomato in the solar greenhouse. *Agricultural Water Management*, *249*, 106777. https://doi.org/10.1016/j.agwat.2021.106777

Li, C., Wang, N., Luo, X., Li, Y., Zhang, T., Ding, D., et al. (2023). Introducing water factors improves simulations of maize stomatal conductance models under plastic film mulching in arid and semi-arid irrigation areas. *Journal of Hydrology*, *617*, 128908. https://doi.org/10.1016/j.jhydrol.2022.128908

Li, F. S., Kang, S. Z., & Zhang, J. H. (2004). Interactive effects of elevated $CO_2$, nitrogen and drought on leaf area, stomatal conductance, and evapotranspiration of wheat. *Agricultural Water Management*, *67*(3), 221–233. https://doi.org/10.1016/j.agwat.2004.01.005

Li, L., & Yu, Q. (2007). Quantifying the effects of advection on canopy energy budgets and water use efficiency in an irrigated wheat field in the North China Plain. *Agricultural Water Management*, *89*(1), 116–122. https://doi.org/10.1016/j.agwat.2006.12.003

Li, Q., Li, H., Zhang, L., Zhang, S., & Chen, Y. (2018). Mulching improves yield and water-use efficiency of potato cropping in China: A meta-analysis. *Field Crops Research*, *221*, 50–60. https://doi.org/10.1016/j.fcr.2018.02.017

Li, S., Kang, S., Zhang, L., Ortega-Farias, S., Li, F., Du, T., et al. (2013). Measuring and modeling maize evapotranspiration under plastic film-mulching condition. *Journal of Hydrology*, *503*, 153–168. https://doi.org/10.1016/j.jhydrol.2013.07.033

Li, S. X., Wang, Z. H., Li, S. Q., Gao, Y. J., & Tian, X. H. (2013). Effect of plastic sheet mulch, wheat straw mulch, and maize growth on water loss by evaporation in dryland areas of China. *Agricultural Water Management*, *116*, 39–49. https://doi.org/10.1016/j.agwat.2012.10.004

Li, X. J., Kang, S. Z., Niu, J., Huo, Z. L., & Liu, J. Z. (2019). Improving the representation of stomatal responses to $CO_2$ within the Penman–Monteith model to better estimate evapotranspiration responses to climate change. *Journal of Hydrology*, *572*, 692–705. https://doi.org/10.1016/j.jhydrol.2019.03.029

Li, X. J., Kang, S. Z., Zhang, X. T., Li, F. S., & Lu, H. N. (2018). Deficit irrigation provokes more pronounced responses of maize photosynthesis and water productivity to elevated $CO_2$. *Agricultural Water Management*, *195*, 71–83. https://doi.org/10.1016/j.agwat.2017.09.017

Liao, Q., Ding, R., Du, T., Kang, S., Tong, L., & Li, S. (2022). Stomatal conductance drives variations of yield and water use of maize under water and nitrogen stress. *Agricultural Water Management*, *268*, 107651. https://doi.org/10.1016/j.agwat.2022.107651

Liebhard, G., Klik, A., Neugschwandtner, R. W., & Nolz, R. (2022). Effects of tillage systems on soil water distribution, crop development, and evaporation and transpiration rates of soybean. *Agricultural Water Management*, *269*, 107719. https://doi.org/10.1016/j.agwat.2022.107719

Liu, B., Asseng, S., Liu, L., Tang, L., Cao, W., & Zhu, Y. (2016). Testing the responses of four wheat crop models to heat stress at anthesis and grain filling. *Global Change Biology*, *22*(5), 1890–1903. https://doi.org/10.1111/gcb.13212

Liu, B., Asseng, S., Wang, A., Wang, S., Tang, L., Cao, W., et al. (2017). Modelling the effects of post-heading heat stress on biomass growth of winter wheat. *Agricultural and Forest Meteorology*, *247*, 476–490. https://doi.org/10.1016/j.agrformet.2017.08.018

Liu, B., Cui, Y., Luo, Y., Shi, Y., Liu, M., & Liu, F. (2019). Energy partitioning and evapotranspiration over a rotated paddy field in Southern China. *Agricultural and Forest Meteorology*, *276–277*, 107626. https://doi.org/10.1016/j.agrformet.2019.107626

Liu, B., Han, H., Liu, X., Li, C., Chen, X., Wu, H., et al. (2022). Quantifying the effects of advection on single crop coefficients over a humid paddy field for sustainable irrigation. *Journal of Hydrology*, *614*, 128552. https://doi.org/10.1016/j.jhydrol.2022.128552

Liu, C., Zhang, X., & Zhang, Y. (2002). Determination of daily evaporation and evapotranspiration of winter wheat and maize by large-scale weighing lysimeter and micro-lysimeter. *Agricultural and Forest Meteorology*, *111*(2), 109–120. https://doi.org/10.1016/s0168-1923(02)00015-1

Liu, C. W., Du, T. S., Li, F. S., Kang, S. Z., Li, S. E., & Tong, L. (2012). Trunk sap flow characteristics during two growth stages of apple tree and its relationships with affecting factors in an arid region of northwest China. *Agricultural Water Management*, *104*, 193–202. https://doi.org/10.1016/j.agwat.2011.12.014

Liu, G., Zuo, Y., Zhang, Q., Yang, L., Zhao, E., Liang, L., & Tong, Y. A. (2018). Ridge-furrow with plastic film and straw mulch increases water availability and wheat production on the Loess Plateau. *Scientific Reports*, *8*(1), 6503. https://doi.org/10.1038/s41598-018-24864-4

Liu, J., Kang, S., Davies, W. J., & Ding, R. (2020). Elevated [$CO_2$] alleviates the impacts of water deficit on xylem anatomy and hydraulic properties of maize stems. *Plant, Cell & Environment*, *43*(3), 563–578. https://doi.org/10.1111/pce.13677

Liu, L., Hu, C., Olesen, J. E., Ju, Z., & Zhang, X. (2016). Effect of warming and nitrogen addition on evapotranspiration and water use efficiency in a wheat-soybean/fallow rotation from 2010 to 2014. *Climatic Change*, *139*(3), 565–578. https://doi.org/10.1007/s10584-016-1825-8

Liu, M., Paredes, P., Shi, H., Ramos, T. B., Dou, X., Dai, L., & Pereira, L. S. (2022). Impacts of a shallow saline water table on maize evapotranspiration and groundwater contribution using static water table lysimeters and the dual Kc water balance model SIMDualKc. *Agricultural Water Management*, *273*, 107887. https://doi.org/10.1016/j.agwat.2022.107887

Liu, M., Shi, H., Paredes, P., Ramos, T. B., Dai, L., Feng, Z., & Pereira, L. S. (2022). Estimating and partitioning maize evapotranspiration as affected by salinity using weighing lysimeters and the SIMDualKc model. *Agricultural Water Management*, *261*, 107362. https://doi.org/10.1016/j.agwat.2021.107362

Liu, Y., Qiu, G., Zhang, H., Yang, Y., Zhang, Y., Wang, Q., et al. (2022). Shifting from homogeneous to heterogeneous surfaces in estimating terrestrial evapotranspiration: Review and perspectives. *Science China Earth Sciences*, *65*(2), 1–18. https://doi.org/10.1007/s11430-020-9834-y

Liu, Y., Yuan, S., Zhu, Y., Ren, L., Chen, R., Zhu, X., & Xia, R. (2023). The patterns, magnitude, and drivers of unprecedented 2022 mega-drought in the Yangtze River Basin, China. *Environmental Research Letters*, *18*(11), 114006. https://doi.org/10.1088/1748-9326/acfe21

Liu, Y. E., Hou, P., Huang, G. R., Zhong, X. L., Li, H. R., Zhao, J. R., et al. (2021). Maize grain yield and water use efficiency in relation to climatic factors and plant population in northern China. *Journal of Integrative Agriculture*, *20*(12), 3156–3169. https://doi.org/10.1016/s2095-3119(20)63428-1

Lu, P. L., Yu, Q., Wang, E. L., Liu, J. D., & Xu, S. H. (2008). Effects of climatic variation and warming on rice development across South China. *Climate Research*, *36*(1), 79–88. https://doi.org/10.3354/cr00729

Lu, Y. Y., & Fricke, W. (2023). Changes in root hydraulic conductivity in wheat (*Triticum aestivum* L.) in response to salt stress and day/night can best be explained through altered activity of aquaporins. *Plant, Cell & Environment*, *46*(3), 747–763. https://doi.org/10.1111/pce.14535

Lv, Y. P., Xu, J. Z., Yang, S. H., Liu, X. Y., Zhang, J. G., & Wang, Y. J. (2018). Inter-seasonal and cross-treatment variability in single-crop coefficients for rice evapotranspiration estimation and their validation under drying-wetting cycle conditions. *Agricultural Water Management*, *196*, 154–161. https://doi.org/10.1016/j.agwat.2017.11.006

Ma, D., Chen, L., Qu, H., Wang, Y., Misselbrook, T., & Jiang, R. (2018). Impacts of plastic film mulching on crop yields, soil water, nitrate, and organic carbon in Northwestern China: A meta-analysis. *Agricultural Water Management*, *202*, 166–173. https://doi.org/10.1016/j.agwat.2018.02.001

Ma, T., Zeng, W., Li, Q., Yang, X., Wu, J., & Huang, J. (2017). Shoot and root biomass allocation of sunflower varying with soil salinity and nitrogen applications. *Agronomy Journal*, *109*(6), 2545–2555. https://doi.org/10.2134/agronj2017.04.0194

Maas, E. V., & Hoffman, G. J. (1977). Crop salt tolerance-current assessment. *Journal of the Irrigation and Drainage Division*, *103*(2), 115–134. https://doi.org/10.1061/jrcea4.0001137

Maggio, A., De Pascale, S., Angelino, G., Ruggiero, C., & Barbieri, G. (2004). Physiological response of tomato to saline irrigation in long-term salinized soils. *European Journal of Agronomy*, *21*(2), 149–159. https://doi.org/10.1016/s1161-0301(03)00092-3

Magliulo, V., Bindi, M., & Rana, G. (2003). Water use of irrigated potato (*Solanum tuberosum* L.) grown under free air carbon dioxide enrichment in central Italy. *Agriculture, Ecosystems & Environment*, *97*(1), 65–80. https://doi.org/10.1016/s0167-8809(03)00135-x

Mahajan, G., & Singh, K. G. (2006). Response of greenhouse tomato to irrigation and fertigation. *Agricultural Water Management*, *84*(1), 202–206. https://doi.org/10.1016/j.agwat.2006.03.003

Makela, A., Givnish, T. J., Berninger, F., Buckley, T. N., Farquhar, G. D., & Hari, P. (2002). Challenges and opportunities of the optimality approach in plant ecology. *Silva Fennica*, *36*(3), 605–614. https://doi.org/10.14214/sf.528

Malik, A. I., Colmer, T. D., Lambers, H., Setter, T. L., & Schortemeyer, M. (2002). Short-term waterlogging has long-term effects on the growth and physiology of wheat. *New Phytologist*, *153*(2), 225–236. https://doi.org/10.1046/j.0028-646x.2001.00318.x

Manoli, G., Bonetti, S., Domec, J., Putti, M., Katul, G., & Marani, M. (2014). Tree root systems competing for soil moisture in a 3D soil–plant model. *Advances in Water Resources*, *66*, 32–42. https://doi.org/10.1016/j.advwatres.2014.01.006

Manoli, G., Huang, C., Bonetti, S., Domec, J., Marani, M., & Katul, G. (2017). Competition for light and water in a coupled soil-plant system. *Advances in Water Resources*, *108*, 216–230. https://doi.org/10.1016/j.advwatres.2017.08.004

Manzoni, S., Vico, G., Katul, G., Fay, P. A., Polley, W., Palmroth, S., & Porporato, A. (2011). Optimizing stomatal conductance for maximum carbon gain under water stress: A meta-analysis across plant functional types and climates. *Functional Ecology*, *25*(3), 456–467. https://doi.org/10.1111/j.1365-2435.2010.01822.x

Manzoni, S., Vico, G., Porporato, A., & Katul, G. (2013). Biological constraints on water transport in the soil–plant–atmosphere system. *Advances in Water Resources*, *51*, 292–304. https://doi.org/10.1016/j.advwatres.2012.03.016

Martins, J. D., Rodrigues, G. C., Paredes, P., Carlesso, R., Oliveira, Z. B., Knies, A. E., et al. (2013). Dual crop coefficients for maize in southern Brazil: Model testing for sprinkler and drip irrigation and mulched soil. *Biosystems Engineering*, *115*(3), 291–310. https://doi.org/10.1016/j.biosystemseng.2013.03.016

Matthews, A., Katul, G., & Porporato, A. (2024). Multiple time scale optimization explains functional trait responses to leaf water potential. *New Phytologist*, *244*(2), 426–435. https://doi.org/10.1111/nph.20035

McMahon, T. A., Finlayson, B. L., & Peel, M. C. (2016). Historical developments of models for estimating evaporation using standard meteorological data. *Wiley Interdisciplinary Reviews: Water*, *3*(6), 788–818. https://doi.org/10.1002/wat2.1172

McNaughton, K. G. (1976). Evaporation and advection I: Evaporation from extensive homogeneous surfaces. *Quarterly Journal of the Royal Meteorological Society*, *102*(431), 181–191. https://doi.org/10.1002/qj.49710243115

Medlyn, B. E., Barton, C. V. M., Broadmeadow, M. S. J., Ceulemans, R., De Angelis, P., Forstreuter, M., et al. (2001). Stomatal conductance of forest species after long-term exposure to elevated $CO_2$ concentration: A synthesis. *New Phytologist*, *149*(2), 247–264. https://doi.org/10.1046/j.1469-8137.2001.00028.x

Mills, G., Pleijel, H., Braun, S., Büker, P., Bermejo, V., Calvo, E., et al. (2011). New stomatal flux-based critical levels for ozone effects on vegetation. *Atmospheric Environment*, *45*(28), 5064–5068. https://doi.org/10.1016/j.atmosenv.2011.06.009

Minhas, P. S., Ramos, T. B., Ben-Gal, A., & Pereira, L. S. (2020). Coping with salinity in irrigated agriculture: Crop evapotranspiration and water management issues. *Agricultural Water Management*, *227*, 105832. https://doi.org/10.1016/j.agwat.2019.105832

Mishra, V., Ambika, A. K., Asoka, A., Aadhar, S., Buzan, J., Kumar, R., & Huber, M. (2020). Moist heat stress extremes in India enhanced by irrigation. *Nature Geoscience*, *13*(11), 722–728. https://doi.org/10.1038/s41561-020-00650-8

Mohammed, A. T., & Irmak, S. (2022). Maize response to coupled irrigation and nitrogen fertilization under center pivot, subsurface drip and surface (furrow) irrigation: Soil-water dynamics and crop evapotranspiration. *Agricultural Water Management*, *267*, 107634. https://doi.org/10.1016/j.agwat.2022.107634

Monin, A. S., & Obukhov, A. M. (1954). Basic laws of turbulent mixing in the surface layer of the atmosphere. *Trudy Instituta Geologicheskikh Nauk Akademii Nauk SSSR*, *24*(151), 163–187.

Montgomery, R. B. (1948). Vertical eddy flux of heat in the atmosphere. *Journal of the Atmospheric Sciences*, *5*(6), 265–274. https://doi.org/10.1175/1520-0469(1948)005<0265:vefohi>2.0.co;2

Morgan, P. B., Ainsworth, E. A., & Long, S. P. (2003). How does elevated ozone impact soybean? A meta-analysis of photosynthesis, growth and yield. *Plant, Cell & Environment*, *26*(8), 1317–1328. https://doi.org/10.1046/j.0016-8025.2003.01056.x

Morgan, P. B., Mies, T. A., Bollero, G. A., Nelson, R. L., & Long, S. P. (2006). Season-long elevation of ozone concentration to projected 2050 levels under fully open-air conditions substantially decreases the growth and production of soybean. *New Phytologist*, *170*(2), 333–343. https://doi.org/10.1111/j.1469-8137.2006.01679.x

Mrad, A., Domec, J. C., Huang, C. W., Lens, F., & Katul, G. (2018). A network model links wood anatomy to xylem tissue hydraulic behaviour and vulnerability to cavitation. *Plant, Cell & Environment*, *41*(12), 2718–2730. https://doi.org/10.1111/pce.13415

Mrad, A., Manzoni, S., Oren, R., Vico, G., Lindh, M., & Katul, G. (2020). Recovering the metabolic, self-thinning, and constant final yield rules in mono-specific stands. *Frontiers in Forests and Global Change*, *3*, 62. https://doi.org/10.3389/ffgc.2020.00062

Mrad, A., Sevanto, S., Domec, J., Liu, Y., Nakad, M., & Katul, G. (2019). A dynamic optimality principle for water use strategies explains isohydric to anisohydric plant responses to drought. *Frontiers in Forests and Global Change*, *2*, 49. https://doi.org/10.3389/ffgc.2019.00049

Munns, R. (2002). Comparative physiology of salt and water stress. *Plant, Cell and Environment*, *25*(2), 239–250. https://doi.org/10.1046/j.0016-8025.2001.00808.x

Munns, R. (2005). Genes and salt tolerance: Bringing them together. *New Phytologist*, *167*(3), 645–663. https://doi.org/10.1111/j.1469-8137.2005.01487.x

Nakad, M., Domec, J., Sevanto, S., & Katul, G. (2022). Radial–axial transport coordination enhances sugar translocation in the phloem vasculature of plants. *Plant Physiology*, *189*(4), 2061–2071. https://doi.org/10.1093/plphys/kiac231

Nakad, M., Sevanto, S., Domec, J., & Katul, G. (2023). Linking the water and carbon economies of plants in a drying and warming climate. *Current Forestry Reports*, *9*(6), 383–400. https://doi.org/10.1007/s40725-023-00202-4

National Bureau of Statistics of China. (2023). Retrieved from https://data.stats.gov.cn/easyquery.htm?cn=C01&zb=A0D0D&sj=2022

Nguyen, T. H., Langensiepen, M., Gaiser, T., Webber, H., Ahrends, H., Hueging, H., & Ewert, F. (2022). Responses of winter wheat and maize to varying soil moisture: From leaf to canopy. *Agricultural and Forest Meteorology*, *314*, 108803. https://doi.org/10.1016/j.agrformet.2021.108803

Niklas, K. J. (1994). *Plant allometry: The scaling of form and process*. University of Chicago Press.

Ogola, J. B. O., Wheeler, T. R., & Harris, P. M. (2002). Effects of nitrogen and irrigation on water use of maize crops. *Field Crops Research*, *78*(2), 105–117. https://doi.org/10.1016/s0378-4290(02)00116-8

Oishi, A. C., Oren, R., Novick, K. A., Palmroth, S., & Katul, G. G. (2010). Interannual invariability of forest evapotranspiration and its consequence to water flow downstream. *Ecosystems*, *13*(3), 421–436. https://doi.org/10.1007/s10021-010-9328-3

Oishi, A. C., Oren, R., & Stoy, P. C. (2008). Estimating components of forest evapotranspiration: A footprint approach for scaling sap flux measurements. *Agricultural and Forest Meteorology*, *148*(11), 1719–1732. https://doi.org/10.1016/j.agrformet.2008.06.013

Oren, R., Phillips, N., Ewers, B. E., Pataki, D. E., & Megonigal, J. P. (1999). Sap-flux-scaled transpiration responses to light, vapor pressure deficit, and leaf area reduction in a flooded *Taxodium distichum* forest. *Tree Physiology*, *19*(6), 337–347. https://doi.org/10.1093/treephys/19.6.337

Oren, R., Phillips, N., Katul, G., Ewers, B. E., & Pataki, D. E. (1998). Scaling xylem sap flux and soil water balance and calculating variance: A method for partitioning water flux in forests. *Annals of Forest Science*, *55*(1–2), 191–216. https://doi.org/10.1051/forest:19980112

Oren, R., Sperry, J. S., Katul, G. G., Pataki, D. E., Ewers, B. E., Phillips, N., & Schäfer, K. (1999). Survey and synthesis of intra-and interspecific variation in stomatal sensitivity to vapour pressure deficit. *Plant, Cell & Environment*, *22*(12), 1515–1526. https://doi.org/10.1046/j.1365-3040.1999.00513.x

Ortega-Farias, S., Olioso, A., Antonioletti, R., & Brisson, N. (2004). Evaluation of the Penman-Monteith model for estimating soybean evapotranspiration. *Irrigation Science*, *23*(1), 1–9. https://doi.org/10.1007/s00271-003-0087-1

Ortega-Farias, S. O., Olioso, A., Fuentes, S., & Valdes, H. (2006). Latent heat flux over a furrow-irrigated tomato crop using Penman–Monteith equation with a variable surface canopy resistance. *Agricultural Water Management*, *82*(3), 421–432. https://doi.org/10.1016/j.agwat.2005.07.028

Oweis, T. Y., Farahani, H. J., & Hachum, A. Y. (2011). Evapotranspiration and water use of full and deficit irrigated cotton in the Mediterranean environment in northern Syria. *Agricultural Water Management*, *98*(8), 1239–1248. https://doi.org/10.1016/j.agwat.2011.02.009

Palmroth, S., Katul, G. G., Maier, C. A., Ward, E., Manzoni, S., & Vico, G. (2013). On the complementary relationship between marginal nitrogen and water-use efficiencies among *Pinus taeda* leaves grown under ambient and $CO_2$-enriched environments. *Annals of Botany*, *111*(3), 467–477. https://doi.org/10.1093/aob/mcs268

Pan, S., Tian, H., Dangal, S. R. S., Yang, Q., Yang, J., Lu, C., et al. (2015). Responses of global terrestrial evapotranspiration to climate change and increasing atmospheric $CO_2$ in the 21st century. *Earth's Future*, *3*(1), 15–35. https://doi.org/10.1002/2014ef000263

Papadopoulos, A. P., & Ormrod, D. P. (1988). Plant spacing effects on light interception by greenhouse tomatoes. *Canadian Journal of Plant Science*, *68*(4), 1197–1208. https://doi.org/10.4141/cjps88-149

Parlange, M. B., & Katul, G. G. (1992). An advection-aridity evaporation model. *Water Resources Research*, *28*(1), 127–132. https://doi.org/10.1029/91wr02482

Parlange, M. B., Katul, G. G., Cuenca, R. H., Kavvas, M. L., Nielsen, D. R., & Mata, M. (1992). Physical basis for a time series model of soil water content. *Water Resources Research*, *28*(9), 2437–2446. https://doi.org/10.1029/92wr01241

Patra, S. K., Poddar, R., Pramanik, S., Bandopadhyay, P., Gaber, A., & Hossain, A. (2023). Growth, yield, water productivity and economics of okra (*Abelmoschus esculentus* L.) in response to gravity drip irrigation under mulch and without-mulch conditions. *Scientia Horticulturae*, *321*, 112327. https://doi.org/10.1016/j.scienta.2023.112327

Paw U, K. T., Qiu, J., Su, H., Watanabe, T., & Brunet, Y. (1995). Surface renewal analysis: A new method to obtain scalar fluxes. *Agricultural and Forest Meteorology*, *74*(1), 119–137. https://doi.org/10.1016/0168-1923(94)02182-j

Peng, S., Piao, S., Ciais, P., Myneni, R. B., Chen, A., Chevallier, F., et al. (2013). Asymmetric effects of daytime and night-time warming on Northern Hemisphere vegetation. *Nature*, *501*(7465), 88–92. https://doi.org/10.1038/nature12434

Pereira, L. S., Gonçalves, J. M., Dong, B., Mao, Z., & Fang, S. X. (2007). Assessing basin irrigation and scheduling strategies for saving irrigation water and controlling salinity in the upper Yellow River Basin, China. *Agricultural Water Management*, *93*(3), 109–122. https://doi.org/10.1016/j.agwat.2007.07.004

Pereira, L. S., Paredes, P., Melton, F., Johnson, L., Mota, M., & Wang, T. (2021). Prediction of crop coefficients from fraction of ground cover and height: Practical application to vegetable, field and fruit crops with focus on parameterization. *Agricultural Water Management*, *252*, 106663. https://doi.org/10.1016/j.agwat.2020.106663

Pereira, L. S., Paredes, P., Melton, F., Johnson, L., Wang, T., López-Urrea, R., et al. (2020). Prediction of crop coefficients from fraction of ground cover and height. Background and validation using ground and remote sensing data. *Agricultural Water Management*, *241*, 106197. https://doi.org/10.1016/j.agwat.2020.106197

Phillips, N., Oren, R., & Zimmermann, R. (1996). Radial patterns of xylem sap flow in non-, diffuse-and ring-porous tree species. *Plant Cell and Environment*, *19*(8), 983–990. https://doi.org/10.1111/j.1365-3040.1996.tb00463.x

Pruitt, W. O., Morgan, D. L., & Lourence, F. J. (1973). Momentum and mass transfers in the surface boundary layer. *Quarterly Journal of the Royal Meteorological Society*, *99*(420), 370–386. https://doi.org/10.1002/qj.49709942014

Qin, J., Dong, W. Y., He, K. N., Yu, Y., Tan, G. D., Han, L., et al. (2010). NaCl salinity-induced changes in water status, ion contents and photosynthetic properties of *Shepherdia argentea* (Pursh) Nutt. seedlings. *Plant Soil Environment*, *56*(7), 325–332. https://doi.org/10.17221/209/2009-pse

Qin, S., Fan, Y., Li, S., Cheng, L., Zhang, L., Xi, H., et al. (2023). Partitioning of available energy in canopy and soil surface in croplands with different irrigation methods. *Agricultural Water Management*, *288*, 108475. https://doi.org/10.1016/j.agwat.2023.108475

Qin, S., Li, S., Kang, S., Du, T., Tong, L., & Ding, R. (2016). Can the drip irrigation under film mulch reduce crop evapotranspiration and save water under the sufficient irrigation condition? *Agricultural Water Management*, *177*, 128–137. https://doi.org/10.1016/j.agwat.2016.06.022

Qin, S., Li, S., Kang, S., Du, T., Tong, L., Ding, R., et al. (2019). Transpiration of female and male parents of seed maize in northwest China. *Agricultural Water Management*, *213*, 397–409. https://doi.org/10.1016/j.agwat.2018.10.016

Qin, S., Li, S., Yang, K., & Hu, K. (2018). Can plastic mulch save water at night in irrigated croplands? *Journal of Hydrology*, *564*, 667–681. https://doi.org/10.1016/j.jhydrol.2018.07.050

Qin, S., Li, S., Yang, K., Zhang, L., Cheng, L., Liu, P., & She, D. (2023). A method for estimating surface albedo and its components for partial plastic mulched croplands. *Journal of Hydrometeorology*, *24*(6), 1069–1086. https://doi.org/10.1175/jhm-d-22-0088.1

Qin, S., Zhang, J., Dai, H., Wang, D., & Li, D. (2014). Effect of ridge–furrow and plastic-mulching planting patterns on yield formation and water movement of potato in a semi-arid area. *Agricultural Water Management*, *131*, 87–94. https://doi.org/10.1016/j.agwat.2013.09.015

Qiu, R. J., Du, T. S., Kang, S. Z., Chen, R. Q., & Wu, L. S. (2015a). Assessing the SIMDualKc model for estimating evapotranspiration of hot pepper grown in a solar greenhouse in Northwest China. *Agricultural Systems*, *138*, 1–9. https://doi.org/10.1016/j.agsy.2015.05.001

Qiu, R. J., Du, T. S., Kang, S. Z., Chen, R. Q., & Wu, L. S. (2015b). Influence of water and nitrogen stress on stem sap flow of tomato grown in a solar greenhouse. *Journal of the American Society for Horticultural Science*, *140*(2), 111–119. https://doi.org/10.21273/jashs.140.2.111

Qiu, R. J., & Katul, G. G. (2020). Maximizing leaf carbon gain in varying saline conditions: An optimization model with dynamic mesophyll conductance. *The Plant Journal*, *101*(3), 543–554. https://doi.org/10.1111/tpj.14553

Qiu, R. J., Katul, G. G., Wang, J. T., Xu, J. Z., Kang, S. Z., Liu, C. W., et al. (2021). Differential response of rice evapotranspiration to varying patterns of warming. *Agricultural and Forest Meteorology*, *298–299*, 108293. https://doi.org/10.1016/j.agrformet.2020.108293

Qiu, R. J., Liu, C. W., Cui, N. B., Wu, Y. J., Wang, Z. C., & Li, G. (2019). Evapotranspiration estimation using a modified Priestley-Taylor model in a rice-wheat rotation system. *Agricultural Water Management*, *224*, 105755. https://doi.org/10.1016/j.agwat.2019.105755

Qiu, R. J., Liu, C. W., Wang, Z. C., Yang, Z. Q., & Jing, Y. S. (2017). Effects of irrigation water salinity on evapotranspiration modified by leaching fractions in hot pepper plants. *Scientific Reports*, *7*(1), 7231. https://doi.org/10.1038/s41598-017-07743-2

Qiu, R. J., Song, J. J., Du, T. S., Kang, S. Z., Tong, L., Chen, R. Q., & Wu, L. S. (2013). Response of evapotranspiration and yield to planting density of solar greenhouse grown tomato in northwest China. *Agricultural Water Management*, *130*, 44–51. https://doi.org/10.1016/j.agwat.2013.08.013

Qiu, R. J., Yang, Z. Q., Jing, Y. S., Liu, C. W., Luo, X. S., & Wang, Z. C. (2018). Effects of irrigation water salinity on the growth, gas exchange parameters, and ion concentration of hot pepper plants modified by leaching fractions. *HortScience*, *53*(7), 1050–1055. https://doi.org/10.21273/hortsci13078-18

Qu, Y., Kang, S., Li, F., Zhang, J., Xia, G., & Li, W. (2007). Xylem sap flows of irrigated Tamarix elongata Ledeb and the influence of environmental factors in the desert region of Northwest China. *Hydrological Processes*, *21*(10), 1363–1369. https://doi.org/10.1002/hyp.6314

Raats, P. A., & Knight, J. H. (2018). The contributions of Lewis Fry Richardson to drainage theory, soil physics, and the soil-plant-atmosphere continuum. *Frontiers in Environmental Science*, *6*, 13. https://doi.org/10.3389/fenvs.2018.00013

Rafi, Z., Merlin, O., Le Dantec, V., Khabba, S., Mordelet, P., Er-Raki, S., et al. (2019). Partitioning evapotranspiration of a drip-irrigated wheat crop: Inter-comparing eddy covariance-sap flow-lysimeter- and FAO-based methods. *Agricultural and Forest Meteorology*, *265*, 310–326. https://doi.org/10.1016/j.agrformet.2018.11.031

Ramos, T. B., Šimůnek, J., Gonçalves, M. C., Martins, J. C., Prazeres, A., & Pereira, L. S. (2012). Two-dimensional modeling of water and nitrogen fate from sweet sorghum irrigated with fresh and blended saline waters. *Agricultural Water Management*, *111*, 87–104. https://doi.org/10.1016/j.agwat.2012.05.007

Rana, G., & Katerji, N. (2000). Measurement and estimation of actual evapotranspiration in the field under Mediterranean climate: A review. *European Journal of Agronomy*, *13*(2–3), 125–153. https://doi.org/10.1016/s1161-0301(00)00070-8

Reavis, C. W., Suvočarev, K., Reba, M. L., & Runkle, B. R. K. (2021). Impacts of alternate wetting and drying and delayed flood rice irrigation on growing season evapotranspiration. *Journal of Hydrology*, *596*, 126080. https://doi.org/10.1016/j.jhydrol.2021.126080

Richards, F. J. (1959). A flexible growth function for empirical use. *Journal of Experimental Botany*, *10*(2), 290–301. https://doi.org/10.1093/jxb/10.2.290

Richards, L. A. (1931). Capillary conduction of liquids through porous mediums. *Physics*, *1*(5), 318–333. https://doi.org/10.1063/1.1745010

Richardson, L. F. (1993). The lines of flow of water in saturated soils. *The Collected Papers of Lewis Fry Richardson*, *1*, 95–118.

Rosa, R., Dicken, U., & Tanny, J. (2013). Estimating evapotranspiration from processing tomato using the surface renewal technique. *Biosystems Engineering*, *114*(4), 406–413. https://doi.org/10.1016/j.biosystemseng.2012.06.011

Rosa, R. D., Paredes, P., Rodrigues, G. C., Alves, I., Fernando, R. M., Pereira, L. S., & Allen, R. G. (2012). Implementing the dual crop coefficient approach in interactive software. 1. Background and computational strategy. *Agricultural Water Management*, *103*, 8–24. https://doi.org/10.1016/j.agwat.2011.10.013

Rosa, R. D., Paredes, P., Rodrigues, G. C., Fernando, R. M., Alves, I., Pereira, L. S., & Allen, R. G. (2012). Implementing the dual crop coefficient approach in interactive software: 2. Model testing. *Agricultural Water Management*, *103*, 62–77. https://doi.org/10.1016/j.agwat.2011.10.018

Rosa, R. D., Ramos, T. B., & Pereira, L. S. (2016). The dual Kc approach to assess maize and sweet sorghum transpiration and soil evaporation under saline conditions: Application of the SIMDualKc model. *Agricultural Water Management*, *177*, 77–94. https://doi.org/10.1016/j.agwat.2016.06.028

Rousseaux, M. C., Figuerola, P. I., Correa-Tedesco, G., & Searles, P. S. (2009). Seasonal variations in sap flow and soil evaporation in an olive (*Olea europaea* L.) grove under two irrigation regimes in an arid region of Argentina. *Agricultural Water Management*, *96*(6), 1037–1044. https://doi.org/10.1016/j.agwat.2009.02.003

Rudnick, D. R., & Irmak, S. (2014). Impact of nitrogen fertilizer on maize evapotranspiration crop coefficients under fully irrigated, limited irrigation, and rainfed settings. *Journal of Irrigation and Drainage Engineering*, *140*(12), 04014039. https://doi.org/10.1061/(asce)ir.1943-4774.0000778

Saeidi, R., Ramezani Etedali, H., Sotoodehnia, A., Kaviani, A., & Nazari, B. (2021). Salinity and fertility stresses modify Ks and readily available water coefficients in maize (case study: Qazvin region). *Irrigation Science*, *39*(3), 299–313. https://doi.org/10.1007/s00271-020-00711-1

Sainju, U. M., Singh, B. P., & Whitehead, W. F. (2005). Tillage, cover crops, and nitrogen fertilization effects on cotton and sorghum root biomass, carbon, and nitrogen. *Agronomy Journal*, *97*(5), 1279–1290. https://doi.org/10.2134/agronj2004.0213

Sandhu, R., & Irmak, S. (2019). Assessment of AquaCrop model in simulating maize canopy cover, soil-water, evapotranspiration, yield, and water productivity for different planting dates and densities under irrigated and rainfed conditions. *Agricultural Water Management*, *224*, 105753. https://doi.org/10.1016/j.agwat.2019.105753

Schlesinger, W. H., & Jasechko, S. (2014). Transpiration in the global water cycle. *Agricultural and Forest Meteorology*, *189*, 115–117. https://doi.org/10.1016/j.agrformet.2014.01.011

Scott, R. L., Knowles, J. F., Nelson, J. A., Gentine, P., Li, X., Barron-Gafford, G., et al. (2021). Water availability impacts on evapotranspiration partitioning. *Agricultural and Forest Meteorology*, *297*, 108251. https://doi.org/10.1016/j.agrformet.2020.108251

Sepaskhah, A. R., Bazrafshan-Jahromi, A. R., & Shirmohammadi-Aliakbarkhani, Z. (2006). Development and evaluation of a model for yield production of wheat, maize and sugarbeet under water and salt stresses. *Biosystems Engineering*, *93*(2), 139–152. https://doi.org/10.1016/j.biosystemseng.2005.11.005

Shang, B., Fu, R., Agathokleous, E., Dai, L., Zhang, G., Wu, R., & Feng, Z. (2022). Ethylenediurea offers moderate protection against ozone-induced rice yield loss under high ozone pollution. *Science of the Total Environment*, *806*, 151341. https://doi.org/10.1016/j.scitotenv.2021.151341

Shang, B., Xu, Y. S., Peng, J. L., Agathokleous, E., & Feng, Z. Z. (2021). High nitrogen addition decreases the ozone flux by reducing the maximum stomatal conductance in poplar saplings. *Environmental Pollution*, *272*, 115979. https://doi.org/10.1016/j.envpol.2020.115979

Shani, U., Ben Gal, A., Tripler, E., & Dudley, L. M. (2007). Plant response to the soil environment: An analytical model integrating yield, water, soil type, and salinity. *Water Resources Research*, *43*(8), W08418. https://doi.org/10.1029/2006wr005313

Shani, U., & Dudley, L. M. (2001). Field studies of crop response to water and salt stress. *Soil Science Society of America Journal*, *65*(5), 1522–1528. https://doi.org/10.2136/sssaj2001.6551522x

Shao, G. C., Lan, J. J., Yu, S. E., Liu, N., Guo, R. Q., & She, D. L. (2013). Photosynthesis and growth of winter wheat in response to waterlogging at different growth stages. *Photosynthetica*, *51*(3), 429–437. https://doi.org/10.1007/s11099-013-0039-9

Sharma, V., & Irmak, S. (2021). Comparative analyses of variable and fixed rate irrigation and nitrogen management for maize in different soil types: Part II. Growth, grain yield, evapotranspiration, production functions and water productivity. *Agricultural Water Management*, *246*, 106653. https://doi.org/10.1016/j.agwat.2020.106653

Shi, P., Tang, L., Lin, C., Liu, L., Wang, H., Cao, W., & Zhu, Y. (2015). Modeling the effects of post-anthesis heat stress on rice phenology. *Field Crops Research*, *177*, 26–36. https://doi.org/10.1016/j.fcr.2015.02.023

Siqueira, M., Katul, G., & Porporato, A. (2008). Onset of water stress, hysteresis in plant conductance, and hydraulic lift: Scaling soil water dynamics from millimeters to meters. *Water Resources Research*, *44*(1), W01432. https://doi.org/10.1029/2007wr006094

Skaggs, T. H., Poss, J. A., Shouse, P. J., & Grieve, C. M. (2006). Irrigating forage crops with saline waters. *Vadose Zone Journal*, *5*(3), 815–823. https://doi.org/10.2136/vzj2005.0119

Smith, D. M., & Allen, S. J. (1996). Measurement of sap flow in plant stems. *Journal of Experimental Botany*, *47*(12), 1833–1844. https://doi.org/10.1093/jxb/47.12.1833

Song, X., Zhou, G., He, Q., & Zhou, H. (2020). Stomatal limitations to photosynthesis and their critical Water conditions in different growth stages of maize under water stress. *Agricultural Water Management*, *241*, 106330. https://doi.org/10.1016/j.agwat.2020.106330

Song, Z., Xia, J., She, D., Zhang, L., Hu, C., & Zhao, L. (2020). The development of a Nonstationary Standardized Precipitation Index using climate covariates: A case study in the middle and lower reaches of Yangtze River Basin, China. *Journal of Hydrology*, *588*, 125115. https://doi.org/10.1016/j.jhydrol.2020.125115

Srivastava, R. K., Panda, R. K., Chakraborty, A., & Halder, D. (2020). Quantitative estimation of water use efficiency and evapotranspiration under varying nitrogen levels and sowing dates for rainfed and irrigated maize. *Theoretical and Applied Climatology*, *139*(3), 1385–1400. https://doi.org/10.1007/s00704-019-03005-5

Sugita, M., Matsuno, A., El-Kilani, R. M. M., Abdel-Fattah, A., & Mahmoud, M. A. (2017). Crop evapotranspiration in the Nile Delta under different irrigation methods. *Hydrological Sciences Journal*, *62*(10), 1618–1635. https://doi.org/10.1080/02626667.2017.1341631

Sun, D., Li, H., Wang, E., He, W., Hao, W., Yan, C., et al. (2020). An overview of the use of plastic-film mulching in China to increase crop yield and water-use efficiency. *National Science Review*, *7*(10), 1523–1526. https://doi.org/10.1093/nsr/nwaa146

Sun, T., Hasegawa, T., Liu, B., Tang, L., Liu, L., Cao, W., & Zhu, Y. (2021). Current rice models underestimate yield losses from short-term heat stresses. *Global Change Biology*, *27*(2), 402–416. https://doi.org/10.1111/gcb.15393

Suyker, A. E., & Verma, S. B. (2009). Evapotranspiration of irrigated and rainfed maize–soybean cropping systems. *Agricultural and Forest Meteorology*, *149*(3), 443–452. https://doi.org/10.1016/j.agrformet.2008.09.010

Swinbank, W. C. (1951). The measurement of vertical transfer of heat and water vapor by eddies in the lower atmosphere. *Journal of Atmospheric Sciences*, *8*(3), 135–145. https://doi.org/10.1175/1520-0469(1951)008<0135:tmovto>2.0.co;2

Tan, W., Meng, Q. W., Brestic, M., Olsovska, K., & Yang, X. (2011). Photosynthesis is improved by exogenous calcium in heat-stressed tobacco plants. *Journal of Plant Physiology*, *168*(17), 2063–2071. https://doi.org/10.1016/j.jplph.2011.06.009

Tao, F. L., Hayashi, Y., Zhang, Z., Sakamoto, T., & Yokozawa, M. (2008). Global warming, rice production, and water use in China: Developing a probabilistic assessment. *Agricultural and Forest Meteorology*, *148*(1), 94–110. https://doi.org/10.1016/j.agrformet.2007.09.012

Tezara, W., Mitchell, V., Driscoll, S. P., & Lawlor, D. W. (2002). Effects of water deficit and its interaction with $CO_2$ supply on the biochemistry and physiology of photosynthesis in sunflower. *Journal of Experimental Botany*, *53*(375), 1781–1791. https://doi.org/10.1093/jxb/erf021

Thidar, M., Gong, D., Mei, X., Gao, L., Li, H., Hao, W., & Gu, F. (2020). Mulching improved soil water, root distribution and yield of maize in the Loess Plateau of Northwest China. *Agricultural Water Management*, *241*, 106340. https://doi.org/10.1016/j.agwat.2020.106340

Tian, F., Yang, P., Hu, H., & Liu, H. (2017). Energy balance and canopy conductance for a cotton field under film mulched drip irrigation in an arid region of northwestern China. *Agricultural Water Management*, *179*, 110–121. https://doi.org/10.1016/j.agwat.2016.06.029

Tillman, J. E. (1972). The indirect determination of stability, heat and momentum fluxes in the atmospheric boundary layer from simple scalar variables during dry unstable conditions. *Journal of Applied Meteorology and Climatology*, *11*(5), 783–792. https://doi.org/10.1175/1520-0450(1972)011<0783:tidosh>2.0.co;2

Triggs, J. M., Kimball, B. A., Pinter, P. J., Wall, G. W., Conley, M. M., Brooks, T. J., et al. (2004). Free-air $CO_2$ enrichment effects on the energy balance and evapotranspiration of sorghum. *Agricultural and Forest Meteorology*, *124*(1), 63–79. https://doi.org/10.1016/j.agrformet.2004.01.005

Tripler, E., Shani, U., Mualem, Y., & Ben-Gal, A. (2011). Long-term growth, water consumption and yield of date palm as a function of salinity. *Agricultural Water Management*, *99*(1), 128–134. https://doi.org/10.1016/j.agwat.2011.06.010

Turnock, S. T., Allen, R. J., Andrews, M., Bauer, S. E., Deushi, M., Emmons, L., et al. (2020). Historical and future changes in air pollutants from CMIP6 models. *Atmospheric Chemistry and Physics*, *20*(23), 14547–14579. https://doi.org/10.5194/acp-20-14547-2020

Urban, D. W., Sheffield, J., & Lobell, D. B. (2017). Historical effects of $CO_2$ and climate trends on global crop water demand. *Nature Climate Change*, *7*(12), 901–905. https://doi.org/10.1038/s41558-017-0011-y

Valentín, F., Nortes, P. A., Domínguez, A., Sánchez, J. M., Intrigliolo, D. S., Alarcón, J. J., & López-Urrea, R. (2020). Comparing evapotranspiration and yield performance of maize under sprinkler, superficial and subsurface drip irrigation in a semi-arid environment. *Irrigation Science*, *38*(1), 105–115. https://doi.org/10.1007/s00271-019-00657-z

Van den Honert, T. H. (1948). Water transport in plants as a catenary process. *Discussions of the Faraday Society*, *3*, 146–153. https://doi.org/10.1039/df9480300146

Vandermeiren, K., Black, C., Pleijel, H., & De Temmerman, L. (2005). Impact of rising tropospheric ozone on potato: Effects on photosynthesis, growth, productivity and yield quality. *Plant, Cell & Environment*, *28*(8), 982–996. https://doi.org/10.1111/j.1365-3040.2005.01316.x

Van Genuchten, M. T., & Hoffman, G. J. (1984). Analysis of crop production. In I. Shainberg & J. Shalhevet (Eds.), *Soil salinity under irrigation* (pp. 258–271). Spinger.

Vanloocke, A., Betzelberger, A. M., Ainsworth, E. A., & Bernacchi, C. J. (2012). Rising ozone concentrations decrease soybean evapotranspiration and water use efficiency whilst increasing canopy temperature. *New Phytologist*, *195*(1), 164–171. https://doi.org/10.1111/j.1469-8137.2012.04152.x

Volpe, V., Manzoni, S., Marani, M., & Katul, G. (2011). Leaf conductance and carbon gain under salt-stressed conditions. *Journal of Geophysical Research*, *116*(G4), G04035. https://doi.org/10.1029/2011jg001848

Von Bertalanffy, L. (1957). Quantitative laws in metabolism and growth. *The Quarterly Review of Biology*, *32*(3), 217–231. https://doi.org/10.1086/401873

Wang, J., Zhang, Y., Gong, S., Xu, D., Juan, S., & Zhao, Y. (2018). Evapotranspiration, crop coefficient and yield for drip-irrigated winter wheat with straw mulching in North China Plain. *Field Crops Research*, *217*, 218–228. https://doi.org/10.1016/j.fcr.2017.05.010

Wang, J. L., Yu, G. R., Wang, B. L., Qi, H., & Xu, Z. J. (2005). Response of photosynthetic rate and stomatal conductance of rice to light intensity and $CO_2$ concentration in northern China. *Chinese Journal of Plant Ecology*, *29*(1), 16–25. https://doi.org/10.17521/cjpe.2005.0003

Wang, K., & Dickinson, R. E. (2012). A review of global terrestrial evapotranspiration: Observation, modeling, climatology, and climatic variability. *Reviews of Geophysics*, *50*(2), RG2005. https://doi.org/10.1029/2011rg000373

Wang, S., Zhu, G., Xia, D., Ma, J., Han, T., Ma, T., et al. (2019). The characteristics of evapotranspiration and crop coefficients of an irrigated vineyard in arid Northwest China. *Agricultural Water Management*, *212*, 388–398. https://doi.org/10.1016/j.agwat.2018.09.023

Wang, T., Alfieri, J., Mallick, K., Arias-Ortiz, A., Anderson, M., Fisher, J. B., et al. (2024). How advection affects the surface energy balance and its closure at an irrigated alfalfa field. *Agricultural and Forest Meteorology*, *357*, 110196. https://doi.org/10.1016/j.agrformet.2024.110196

Wang, W. L., Cai, C., Lam, S. K., Liu, G., & Zhu, J. G. (2018). Elevated $CO_2$ cannot compensate for japonica grain yield losses under increasing air temperature because of the decrease in spikelet density. *European Journal of Agronomy*, *99*, 21–29. https://doi.org/10.1016/j.eja.2018.06.005

Wang, X., Guan, H., Huo, Z., Guo, P., Du, J., & Wang, W. (2020). Maize transpiration and water productivity of two irrigated fields with varying groundwater depths in an arid area. *Agricultural and Forest Meteorology*, *281*, 107849. https://doi.org/10.1016/j.agrformet.2019.107849

Wang, X., Huo, Z., Guan, H., Guo, P., & Qu, Z. (2018). Drip irrigation enhances shallow groundwater contribution to crop water consumption in an arid area. *Hydrological Processes*, *32*(6), 747–758. https://doi.org/10.1002/hyp.11451

Wang, Y., Horton, R., Xue, X., & Ren, T. (2021). Partitioning evapotranspiration by measuring soil water evaporation with heat-pulse sensors and plant transpiration with sap flow gauges. *Agricultural Water Management*, *252*, 106883. https://doi.org/10.1016/j.agwat.2021.106883

Wang, Y., Li, S., Qin, S., Guo, H., Yang, D., & Lam, H. (2020). How can drip irrigation save water and reduce evapotranspiration compared to border irrigation in arid regions in northwest China. *Agricultural Water Management*, *239*, 106256. https://doi.org/10.1016/j.agwat.2020.106256

Wei, Z., Abdelhakim, L. O. A., Fang, L., Peng, X., Liu, J., & Liu, F. (2022). Elevated $CO_2$ effect on the response of stomatal control and water use efficiency in amaranth and maize plants to progressive drought stress. *Agricultural Water Management*, *266*, 107609. https://doi.org/10.1016/j.agwat.2022.107609

Wei, Z., Fang, L., Li, X., Liu, J., & Liu, F. (2021). Endogenous ABA level modulates the effects of $CO_2$ elevation and soil water deficit on growth, water and nitrogen use efficiencies in barley and tomato plants. *Agricultural Water Management*, *249*, 106808. https://doi.org/10.1016/j.agwat.2021.106808

Williams, D. G., Cable, W., Hultine, K., Hoedjes, J. C. B., Yepez, E. A., Simonneaux, V., et al. (2004). Evapotranspiration components determined by stable isotope, sap flow and eddy covariance techniques. *Agricultural and Forest Meteorology*, *125*(3), 241–258. https://doi.org/10.1016/j.agrformet.2004.04.008

Wu, H., Yue, Q., Guo, P., Xu, X., & Huang, X. (2022). Improving the AquaCrop model to achieve direct simulation of evapotranspiration under nitrogen stress and joint simulation-optimization of irrigation and fertilizer schedules. *Agricultural Water Management*, *266*, 107599. https://doi.org/10.1016/j.agwat.2022.107599

Wu, Y., Liu, S., & Abdul-Aziz, O. I. (2012). Hydrological effects of the increased $CO_2$ and climate change in the Upper Mississippi River Basin using a modified SWAT. *Climatic Change*, *110*(3), 977–1003. https://doi.org/10.1007/s10584-011-0087-8

Xiao, L., Wei, X., Wang, C., & Zhao, R. (2023). Plastic film mulching significantly boosts crop production and water use efficiency but not evapotranspiration in China. *Agricultural Water Management*, *275*, 108023. https://doi.org/10.1016/j.agwat.2022.108023

Xiao, W., Wei, Z., & Wen, X. (2018). Evapotranspiration partitioning at the ecosystem scale using the stable isotope method—A review. *Agricultural and Forest Meteorology*, *263*, 346–361. https://doi.org/10.1016/j.agrformet.2018.09.005

Xie, Z. K., Wang, Y. J., & Li, F. M. (2005). Effect of plastic mulching on soil water use and spring wheat yield in arid region of northwest China. *Agricultural Water Management*, *75*(1), 71–83. https://doi.org/10.1016/j.agwat.2004.12.014

Xiong, L., Xu, X., Ren, D., Huang, Q., & Huang, G. (2019). Enhancing the capability of hydrological models to simulate the regional agro-hydrological processes in watersheds with shallow groundwater: Based on the SWAT framework. *Journal of Hydrology*, *572*, 1–16. https://doi.org/10.1016/j.jhydrol.2019.02.043

Xu, C., & Huang, B. (2008). Root proteomic responses to heat stress in two Agrostis grass species contrasting in heat tolerance. *Journal of Experimental Botany*, *59*(15), 4183–4194. https://doi.org/10.1093/jxb/ern258

Xu, J. Z., Liu, X. Y., Yang, S. H., Qi, Z. M., & Wang, Y. J. (2017). Modeling rice evapotranspiration under water-saving irrigation by calibrating canopy resistance model parameters in the Penman-Monteith equation. *Agricultural Water Management*, *182*, 55–66. https://doi.org/10.1016/j.agwat.2016.12.010

Xu, Y. S., Shang, B., Peng, J. L., Feng, Z. Z., & Tarvainen, L. (2021). Stomatal response drives between-species difference in predicted leaf water-use efficiency under elevated ozone. *Environmental Pollution*, *269*, 116137. https://doi.org/10.1016/j.envpol.2020.116137

Yang, D., Li, S., Kang, S., Du, T., Guo, P., Mao, X., et al. (2020). Effect of drip irrigation on wheat evapotranspiration, soil evaporation and transpiration in Northwest China. *Agricultural Water Management*, *232*, 106001. https://doi.org/10.1016/j.agwat.2020.106001

Yang, D., Li, S., Wu, M., Yang, H., Zhang, W., Chen, J., et al. (2023). Drip irrigation improves spring wheat water productivity by reducing leaf area while increasing yield. *European Journal of Agronomy*, *143*, 126710. https://doi.org/10.1016/j.eja.2022.126710

Yang, H., Du, T. S., Qiu, R. J., Chen, J. L., Wang, F., Li, Y., et al. (2016). Improved water use efficiency and fruit quality of greenhouse crops under regulated deficit irrigation in northwest China. *Agricultural Water Management*, *179*, 193–204. https://doi.org/10.1016/j.agwat.2016.05.029

Yang, P., Wu, L., Cheng, M., Fan, J., Li, S., Wang, H., & Qian, L. (2023). Review on drip irrigation: Impact on crop yield, quality, and water productivity in China. *Water*, *15*(9), 1733. https://doi.org/10.3390/w15091733

Yang, Q., Zuo, H., Xiao, X., Wang, S., Chen, B., & Chen, J. (2012). Modelling the effects of plastic mulch on water, heat and $CO_2$ fluxes over cropland in an arid region. *Journal of Hydrology*, *452–453*, 102–118. https://doi.org/10.1016/j.jhydrol.2012.05.041

Yang, Y., Roderick, M. L., Guo, H., Miralles, D. G., Zhang, L., Fatichi, S., et al. (2023). Evapotranspiration on a greening Earth. *Nature Reviews Earth & Environment*, *4*(9), 626–641. https://doi.org/10.1038/s43017-023-00464-3

Yang, Y., Yang, Y., Han, S., Li, H., Wang, L., Ma, Q., et al. (2023). Comparison of water-saving potential of fallow and crop change with high water-use winter-wheat – Summer-maize rotation. *Agricultural Water Management*, *289*, 108543. https://doi.org/10.1016/j.agwat.2023.108543

Yang, Y. T., Roderick, M. L., Zhang, S. L., McVicar, T. R., & Donohue, R. J. (2019). Hydrologic implications of vegetation response to elevated $CO_2$ in climate projections. *Nature Climate Change*, *9*(1), 44–48. https://doi.org/10.1038/s41558-018-0361-0

Yang, Z. Q., Jiang, Y. H., Qiu, R. J., Gong, X. W., Agathokleous, E., Hu, W., & Clothier, B. (2023). Heat stress decreased transpiration but increased evapotranspiration in gerbera. *Frontiers in Plant Science*, *14*, 1119076. https://doi.org/10.3389/fpls.2023.1119076

Yoshimoto, M., Oue, H., & Kobayashi, K. (2005). Energy balance and water use efficiency of rice canopies under free-air $CO_2$ enrichment. *Agricultural and Forest Meteorology*, *133*(1), 226–246. https://doi.org/10.1016/j.agrformet.2005.09.010

Zahn, E., Dias, N. L., Araújo, A., Sá, L. D., Sörgel, M., Trebs, I., et al. (2016). Scalar turbulent behavior in the roughness sublayer of an Amazonian forest. *Atmospheric Chemistry and Physics*, *16*(17), 11349–11366. https://doi.org/10.5194/acp-16-11349-2016

Zahra, N., Hafeez, M. B., Ghaffar, A., Kausar, A., Al Zeidi, M., Siddique, K. H., & Farooq, M. (2023). Plant photosynthesis under heat stress: Effects and management. *Environmental and Experimental Botany*, *206*, 105178. https://doi.org/10.1016/j.envexpbot.2022.105178

Zhang, B. Z., Kang, S. Z., Li, F. S., Tong, L., & Du, T. S. (2010). Variation in vineyard evapotranspiration in an arid region of northwest China. *Agricultural Water Management*, *97*(11), 1898–1904. https://doi.org/10.1016/j.agwat.2010.06.010

Zhang, B. Z., Kang, S. Z., Li, F. S., & Zhang, L. (2008). Comparison of three evapotranspiration models to Bowen ratio-energy balance method for a vineyard in an arid desert region of northwest China. *Agricultural and Forest Meteorology*, *148*(10), 1629–1640. https://doi.org/10.1016/j.agrformet.2008.05.016

Zhang, B. Z., Liu, Y., Xu, D., Zhao, N. N., Lei, B., Rosa, R. D., et al. (2013). The dual crop coefficient approach to estimate and partitioning evapotranspiration of the winter wheat–summer maize crop sequence in North China Plain. *Irrigation Science*, *31*(6), 1303–1316. https://doi.org/10.1007/s00271-013-0405-1

Zhang, C., Dong, J., Leng, G., Doughty, R., Zhang, K., Han, S., et al. (2023). Attenuated cooling effects with increasing water-saving irrigation: Satellite evidence from Xinjiang, China. *Agricultural and Forest Meteorology*, *333*, 109397. https://doi.org/10.1016/j.agrformet.2023.109397

Zhang, F., Eldoma, I. M., Li, M., Kong, M., Siddique, K. H. M., & Li, F. (2019). Integrated model and field experiment to determine the optimum planting density in plastic film mulched rainfed agriculture. *Agricultural and Forest Meteorology*, *268*, 331–340. https://doi.org/10.1016/j.agrformet.2019.01.040

Zhang, T., Zou, Y., Kisekka, I., Biswas, A., & Cai, H. (2021). Comparison of different irrigation methods to synergistically improve maize's yield, water productivity and economic benefits in an arid irrigation area. *Agricultural Water Management*, *243*, 106497. https://doi.org/10.1016/j.agwat.2020.106497

Zhang, T. Y., Huang, Y., & Yang, X. G. (2013). Climate warming over the past three decades has shortened rice growth duration in China and cultivar shifts have further accelerated the process for late rice. *Global Change Biology*, *19*(2), 563–570. https://doi.org/10.1111/gcb.12057

Zhang, X., Yang, L., Xue, X., Kamran, M., Ahmad, I., Dong, Z., et al. (2019). Plastic film mulching stimulates soil wet-dry alternation and stomatal behavior to improve maize yield and resource use efficiency in a semi-arid region. *Field Crops Research*, *233*, 101–113. https://doi.org/10.1016/j.fcr.2019.01.002

Zhang, Y., Wang, J., Gong, S., Xu, D., Sui, J., Wu, Z., & Mo, Y. (2018). Effects of film mulching on evapotranspiration, yield and water use efficiency of a maize field with drip irrigation in Northeastern China. *Agricultural Water Management*, *205*, 90–99. https://doi.org/10.1016/j.agwat.2018.04.029

Zhang, Y., Wang, R., Wang, S., Ning, F., Wang, H., Wen, P., et al. (2019). Effect of planting density on deep soil water and maize yield on the Loess Plateau of China. *Agricultural Water Management*, *223*, 105655. https://doi.org/10.1016/j.agwat.2019.05.039

Zhang, Y. L., Wang, F. X., Shock, C. C., Yang, K. J., Kang, S. Z., Qin, J. T., & Li, S. E. (2017). Effects of plastic mulch on the radiative and thermal conditions and potato growth under drip irrigation in arid Northwest China. *Soil and Tillage Research*, *172*, 1–11. https://doi.org/10.1016/j.still.2017.04.010

Zhang, Y. Q., Kang, S. Z., Ward, E. J., Ding, R. S., Zhang, X., & Zheng, R. (2011). Evapotranspiration components determined by sap flow and microlysimetry techniques of a vineyard in northwest China: Dynamics and influential factors. *Agricultural Water Management*, *98*(8), 1207–1214. https://doi.org/10.1016/j.agwat.2011.03.006

Zhao, J., Xue, Q., Hao, B., Marek, T. H., Jessup, K. E., Xu, W., et al. (2019). Yield determination of maize hybrids under limited irrigation. *Journal of Crop Improvement*, *33*(3), 410–427. https://doi.org/10.1080/15427528.2019.1606129

Zhao, N., Liu, Y., Cai, J., Paredes, P., Rosa, R. D., & Pereira, L. S. (2013). Dual crop coefficient modelling applied to the winter wheat-summer maize crop sequence in North China Plain: Basal crop coefficients and soil evaporation component. *Agricultural Water Management*, *117*, 93∼105–105. https://doi.org/10.1016/j.agwat.2012.11.008

Zhao, P., Kang, S., Li, S., Ding, R., Tong, L., & Du, T. (2018). Seasonal variations in vineyard ET partitioning and dual crop coefficients correlate with canopy development and surface soil moisture. *Agricultural Water Management*, *197*, 19–33. https://doi.org/10.1016/j.agwat.2017.11.004

Zhao, Y., Mao, X., Shukla, M. K., Tian, F., Hou, M., Zhang, T., & Li, S. (2021). How does film mulching modify available energy, evapotranspiration, and crop coefficient during the seed–maize growing season in northwest China? *Agricultural Water Management*, *245*, 106666. https://doi.org/10.1016/j.agwat.2020.106666

Zhong, Y., & Shangguan, Z. (2014). Water consumption characteristics and water use efficiency of winter wheat under long-term nitrogen fertilization regimes in Northwest China. *PLoS One*, *9*(6), e98850. https://doi.org/10.1371/journal.pone.0098850